ISTANBUL TECHNICAL UNIVERSITY ★ GRADUATE SCHOOL

MECHANICAL BEHAVIOR OF THE BI-DIRECTIONAL BEAMS

Ph.D. THESIS

Murat ÇELİK

Department of Civil Engineering

Structure Engineering Programme

AUGUST 2021

ISTANBUL TECHNICAL UNIVERSITY ★ GRADUATE SCHOOL

MECHANICAL BEHAVIOR OF THE BI-DIRECTIONAL BEAMS

Ph.D. THESIS

Murat ÇELİK
(501152009)

Department of Civil Engineering

Structure Engineering Programme

Thesis Advisor: Prof. Dr. Reha ARTAN

AUGUST 2021

İSTANBUL TEKNİK ÜNİVERSİTESİ ★ LİSANSÜSTÜ EĞİTİM ENSTİTÜSÜ

MALZEME ÖZELLİKLERİ İKİ DOĞRULTUDA DEĞİŞEN KİRİŞLERİN MEKANİK DAVRANIŞLARI

DOKTORA TEZİ

Murat ÇELİK
(501152009)

İnşaat Mühendisliği Anabilim Dalı

Yapı Mühendisliği Programı

Tez Danışmanı: Prof. Dr. Reha ARTAN

AĞUSTOS 2021

Murat ÇELİK, a Ph.D. student of ITU Graduate School student ID 501152009, successfully defended the thesis entitled "MECHANICAL BEHAVIOR OF THE BI-DIRECTIONAL BEAMS", which he prepared after fulfilling the requirements specified in the associated legislations, before the jury whose signatures are below.

Thesis Advisor :	**Prof. Dr. Reha ARTAN** Istanbul Technical University	.....
Jury Members :	**Prof. Dr. Abdullah GEDİKLİ** Istanbul Technical University	.....
	Prof. Dr. Fethi KADIOĞLU Istanbul Technical University	.....
	Prof. Dr. İrfan COŞKUN Yıldız Technical University	.....
	Asst.Prof. Dr. Gülçin TEKİN ÖZKAN Yıldız Technical University	.....

Date of Submission : 07 July 2021
Date of Defense : 13 August 2021

To the woman who is both the heroine and architect of this great success, my mother.

FOREWORD

I would like to express my sincere gratitude to my doctoral supervisor, Prof. Dr. Reha ARTAN, who supported me in every way with his knowledge and experience during the thesis work.

I would also like to extend my love and respect to my dear colleague Dr. Erol DEMİRKAN, who has always supported me throughout my doctoral study, and to my dear students, who have encouraged me in many subjects and always made me feel their love.

August 2021

Murat ÇELİK
(M.Sc. Engineer)

TABLE OF CONTENTS

Page

ABBREVIATIONS

CNT **:** Carbon Nanotube

BDSGEB **:** Bi-directional Strain-Gradient Euler-Bernoulli Beam

FGM **:** Functionally Graded Materials

IVP **:** Initial Values Problem

MEMS **:** Microelectromechanical Systems

NEMS **:** Nanoelectromechanical Systems

SWNT **:** Single-walled nanotube

MWNT **:** Multi-walled nanotube

SYMBOLS

t	**:** Time
m	**:** Mass
a	**:** Acceleration
v	**:** Velocity
s	**:** Position
S	**:** Coordinate
S(z)	**:** State vector
D	**:** Differential transition matrix
F(z)	**:** Transport matrix
K(ζ)	**:** Discontinuity matrix
v	**:** Deflection
Ω	**:** Rotation angle
ρ	**:** Radius of curvature
M	**:** Bending moment
E	**:** Modulus of elasticity
I	**:** Moment of inertia
T	**:** Shear force
P	**:** Axial load/force
q	**:** Distributed load
ε	**:** Strain
γ_{zy}	**:** Shear angle
σ	**:** Normal stress
τ	**:** Shear stress
TM(z)	**:** Transformation matrix
G	**:** Shear modulus
F	**:** Cross-sectional area
κ	**:** Shear coefficient

$\mathbf{y(z)}$: State vector

$\mathbf{A}$: Differential transition matrix

$\boldsymbol{\sigma_{ij}}$: Non-local stress tensor

$\boldsymbol{\tau_{ij}}$: Local stress tensor

$\boldsymbol{C_{ijkl}}$: Elastic module tensor

$\boldsymbol{\varepsilon_{kl}}$: Local strain tensor

$\boldsymbol{\nabla}$: Laplace operator

$\boldsymbol{a}$: Atomic distance

$\boldsymbol{e_0}$: Material constant

$\boldsymbol{\sigma_{loc}}$: Local stress

$\boldsymbol{\sigma_{nonloc}}$: Non-local stress

$\mathbf{L}$: Length of the bar

$\boldsymbol{\gamma}$: Material characteristic length

$\boldsymbol{u}$: Discontinuity matrix

$\boldsymbol{\beta}$: Inhomogeneous material constant

$\boldsymbol{\nabla_x}$: Gradient

$\boldsymbol{\chi}$: Reference position

$\boldsymbol{C}$: Fourth order tensor

$\boldsymbol{H}$: Fifth order tensor

$\boldsymbol{G}$: Sixth order tensor

$\boldsymbol{\varepsilon}$: Green-Lagrange tensor

$\boldsymbol{\delta_{ij}}$: Kronecker delta

$\boldsymbol{\lambda, \mu}$: Lame constants

$\boldsymbol{\tau_{ij}}$: Cauchy stress

$\boldsymbol{\mu_{zz}}$: Double stress

$\boldsymbol{\sigma_{zz}}$: Total stress

LIST OF TABLES

Page

LIST OF FIGURES

Page

MECHANICAL BEHAVIOR OF THE BI-DIRECTIONAL BEAMS

SUMMARY

Nanotechnology, which is one of the most developed areas of today's technology, has a widespread usage area because it can be easily integrated into many areas of engineering. The design and production of very small-scale functional materials in fields such as aerospace and aviation industry, medicine, energy and civil engineering, and their effective use in related fields make significant contributions to engineering science.

The fact that these very small-scale materials used in many areas of technology have spread to almost every field of engineering has revealed the need to determine their internal structure and mechanical properties. Materials exhibit some mechanical behavior such as bending, torsion and buckling under loads. It is an important issue for the stability of the structure to be able to detect such mechanical effects in the most accurate way. In this sense, the dimensions of nanoscale structures, which are comparable to the distance between atoms that make up that material, have shown that the classical elasticity theory, which is currently widely used, is not sufficient in determining the mechanical behavior of such structures. Since the size effect is an important factor in nanoscale structures, defining a more general continuum model that includes such parameters increases the accuracy of the solution of the related problems.

In this thesis, the bending and buckling behavior of beams is investigated within the framework of the strain gradient theory. In determining the mechanical behavior of nanostructures, the non-local elasticity theory, the couple stress theory and the strain gradient theory, which are proposed by respectable scientists such as Eringen and Mindlin, are widely used. The calculation load of the problem may increase depending on the loading, boundary conditions and geometric properties of the analyzed structure. Thus, the Initial Values Method is used to solve the problem in the thesis. The transport matrix approach is used for the static bending analysis of the beam within the scope of Initial Values Method.

In the first part of the study, the bending behavior of the Euler-Bernoulli nano beam whose material properties change in two directions (bi-directional) is investigated. Therefore, it is assumed that the modulus of elasticity is variable along the axis and thickness of the beam. In the literature, the modulus of elasticity for a functionally graded material (FGM) is expressed in terms of arbitrary functions and the bending behavior is investigated for the first time within the scope of the gradient elasticity theory. In this context, the basic equations and boundary conditions (simply supported and fixed at both ends) are obtained with the help of Hamilton’s principle for the beam under uniformly distributed load. While 4 end conditions can be written depending on the boundary conditions in the classical elasticity approach, 6 end conditions are obtained by using the gradient elasticity theory. While each loading case is required for the solution of the 6th order differential equation in the classical solution, the vertical displacements for two different types of loading cases are calculated by

solving 3 linear equation systems based on 3 unknowns using the initial values method. As a result of the study, it was observed that the size effect decreased depending on the increase of nano beam length. In other words, the difference between local and non-local theory becomes important in small scales. However, it was observed that there is a lower vertical displacement in the bi-directional Euler-Bernoulli nano beam due to the increase in the inhomogeneous material constant (β). The accuracy and importance of the study for both boundary conditions are demonstrated with the help of graphics.

In the second part of the study, the buckling behavior of the Euler-Bernoulli nano beam (FGM) whose material properties change in two directions (bi-directional) is investigated. Basic equations and boundary conditions are derived with the help of Hamilton's principle. Since the transport matrix cannot be calculated analytically for buckling analysis, the approximate transport matrix (Matricant) is used in the solution. Critical buckling loads are calculated for the classical theory of elasticity and the gradient elasticity theory depending on the number of intervals. In the results of study; It is observed that the first two terms of the transport matrix reflect the exact result if the number of intervals is chosen large enough. Remarkably, it is concluded that the first and second type of boundary conditions in the buckling calculation may depend on the type of material used. The accuracy of such a proposition can only be demonstrated more clearly by experimental studies. In addition, it is observed that the buckling resistance of the beam increases depending on the increase in the material characteristic length (γ). The accuracy and scientific contribution of the study is expressed with the help of the diagrams.

The greatest contribution of the subject investigated herein to science is that it can guide the analysis and design of nanostructures used in many areas of technology. The importance of parameters such as the size effect and inhomogeneous material coefficient in the analysis of very small-scale structures has once again been demonstrated with strong propositions and results. Thus, it is supported by previous studies that theories such as the non-local elasticity theory and the gradient elasticity theory give more realistic results compare to the classical theory.

With the design of micro and nano electro-mechanical systems (MEMS and NEMS), which are frequently encountered in the electronic device industry, as functional graded materials, it has become more important to determine the mechanical properties of such small-scale structures. In this sense, it is aimed that the relevant thesis study and the international publications published by us will make significant contributions to the literature.

MALZEME ÖZELLİKLERİ İKİ DOĞRULTUDA DEĞİŞEN KİRİŞLERİN MEKANİK DAVRANIŞLARI

ÖZET

Günümüz teknolojisinin en çok gelişme gösteren alanlarından olan nanoteknoloji, mühendisliğin birçok alanına kolayca entegre edilebildiği için yaygın bir kullanım alanına sahiptir. Özellikle uzay ve havacılık sanayi, tıp, enerji ve inşaat mühendisliği gibi alanlarda çok küçük ölçeklerdeki fonksiyonel malzemelerin tasarımı ve üretimi, onların ilgili alanlarda efektif kullanımı mühendislik bilimine önemli katkılar sağlamaktadır.

Mühendislik yapılarında sıklıkla kullanılan bu tür malzemelerin çok küçük ölçeklerde olması onların iç yapısını ve mekanik özelliklerini tespit etme gereksinimini doğurmuştur. Malzemeler yükler altında eğilme, burulma ve burkulma gibi bazı mekanik davranışlar sergiler. Bunun gibi mekanik etkilerin en doğru biçimde tespit edilebilmesi yapı stabilitesi açısından önemli bir husustur. Bu manâda bilhassa nano ölçekteki yapıların boyutlarının o malzemeyi oluşturan atomlar arası mesafelerle kıyaslanabilecek ölçüde olması halihazırda yaygın olarak kullanılan klasik elastisite teorisinin bu tür yapıların mekanik davranışlarını belirlemede yeterli olmadığını göstermiştir. Nano ölçekteki yapılarda boyut etkisi önemli bir faktör olduğu için, içerisinde boyut parametrelerini de barındıran daha genel bir sürekli ortam modeli tanımlamak ilgili problemlerin çözümünün doğruluğunu artırmaktadır. Yirminci yüzyılın ortalarından itibaren yapılan çalışmalarda nano yapıların mekanik davranışlarının belirlenmesinde Eringen ve Mindlin gibi önemli bilim insanları tarafından önerilen yerel olmayan elastisite teorisi (non-local), gerilme çifti teorisi (couple stress theory) ve şekil değiştirme gradyanı teorisi (strain gradient theory) gibi teoriler ön plana çıkmaktadır. Eringen tarafından önerilen yerel olmayan elastisite teorisi -klasik teoriden farklı olarak- elaman içerisindeki bir noktaya ait gerilme durumunu ilgili noktaya komşu olan tüm noktaların bir fonksiyoneli olarak ifade edilebildiği zenginleştirilmiş yeni bir sürekli ortam modeli sunmaktadır. Oysa ki yerel teori bizlere belirli bir noktaya ait fiziksel tanımlamanın yalnızca o noktaya ait gerilmeler cinsinden ifade edilebildiğini önermekteydi. Şekil değiştirmenin hesaba katılmadığı bu yaklaşımın özellikle mikro ve nano ölçeklerdeki yapıların mekanik davranışlarını belirlemede yetersiz olduğu Eringen ve Edelen tarafından 1972 yılında yapılan öncül çalışmalarla ortaya konmuştur. Analiz edilen yapının yükleme durumu, sınır şartları ve geometrik özelliklerine bağlı olarak problemin hesap yükü artabilmektedir.

Bu tez çalışmasında nanomekanik alanında yapılan çalışmalarda yaygın olarak kullanılan Euler-Bernoulli kirişlerinin eğilme ve burkulma davranışları şekil değiştirme gradanı teorisi kapsamında araştırılmıştır. Bilindiği üzere genel anlamda nano yapıların modellenmesi ve analizi için Euler-Bernoulli kiriş modeli ve kesme etkisinin de hesaba katıldığı Timoshenko kiriş modeli gibi teoriler bulunmaktadır. Geçmiş çalışmalarda nano kirişlerin eğilme ve burkulma davranışlarının çözümü için birçok farklı yöntem kullanılmıştır. Bununla beraber kiriş üzerinde malzeme

özelliklerinin, eğilme rijitliğinin değişken olması ve/veya süreksizlik sayısının artması gibi durumlar problemin çözümünü zorlaştırmaktadır. Mustafa İnan tarafından 1964 yılında önerilen "Başlangıç Değerleri Yöntemi" birçok mekanik probleme uygulanabilmesi açısından önemli bir çözüm yöntemidir. Bu nedenle tez çalışmasında literatürde nano kirişlerin çözümünde de sıklıkla kullanılan başlangıç değerleri yönteminden faydalanılmıştır. Başlangıç değerleri yönteminde kirişin statik eğilme ve burkulma analizi için taşıma matrisi yaklaşımı kullanılmıştır.

İlk bölümde malzeme özellikleri iki doğrultuda değişen (bi-directional) Euler-Bernoulli nano kirişin eğilme davranışı araştırılmıştır. Buna binaen kirişin ekseni ve kalınlığı boyunca elastisite modülünün değişken olduğu kabul edilmiştir. Literatürde ilk defa fonskiyonel olarak derecelendirilmiş bir eleman için elastisite modülü keyfi fonskiyonlar cinsinden ifade edilerek eğilme davranışı gradyan elastisite teorisi kapsamında incelenmiştir. Şekil değiştirme gradyanı (Strain Gradient Theory) teorisinde toplam gerilmeye ek olarak Cauchy gerilmesi ve gerilme çifti de yazılmaktadır. Bu bağlamda temel denklemler ve sınır şartları (basit mesnetli ve iki ucu ankastre olarak) düzgün yayılı yük etkisi altındaki kiriş için Hamilton prensipi yardımıyla elde edilmiştir. Klasik elastisite yaklaşımında mevzu bahis menetlenme koşullarına bağlı olarak 4 adet uç koşulu yazılabilirken, gradyan elastisite teorisi kullanılarak 6 adet uç koşulu elde edilmiştir. Problemin daha sade bir forma indirgenmesi ve böylece çözümün kolaylaşması açısından bazı boyutsuz parametreler tanımlanmıştır. Klasik çözümde 6'ncı dereceden diferansiyel denklemin çözümü için her bir yükleme durumuna ihtiyaç duyulurken, başlangıç değerleri yöntemi kullanılarak 3 bilinmeyene bağlı olarak oluşturulan 3 lineer denklem sistemi çözülerek iki farklı tip sınır koşulu için düşey yer değiştirmeler hesaplanmıştır. Çalışma sonucunda nono kiriş uzunluğunun artmasına bağlı olarak boyut etkisinin küçüldüğü görülmüştür. Başka bir deyişle eleman boyutu küçüldükçe boyut etkisinin önemi artmaktadır. Bununla beraber homojen olmayan malzeme sabiti (β)'nin artışına bağlı olarak bi-directional Euler-Bernoulli nano kirişte daha düşük bir düşey yer değiştirme olduğu gözlenmiştir. Her iki sınır şartına bağlı olarak çalışmanın doğruluğu ve önemi grafikler yardımıyla ortaya konmuştur.

İkinci bölümünde ise yine malzeme özellikleri iki doğrultuda değişen (bi-directional) Euler-Bernoulli nano kirişin (FGM) burkulma davranışı araştırılmıştır. Yine bu çalışma ile FGM olarak üretilmiş Euler-Bernoulli kirişinin burkulma davranışı ilk kez gradyan elastisite teorisi kapsamında başlangıç değerleri yöntemi ile ele alınmıştır. Temel denklemler ve sınır koşulları Hamilton prensibi yardımıyla türetilmiştir. Burkulma hesabı için taşıma matrisi analitik olarak hesap edilemediğinden çözümde yaklaşık taşıma matrisi (Matricant) kullanılmıştır. Kritik burkulma yükleri klasik elastisite teorisi ve gradyan elastisite teorisi için farklı aralık sayısına bağlı olarak hesaplanmıştır. Problemin çözümünde hesap kolaylığı açısından boyutsuz parametreler tanımlanmıştır. Kritik burkulma yüklerinin hesabı için homojen lineer denklem sisteminde katsayılar matrisinin determinantı sıfıra eşitlenerek matrisin öz değerleri hesaplanmıştır.

Bu çalışmayla birlikte aralık sayısının yeterli genişlikte seçilmesi durumunda taşıma matrisine ait ilk iki terimin kesin sonucu büyük ölçüde yansıttığı görülmüştür. İkinci tip sınır koşulu için elde edilen kritik burkulma yüklerinin, birinci tip sınır şartı için hesaplanan kriitik burkulma yüklerinden her zaman daha küçük olduğu görülmüştür. Burkulma hesabı için kabul edilen birinci ve ikinci tip sınır şartlarının kullanılan malzemeye göre değişebileceği fikrine varılmıştır. Böyle bir önermenin doğruluğu ancak yapılacak deneysel çalışmalarla daha net bir şekilde ortaya konulabilir. Bununla

beraber malzeme karakteristik uzunluğu γ'nın artışına bağlı olarak kirişin burkulma direncinin de arttığı görülmüştür.

Çalışmanın doğruluğu ve bilimsel katkısı kullanılan diagramlar yardımıyla ifade edilmiştir.

Burada araştırılan konunun bilime en büyük katkısı teknolojinin birçok alanında kullanılan nano yapıların analizine ve tasarımına yön gösterebilecek nitelikte olmasıdır. Çok küçük ölçekteki yapıların analizinde boyut faktörünün ve homojen olmayan malzeme katsayısı gibi parametrelerin önemi yapılan çalışmayla bir kez daha kuvvetli önermeler ve sonuçlarla ortaya konmuştur. Böylece yerel olmayan elastisite torisi, gradyan elastisite teorisi vb. teorilerin klasik teoriye göre daha gerçekçi sonuçlar verdiği geçmiş çalışmalarla birlikte desteklenmiştir.

Ek olarak, özellikle elektronik aygıt sanayisinde sıklıkla karşımıza çıkan mikro ve nano elektro-mekanik sistemler (MEMS ve NEMS)'in fonskiyonel derecelendirilmiş malzemeler olarak dizayn edilmesi ile bu tür küçük çaptaki yapıların mekanik özelliklerinin belirlenmesi daha da önem kazanmıştır. MEMS ve NEMS gibi yapıların eğilme, burulma, burkulma, titreşim ve sıcaklık gibi etkilere bağlı olarak deformasyonu önemli bir fenomen olarak karşımıza çıkmaktadır. Geçmiş çalışmalar bilhassa bu gibi mekanik etkileri azaltmak ya da öneleyebilmenin ilgili elemanları kompozit ya da fonksiyonel derecelendirilmiş olarak dizayn etmek ile mümkün olduğunu göstermiştir.

Bu bağlamda ilgili tez çalışmasının ve bu kapsamda üretilen uluslararası yayınların litüratüre önemli katkılar sunması amaçlanmıştır.

1. INTRODUCTION

Have you ever thought about the meaning of "small"? In the literature B.C, the concept of small was scientifically put forward by Democritus with the word "Atomus", which means indivisible. It is very clear that over the centuries no civilization and / or person could predict that this magic word could actually be the smallest building block of everything observed. In fact, how small a substance is can only be interpreted by the dimensional accuracy of the instrument observing it.

Although there were many attempts in the name of scientific work in the past, it is known that the scientific study in the real sense started with the Italian scientist Galileo Galilei. Due to the necessity of science to be dependent on experimentation and observation, studies conducted before the relevant period are called "occupation" in the history of science literature.

Looking at the recent history, the beginning of nanotechnology, which is also one of the fields of study of this thesis, is regarded as "There is plenty of room at the bottom", that magnificent sentence that Nobel Prize-winning physicist Richard P. Feynman said at a meeting held in CalTech in 1959.

Since the beginning of the 19th century, the necessity of deriving field equations was revealed with the studies of scientists such as Claude Navier and Augustin Cauchy on linear elastic materials. The idea of linear elasticity was first put forward by the British scientist Robert Hooke in 1660. He stated that the deformation of many materials under loads is proportional to the applied load. Despite this proposition he made, he could not express this concept in terms of stress and strain. The Swiss mathematician Jacob Bernoulli in 1705, in his last article published, showed that the most correct way to describe deformation is to define stress as a function of force per unit area or elongation per unit. In 1727, the Swiss scientist Leonhard Euler, who was also a student of Johann Bernoulli, proposed the linear relationship in the equation $\sigma = E \cdot \varepsilon$ including the E coefficient. Due to Thomas Young's similar studies in 1807, this coefficient was later called the Young's module.

The classical elasticity theory, which is widely used in solving mechanical problems, is not sufficient to describe the mechanical behavior of very small scale materials. In this context, Cosserat (1909) presented an important source for modeling elastic and inelastic homogeneous deformations with his book titled “Theory of deformable boddies."

In the 20th century, methods such as the non-local elasticity theory (Eringen, 1972), the strain gradient theory (Mindlin, 1960), and the couple stress theory (Mindlin and Tiersten,1962) were developed in order to express the size effect at nanoscale structures in the most accurate way.

Today, nanotechnology is one of the fields of engineering for many more such as aviation and space industry, energy, medicine, construction, electronics, and biotechnology. In this context, there are many important studies in the literature. In addition to the theoretical studies, the fact that such structures can be tested experimentally is a scientifically important achievement.

1.1 Purpose of Thesis

The classical elasticity theory, which is widely used in solving mechanical problems, is insufficient in determining the mechanical behavior of structures such as bending, buckling and vibration, especially of nanoscale structures. Because of this requirement, approaches such as gradient elasticity theory, non-local elasticity theory and couple stress theory have been put forward by scientists such as Eringen and Mindlin.

In this thesis, the bending and buckling behaviors of nano beams, which are frequently used in many areas of engineering today, are investigated within the framework of the strain gradient theory. Although there are many studies in the literature to determine the mechanical behavior of nano beams, the bending and buckling behaviors of nano beams whose material properties change in two directions (bi-directional) are investigated for the first time using the Initial Values Method within the framework of “Strain Gradient Elasticity Theory.”

Transport matrix is expressed analytically for the bending behavior of nano beams. As is known, the transport matrix is unique for the initial values problems.

The bending and buckling behavior of nano beams are investigated within the scope of this thesis.

i) Basic equations and boundary conditions are obtained with the help of Hamilton's principle, and the effect of the size effect and characteristic length on the bending behavior for different end conditions is presented with graphs.

ii) For the buckling behavior of nano beams, Matricant, also known as the approximate transport matrix, is used since the transport matrix could not be obtained analytically. This method is one of the methods used to analyze the buckling behavior of functionally graded materials (FGMs). Basic equations and boundary conditions are obtained with the help of Hamilton's principle. Critical buckling loads are presented with the help of graphs depending on different dimensional ($\bar{\gamma}, \beta$) parameters.

The greatest contribution of the scientific study conducted in this thesis to the literature is the determination of the mechanical properties of nanostructures used in many areas of technology. Thus, the information required for the design and production of such structures can be used.

2. NANOTECHNOLOGY

Nanotechnology is a branch of science that includes engineering and technology studies carried out in sizes ranging from 1 to 100 nanometers. The idea and concept of nanoscience and nanotechnology was brought up by physicist Richard Feynman in his speech titled "There is Plenty of Room at the Bottom" at the American Physical Society meeting held at the California Institute of Technology (CalTech) in 1959, long before the term nanotechnology was introduced. It is not only the size that distinguishes nanoparticles from large materials. These particles also appear as a different structure from large materials in terms of physical, chemical and biological properties (Solmaz, 2017). There are two different issues on the basis of nanotechnological studies. The first is that atoms can be moved as desired and also their order can be changed as required (Solmaz, 2017; Toksöz, 2010). When the atomic structures of materials are observed, many different properties belonging to them come in sight. Second, when the atomic structure is descended, the classical physics rules begin to lose their validity and the effects stem from atomic dimensions begin to show themselves in the problem under investigation.

Nanotechnology or nanoscience is a science that has increased its popularity today with the increasing use of quantum properties and atomic metrics. This science which combines physics, chemistry and biology and associates it with engineering branches such as mechanics, electronics, industry, and space, uses functional materials that are reduced to nano-dimensions at the atomic and molecular level and uses them for the production and development of devices or systems (Erkoç, 2007). In recent decades, with the development of nanotechnology and softwares in this field, important technological developments have been achieved in many other important fields such as defense industry, space aviation and medicine.

The properties of matter at nanoscale are different from that on a larger scale. The main reason of this is the effect that occurs in the quantum dimension. As the dimensions of a material decrease, its properties initially remain the same, however, in time small changes in material properties are observed. When the material size is less than 100 nm, its properties change dramatically. These properties can differ

significantly from the properties of bulky materials and single atoms or molecules (Clayton, 2018).

Materials at nanoscale show different properties for two main reasons:

i) First, nanomaterials have greater surface area when compared to material produced in larger form with the same mass of material. Since most atoms are located on the surface, as the size of a particle decreases, the ratio of atoms on the surface to the atoms in the particle increases. For example, there are 5% of all atoms on the surface of a 30 nm particle, 20% of all atoms on the surface of a 10 nm particle, 50% of all atoms on the surface of a 3 nm particle, and almost all of the atoms on the surface of a 1 nm particle (Taourirte et al., 2016). Increasing the surface area makes materials more chemically reactive (in some cases, materials that do not react in their larger form become reactive when produced in nanoscale form) and may affect their strength and / or electrical properties.

ii) The second reason is that quantum effects can affect the optical, electrical and magnetic behavior of the material effectively on the behavior of matter at the nanoscale. For example; opaque materials can become transparent (copper), chemically non-reactive materials can become catalysts (platinum), stable materials can become flammable (aluminum), solids can turn into liquids at ambient temperature (gold), insulators can become conductive (silicon) (Güçlü, 2020). With the quantum effects on the nanoscale and the increase in surface area, researchers have enabled the production of many different materials by taking advantage of these new properties that materials have acquired (Berger, 2016).

The emergence of nano-scale structures and developments in nanotechnology; Its mechanical, electrical, chemical and biological properties have enabled the production of new generation materials, devices and equipment that are far superior to those produced by conventional methods (Ansari and Sahmani, 2011). Nanotechnology has become a rich field of study due to the contributions of physicists, chemists, engineers, manufacturing technology workers, biologists and medical professionals (Chakraverty and Behera, 2016).

An indication that nanotechnology is actively studied and used by different disciplines around the world is the amount of investments made in nanotechnology. For example, between 2001-2015, United States of America (USA) Congress allocated approximately 20 billion US dollars to research and development in nanotechnology. It is seen that there is an enormous return on income compared to the investments made with the revenues obtained. In 2012, the revenue generated from nano products in the USA alone was 200 billion US dollars, while the whole figure was 700 billion US dollars in the world (The National Nanotechnology Initiative, 2015). In 2014, the European Union launched the Horizon 2020 Research and Innovation Framework Program with a budget of 77 billion Euros. Six main research areas have been determined in the Horizon 2020 program. These areas are nanotechnology, advanced manufacturing, advanced materials, nanoelectronics, photonics and biotechnology. A total budget of 6.6 billion Euros was allocated for these areas (de Oliveira et al.,2017).

Nanotechnology is considered as the fastest growing technology of the current decade (Mangematin and Walsh, 2012). The main reason behind this exponential growth is the invention of devices such as scanning tunneling microscopy (STM) and electron microscopy, allowing scientists to research at the nanoscale level in matter, and then synthesize, characterize and use nanoscale materials (Rao and Cheetham, 2001). Researchers and industrialists believe that smart nanomaterials have an important potential that can be adapted to almost every area of modern life. Nano structures play a very important role in modern world technology due to their economic potential, optimized product development capability and most importantly the possibility of reducing the pressure on natural resources and the environment (Bhagyaraj and Oluwafemi, 2018).

In the future, it is predicted that nanotechnology will lead to applications that provide more added-value, it will enable the production of new diagnostic devices, and will lead to the emergence of new sectors such as nanoenergy, nanofood, nanotechnology, nanomedicine, nanobiotechnology and nanoelectronics (Lee and Song, 2007; Allarakhia and Walsh, 2011). In addition, by helping other technologies that can bring solutions to industrial problems, scientific fields such as biotechnology, physics, computer science, psychology will be able to advance faster than ever before. Moreover, nano technology will provide sustainability in many areas of our lives (Loveridge et al., 2008).

2.1 Application Fields of Nanotechnology

Nano sized materials are presented to the market after being designed in an innovative way thanks to the advantage of being functional and useful. The qualities of these products have shown the variety of uses of nanotechnology and how widely they can be used (Allhoff et al., 2007).

Computer technologies, another of the fields where nanotechnology is used, are developing rapidly as a result of the production of nano-scale electronic circuit components. The systems used in electronic devices become more useful and effective by increasing their processing power thanks to their nano structures (Demirkan,2020).

Quantum computers come to the forefront as another innovation that nanotechnology has shown its effect on. In addition, thanks to nanotechnology, great advances were made in industries such as sensors, every product that can transmit signals and navigation display systems (Toksöz, 2010).

Nano materials are used as many tools in the field of medicine and health in the diagnosis and treatment process. These tools, with their correct results, allow not only to affect the diseased area but also to produce more sensitive measurement devices and to integrate them in harmony with foreign tissues.

Products made of nano structures in aviation and space fields have an important place in the construction of space and rocket stations because they are more durable and resistant to temperature changes. Nano-structures are also very light materials and this feature makes them important to construct engineering elements. Examples of applications on this subject are: The production of computers that require less energy, more resistant to radiation, and high efficiency, nano-sized instruments that can be used in micro-sized spacecraft, nano-material sensors and flight mechanisms provided with nano-electronics, heat-resistant nano-structured coating materials.

Today, one of the most prominent sectors is the energy industry. For example, nanomaterials increase efficiency in fossil fuels and enable transportation and production sectors to work properly (Toksöz, 2010). There are also some application areas such as storage and production of energy in nanotechnology to use energy effectively. With the hydrogen storage method, cars that operate with the help of hydrogen energy will be developed, and environmentally friendly fuel consumption will be achieved. Moreover, with the development of nano filters regarding water

consumption, which is one of the fundamental problems of humanity, clean water will be obtained (Ersöz, Işıtan, and Balaban, 2018).

2.2 Nanomaterials

2.2.1 Graphenes

Graphene is the name given to a single-atom-thick full planar layer in which sp2-form bonded carbon atoms are densely arranged to form a honeycomb crystal lattice. Graphene is also a crystalline allotrope of carbon. Graphene, which is harder than diamond but more elastic than rubber, as well as more durable than steel but lighter than aluminum, is the strongest material known (Ovid'ko, 2013). This method is based on the use of a piece of tape made to remove graphite flakes from a highly regular pyrolytic graphite sheet, which is then deposited on a silica tape. The flakes are then exfoliated using more adhesive tape and finally applied to other silica slides until they have a graphite layer at an atomic thickness, while viz.graphene is left immobilized and is kept in a rest position on the slide. With this breakthrough, which allows graphene to be easily isolated, it has not only shown a remarkable high load-bearing mobility of 2000-5000 cm2 / Vs, but also allowed its unique properties to be measured (Novoselov et al., 2005).

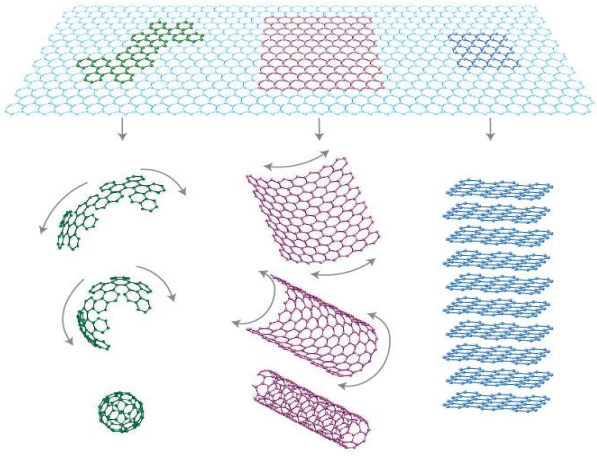

Figure 2.1 : Graphene and related structures: fullerene carbon nanotube and graphene structures (Geim and Novoselov, 2007).

In fact, this was not the first time that ultra-thin carbon films were observed. Before 2005, there were some reports that graphene was observed but its unique properties have yet to be determined (Brownson et al., 2012; Geim, 2012; Wallace, 1947). For

example, graphite oxide was independently synthesized in 1859 by Brodie (Brodie,1859), Hummers in the late 1950s, and Staudenmaier (Staudenmaier, 1898) in 1898.

Geim and Novoselov were awarded the Nobel Prize in physics in 2010 for their pioneering work on two-dimensional atomic crystals (T.N. Foundation, 2013). For some researchers since the aforesaid study, the focus has been to explore the large-scale synthesis of graphene, while for others, manipulating the structure so that its properties can be utilized. The adhesive tape method has become a problem for the production of graphene only because it can isolate both small amounts of graphene and is a laborious process (Randviir et al., 2014).

Some important fields of usage of graphene:

- High-speed electronics
- Data storage
- LCD smart windows and OLED displays
- Supercapacitors
- Solar cells
- Electrochemical sensing

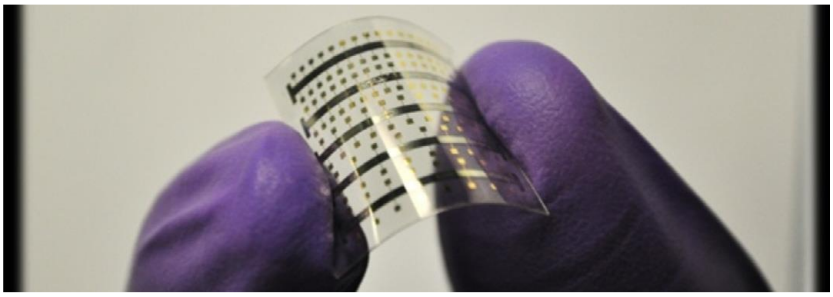

Figure 2.2 : Ultra-thin flexible graphene transistor (Mattevi et al., 2012).

Graphene; It is a material with impressive properties such as hardness, strength and toughness. In addition, graphene can be used both as a material itself and also to reinforce composites. The modulus of elasticity of graphene calculated from both experimental studies and simulations is almost the same, and it was calculated as 1.0 ± 0.1 TPa for single layer graphene. Single layer graphenes without defects are the strongest material tested thus far. Tensile strength of graphene is 130 GPa. Fracture toughness, a property related to engineering applications, is one of the most important

mechanical properties of graphene and has a critical stress density factor of 4.0 ± 0.6 MPa (Papageorgiou ve diğ, 2017).

2.2.2 Carbon nanotubes (CNTs)

CNTs are cylindrical molecules obtained by bending graphene. They can be single or double layered. The lengths of these tubes can reach several micrometers and / or millimeters (Aqel et al., 2012). Like the building block graphenes, CNTs are chemically bound in the form of sp^2, which is a very strong form of molecular interaction. In addition to this feature, CNTs offer the opportunity to develop ultra-high strength, low-weight materials with high electrical and thermal conductivity properties, as they naturally tend to join each other in the form of rope through van der Waals forces.

Carbon nanotubes discovered by Iijima in 1991 have a wide range of applications in structures such as bio sensors, actuators, bulletproof vests, and high performance composites, and many more.

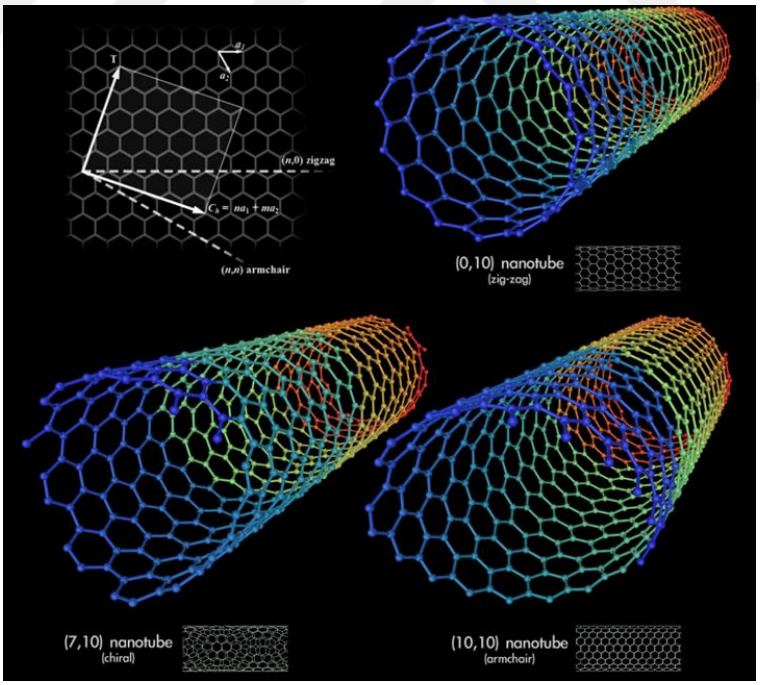

Figure 2.3 : SWNT and MWNT (URL-1).

Carbon nanotubes can be obtained by several different methods. One of them is the arc evaporation method. The arc evaporation method is carried out by applying electric current between two electrodes in the atmosphere where helium and argon are present. In this method applied with electrodes consisting of two graphene rods, the intensity

of the current applied is 50-100 amperes. Some of the carbon evaporating from the anode is re-evaporated cylindrically at the cathode. Nanotubes and nanoparticles are formed in the center of this cylindrical sediment (Yükseltürk, 2008).

In the laser evaporation method, single-walled carbon nanotubes are obtained by evaporating carbon. The first efficient single-walled carbon nanotube production was carried out using this method. This method is disadvantageous compared to other methods in that it is high cost and requires high temperature for its application (Yükseltürk, 2008).

In another method, chemical evaporation, a substrate containing magnetic metals such as iron, nickel or cobalt is prepared. These materials act as catalysts in the process. The prepared substrate is heated to a temperature of 700 °C. In order to start the nanotube formation, ammonia, nitrogen, one of hydrogen gases and carbon containing gases such as acetylene, ethylene, ethanol, methane are introduced into the reactor. These gases ruptured at the surface of the catalyst and stick to the catalyst. Consequently, nanotube formation occurs around the metal catalyst (Yükseltürk, 2008).

2.2.2.1 Mechanical properties of the CNTs

Although carbon nanotubes are very light, their elastic modulus are quite high compared to other building materials. Carbon nanotubes can withstand a weight of 300 million times their weight, yet they are many times stronger than steel (Çıracı, 2005). The tensile strength of single-walled small-scale CNTs was determined as $45x10^3$ MPa (Erkoç, 2001). The first experimental review of the modulus of elasticity of MWCNTs was conducted by Treacy et al. (1996). Using the thermal vibration method, the modulus of elasticity of the carbon nanotubes was measured in the range of 0.40-4.15 TPa. Krishnan et al. (1997) also determined that the elastic modulus of SWCNTs is in the range of 0.9-1.9 TPa.

3. INITIAL VALUES METHOD AND TRANSPORT MATRIX

While calculating the elastic curves of the bearing elements, the solution is made by applying the differential or integration method. However, it is necessary to divide the element into regions due to discontinuities such as concentrated moment, singular load, and hinge. The number of regions will increase depending on the number of discontinuities. When calculating with the integration method, it is necessary to calculate the integral constant for each region and the amount of integral constant to be calculated increases with the increase in the number of regions. Boundary conditions on the bearing element are used to determine the aforementioned integration constants. Since the solution of integration constants is not easy due to its computational load, different types of solutions are investigated in such cases to minimize the number of unknowns (Demirkan and Artan, 2019).

Initial values method, which is a method to simplify the solution, is used in the solution of such problems. This solution method is suitable for solving univariate systems (Tepe, 2007).

Let us investigate a system whose coordinate systems are;

$$S_1, S_2, S_3, ..., S_{n-1}, S_n \tag{3.1}$$

If we assume that these coordinates change due to a free variable of z, the coordinates of the system are expressed as S_i (z). In some problems, this parameter can also represent the location or time in a one-dimensional continuum.

S_i (z) can be written as a vector coordinate according to the type of problem as follows

$$S(z) = \begin{bmatrix} S_1(z) \\ S_2(z) \\ \vdots \\ S_n(z) \end{bmatrix} \tag{3.2}$$

This vector is called the state vector. In order to express the vector $S(z)$, the derivatives of $S_i(z)$ functions are calculated. If we assume that all elements belonging to the vector $S(z)$ have first derivatives, the derivative of the state vector can be written as follows;

$$S'(z) = \begin{bmatrix} S_1'(z) \\ S_2'(z) \\ \vdots \\ S_n'(z) \end{bmatrix} \tag{3.3}$$

In order to describe how the transition from the state of the parameters in z to the state at $z + dz$ will be, it is necessary to explain the system in canonical form showing the relations between the vectors $S'(z)$ and $S(z)$. Assuming that these relations consist of n linear equations, the linear differential equations of the system are written as;

$$S_1'(z) = d_{11} \cdot S_1(z) + d_{12} \cdot S_2(z) + \ldots\ldots + d_{1n} \cdot S_n(z) \tag{3.4}$$

$$\begin{matrix} S_2'(z) = d_{21} \cdot S_1(z) + d_{22} \cdot S_2(z) + \ldots\ldots + d_{2n} \cdot S_n(z) \\ \vdots \end{matrix} \tag{3.5}$$

$$S_n'(z) = d_{n1} \cdot S_1(z) + d_{n2} \cdot S_2(z) + \ldots\ldots + d_{nn} \cdot S_n(z) \tag{3.6}$$

These equations are of great importance as they express the conformity between the state coordinates, the balance of the system and the position of the object in many cases. The coefficients d_{ik} in linear equations is independent of the $S_i(z)$ parameter, however they can depend on the z parameter.

If linear equations are written more regularly:

$$S_n'(z) = D \cdot S(z) \tag{3.7}$$

If D is expressed as a matrix,

$$D = \begin{bmatrix} d_{11} & d_{12} & d_{13} & \ldots & d_{1n} \\ d_{21} & d_{22} & d_{23} & \ldots & d_{2n} \\ d_{31} & d_{32} & d_{33} & \ldots & d_{3n} \\ \vdots & \vdots & \vdots & \cdots & \vdots \\ d_{n1} & d_{n2} & d_{n3} & \cdots & d_{nn} \end{bmatrix} \tag{3.8}$$

Matrix *D* is called as "**differential transition matrix**". The relationship between *z* and *z* + *dz*, which are close to each other by the definition of the linear differential equation derivative in equation (3.8), is expressed as follows.

$$S(z+dz) = S(z) + \left[D \cdot S(z)\right] dz \tag{3.9}$$

Provided that the *z* parameter starts from a certain value for instance, when *z* = 0; the obtained value of *z* can be calculated by making a large number of partial differential transitions in infinitesimal steps. In fact, the finite value of the *z* parameter can be calculated with a single integral using the initial condition *z* = 0 instead of the piecewise transition. The matrix that makes this transition possible with a single step is called the "**Transport Matrix**".

The transport matrix, which can be used in many areas of mechanics, is used by researchers in the past studies to examine the mechanical behavior of nanostructures with the development of calculation methods (Celik and Artan, 2020). First proposed by Holzer Van Dungen in 1856, the transport matrix was introduced by Mustafa Inan under the name of "Initial Values Method" in the following century (Inan, 1964). Nam and Lee (2000) investigated the problem of cylindrical tanks placed on elastic ground using the transport matrix method in their studies. Lin (2004) examined of simply supported beams with open cracks using the transfer matrix method in his study.

Thanks to the transport matrix method it is predicted that the solution of any differential equation system can be solved easily. However, with the increase in the number of variables in the equations written in matrix form, the solution of the problem getting difficult. In such cases, the approximate transport matrix method (Matricant) is used (Celik and Artan, 2020).

The transport matrix is calculated with the help of the equation given below;

$$S(z) = F(z) \cdot S(0) \tag{3.10}$$

Where *S*(*0*) indicates the state of the system at an initial position. The state vector:

$$S(0) = \begin{bmatrix} S_1(0) \\ S_2(0) \\ \vdots \\ S_n(0) \end{bmatrix} \tag{3.11}$$

And the transform matrix $F(z)$ can be written as,

$$F(z)=\begin{bmatrix} f_{11}(z) & f_{12}(z) & \cdots & f_{1n}(z) \\ f_{21}(z) & f_{22}(z) & \cdots & f_{2n}(z) \\ \vdots & \vdots & \cdots & \vdots \\ f_{n1}(z) & f_{n2}(z) & \cdots & f_{nn}(z) \end{bmatrix} \tag{3.12}$$

As seen in matrix above the $F(z)$ transport matrix consists of n^2 number of f_{ik} elements. The expression given in (3.10) is a homogeneous equation. That is, the system is unloaded. Herein, $F(z)$ expresses the integral character of the system, while $D(z)$ expresses the differential character of the system. If it is to explain how the $F(z)$ matrix is derived from the $D(z)$ matrix;

Darivation of the both sides of the equation (3.10),

$$S'(z)=F'(z)\cdot S(0) \tag{3.13}$$

And with the help of the eqn. (3.7),

$$D\cdot S(z)=F'(z)\cdot S(0) \tag{3.14}$$

If the equation (3.10) substitute into the eqn (3.14), then,

$$D\left[F(z)\cdot S(0)\right]=F'(z)\cdot S(0) \tag{3.15}$$

The arranged form of the expression (3.15) can be written as follows:

$$\left[D\cdot F(z)-F'(z)\cdot S(0)\right]=0 \tag{3.16}$$

Also $S(0)\neq 0$ and the column matrix is,

$$F'(z)=D\cdot F(z) \tag{3.17}$$

$F(z)$ and $S(z)$ satisfy the same type of differential equations. If all the elements that construct the D matrix are constant values, the solution of the differential equation becomes very easy.

$$F(z)=F(0)\cdot e^{z\cdot D}=e^{z\cdot D} \tag{3.18}$$

This equation transforms into an exponential matrix form as above. The value of $F(0)$ in the expression (3.18) represents the situation at $z = 0$ and is called the identity matrix.

$$F(0) = I = \begin{bmatrix} 1 & 0 & \cdots & 0 \\ 0 & 1 & \cdots & 0 \\ \vdots & \vdots & \vdots & \vdots \\ 0 & 0 & \cdots & 1 \end{bmatrix} \tag{3.19}$$

If the expression of $e^{z \cdot D}$ described as a matrix polynomial,

$$F(z) = e^{z \cdot D} = I + z \cdot D + \frac{z^2}{2!} \cdot D^2 + \frac{z^3}{3!} \cdot D^3 + \cdots + \frac{z^k}{k!} \cdot D^k + \cdots \tag{3.20}$$

The $F(z)$ transport matrix is solved using the Cayley-Hamilton equation. The point to be noted here is that the coefficients of matrices consist of scalar quantities.

When the rod/beam is loaded, the transition expression is not same with the eqn (3.10). In some cases, there may be discontinuities due to external loads at a location such as $z = \xi$. Situations with such transitions are called non-homogeneous conditions. If the calculation for transition is written for $z \geq \xi$;

$$S(z) = F(z) \cdot S(0) + F(z - \xi) \cdot K(\xi) \tag{3.21}$$

For $z < \xi$, the equation (1) is valid. If $z = \xi$, it means that there is discontinuity in the state vector. Where $K(\xi)$ indicates the discontinuity matrix. This means that,

$$S(z) = F(z) \cdot S(0), \qquad \text{if} \quad z < \xi \tag{3.22}$$

$$S(z) = F(z) \cdot S(0) + F(z - \xi) \cdot K(\xi), \qquad \text{if} \quad z \geq \xi \tag{3.23}$$

In case of discontinuity at more than one point:

$$S(z) = F(z) \cdot S(0) + \sum_{i=1}^{n} F(z - \xi) \cdot K(\xi), \quad (\xi_1, \xi_2, \xi_3 \cdots, \xi_m < x) \tag{3.24}$$

In this case, it means that the discontinuity in the state vector exists at m different points. If the external effects are distributed loads, the integral is written instead of the finite sum in the above equation.

$$S(z) = F(z) \cdot S(0) + \int_0^z F(z-\xi) \cdot K(\xi) \cdot d(\xi) \tag{3.25}$$

Where $k(\xi)$ is,

$$k(\xi) = \begin{bmatrix} k_1(\xi) \\ k_2(\xi) \\ \vdots \\ k_{n1}(\xi) \end{bmatrix} \tag{3.26}$$

3.1 Cayley-Hamilton Equation

Assume that ***A*** is an arbitrary square matrix and size of *nxn*. The characteristic polynomial of this matrix can be expressed for eigenvalues $\lambda_1, \lambda_2, \lambda_3 \ldots, \lambda_n$ as follows,

$$p(\lambda) = \det(\lambda I - A) = \lambda^n + a_{n-1} \cdot \lambda^{n-1} + \cdots\cdots + a_1 \cdot \lambda + a_0 \tag{3.27}$$

The Cayley-Hamilton theorem states that each square matrix satisfies its own characteristic equation. According to this definition, matrix ***A*** satisfy the Cayley-Hamilton equation. Hence, by replacing the eigenvector (λ) in the above equation with ***A***, the matrix polynomial *p* (*A*) becomes equal to zero.

$$p(A) = A^n + a_{n-1} \cdot A^{n-1} + \cdots\cdots + a_1 \cdot A + a_0 \cdot I = 0 \tag{3.28}$$

3.1.1 Calculation of exponential function $e^{A \cdot t}$

The exponantiıal function $e^{A \cdot t}$ can be calculated as follows:

$$e^{At} = \sum_{k=0}^{n-1} \alpha_k \cdot A^k \tag{3.29}$$

Where α_k values are found by solving the systems of equations created by the eigenvalues of ***A***. These eigenvalues (λ_i) are expressed in the exponential matrix as follows;

$$e^{\lambda_i t} = \sum_{k=0}^{n-1} \alpha_k \cdot \lambda_i^{\,k} \tag{3.30}$$

3.1.2 Example: Calculation of *Sin(Az)* for a square matrix

Let ***A*** square matrix is given as,

$$A = \begin{bmatrix} 3 & 2 \\ 2 & 0 \end{bmatrix} \tag{3.31}$$

Characteristic equation of the matrix ***A*** is,

$$p(\lambda) = \det(\lambda I - A) = 0 \tag{3.32}$$

$$\begin{vmatrix} \lambda - 3 & -2 \\ -2 & \lambda \end{vmatrix} = 0 \tag{3.33}$$

In order to determine eigenvalues λ_1 and λ_2, we must solve second order polynomial.

$$\lambda^2 - 3\lambda - 4 = 0 \tag{3.34}$$

The eigenvalues of the above equations are obtained as; $\lambda_1 = 4, \quad \lambda_1 = -1$. Then,

$$\mathrm{Sin}(At) = a_0 \cdot I + a_1 \cdot A \tag{3.35}$$

$$\mathrm{Sin}(\lambda t) = a_0 + a_1 \cdot \lambda \tag{3.36}$$

For $\lambda_1 = 4$,

$$\mathrm{Sin}(4t) = a_0 + 4a_1 \tag{3.37}$$

For $\lambda_2 = -1$,

$$\mathrm{Sin}(-t) = -\mathrm{Sin}(t) = a_0 - a_1 \tag{3.38}$$

If the above two equations are solved together, the coefficients are found as;

$$a_1 = \frac{\mathrm{Sin}(z) + \mathrm{Sin}(4z)}{5} \tag{3.39}$$

$$a_0 = \frac{\mathrm{Sin}(4z) - 4 \cdot \mathrm{Sin}(z)}{5} \tag{3.40}$$

The Transform Matrix, $\mathrm{Sin}(Az) = a_0 \cdot I + a_1 \cdot A$

And let us substitute the real values of the coefficients a_0 and a_1 into the transfer matrix, we obtain,

$$\mathrm{Sin}(Az) = \left(\frac{\mathrm{Sin}(4z) - 4 \cdot \mathrm{Sin}(z)}{5}\right) \cdot \begin{bmatrix} 1 & 0 \\ 0 & 5 \end{bmatrix} + \left(\frac{\mathrm{Sin}(z) + \mathrm{Sin}(4z)}{5}\right) \cdot \begin{bmatrix} 3 & 2 \\ 2 & 0 \end{bmatrix} \qquad (3.41)$$

Simplified form of the Transform Matrix is found as:

$$\mathrm{Sin}(Az) = \begin{bmatrix} \frac{4\mathrm{Sin}(4z)}{5} - \frac{\mathrm{Sin}(z)}{5} & \frac{2\mathrm{Sin}(z)}{5} + \frac{2\mathrm{Sin}(4z)}{5} \\ \frac{2\mathrm{Sin}(z)}{5} + \frac{2\mathrm{Sin}(4z)}{5} & \frac{\mathrm{Sin}(4z)}{5} - \frac{4\mathrm{Sin}(z)}{5} \end{bmatrix} \qquad (3.42)$$

4. NON-LOCAL ELASTICITY

4.1 Eringen's Non-Local Elasticity

Nonlocal elasticity theory is an important issue in engineering mechanics problems and has an important place in cases where local elasticity theory is insufficient. In the classical elasticity theory, while calculating the stress at a point, the stress and strain of other points adjacent to that point are not taken into account. Since the classical elasticity theory was not suitable for the analysis of nano-sized elements, scientists were manipulated to another theory and the scope of the non-local elasticity theory was first presented to the scientific world by Eringen (1983).

The most realistic approach for these circumstances is to express the mechanical behaviour of micro-sized structures by defining the stress at a point as a function of all adjacent points. When objects are displaced, geometric discontinuity caused by these displacements create stresses in the body. The calculation of these stresses arising from displacements within the framework of classical elasticity theory shows some irregularities. For instance, when some objects deformed, both the stresses and the deformation energies that occur in the object go to infinity. The nonlocal elasticity theory is a very important method for dealing with such problems (Artan, 1992). When the distance between the stresses occurring in the internal structure of the body is in atomic dimensions, it is appropriate to calculate the stresses within the framework of classical elasticity theory (Tepe, 2007).

Mercan and Civalek (2017) examined the stability analysis of silicon carbide nanotube by taking into account the surface effect. Peddieson et al. (2003) have extended the Euler-Bernoulli beam model and presented some closed form solutions based on boundary conditions.

Demirkan and Artan (2020) investigated the buckling problem of non-local Timoshenko rods within the framework of nonlocal elasticity theory using the method of initial values. Gurtin (1965) made preliminary work on non-local continuum mechanics.

Körner (1968) made an evaluation of the non-local theory according to other theories in his study on the mechanics of continuum theory.

Edelen (1969) has published articles and books on the basics of calculus of variation in non-local theory.

Eringen (1972) obtained constitutive equations of non-local elasticity for non-local elastic media.

Eringen and Edelen (1972) carried out a series of studies on the derivation of constitutive equations for elastic media by both mechanical and variational method.

Eringen (1973) obtained constitutive equations for nonlocal microfluidics.

Mawphlang et al. (2020) investigated the buckling behavior of a non-uniform single-wall carbon nanotube using the non-local elasticity theory. They analyzed the buckling loads for different boundary conditions using the differential transformation method. Norouzzadeha, Ansaria and Rouhi (2018) tackled the buckling, bending and wave propagation problems of nano-beams made of FGM materials analytically with the integral formulation of the non-local elasticity theory of Eringen.

Nonlocal Cauchy equation of motion in a homogeneous and isotropic material:

$$\partial_j \cdot \sigma_{ij} + \rho \cdot \left[f_i - \frac{\partial^2 u_i}{\partial t^2} \right] \tag{4.1}$$

Constitutive equation is defined as follows,

$$\sigma_{ij}(z) = \int_v \alpha\left(|z' - z|\right) \cdot \tau_{ij}(z')\, dv(z') \tag{4.2}$$

Where σ_{ij} , τ_{ij} are indicate non-local stress tensor and local stress tensor, respectively. In equation (4.2), it is shown that the stress in the material at any *z* point depends on the deformations of the material at z' points.

$$\tau_{ij}(z') = \lambda \cdot \varepsilon_{\min}(z')\,\delta_{ij} + 2 \cdot \mu \cdot \varepsilon_{ij}(z') \tag{4.3}$$

$$\varepsilon_{ij}(z') = \frac{1}{2} \cdot \left[\frac{\partial u_i(z')}{\partial z'_j} + \frac{\partial u_j(z')}{\partial z'_i} \right] \tag{4.4}$$

$$\tau_{ij}(z') = C_{ijkl} \cdot \varepsilon_{kl}(z') \tag{4.5}$$

Where λ and μ are the Lame constants, *C* is the elastic modulus tensor, and ε_{kl} is the local strain tensor.

$$L \cdot \alpha\left(|z' - z|\right) = \delta \cdot \left(|z' - z|\right) \tag{4.6}$$

Nonlocal relation in the equation is as follows:

$$L \cdot \sigma_{ij} = \tau_{ij} \tag{4.7}$$

Considering the partial differential relation given in the equation (4.1),

$$\partial_j \cdot \tau_{ij} + L \cdot \left(\rho \cdot f_i - \rho \cdot \frac{\partial^2 u_i}{\partial t^2} \right) = 0 \tag{4.8}$$

Eringen proposed a non-local method for the above differential relation expressed as follows;

$$L = 1 - \left(e_0 \cdot a\right)^2 \cdot \nabla^2 \tag{4.9}$$

Where strain $\varepsilon = e_0 \cdot a$, ∇^2 indicates Laplace operator, *a* is the distance between the atoms, and e_0 is material constant.

The strain tensor ε_{kl},

$$\varepsilon_{kl} = \frac{1}{2}\left(u_{k,l} + u_{l,k}\right) \tag{4.10}$$

Where $u_{k,l}$ is the displacement and defined as,

$$u_{k,l} = \frac{\partial u_k}{\partial z_1} \tag{4.11}$$

If the constitutive equation is written in a more suitable form,

$$\left[1 - \left(e_0 \cdot a\right)^2 \cdot \nabla^2\right] \cdot \sigma_{ij} = \tau_{ij} \tag{4.12}$$

Equation (4.12) represents the uniaxial constitutive equation.

The plane state stress for non local elasticity can be stated with the help of three equations:

$$\left(\sigma_{zz}\right)_{\substack{non\\local}} - \left(e_0 \cdot a\right)^2 \cdot \left[\frac{\partial^2 \sigma_{zz}}{\partial z^2} + \frac{\partial^2 \sigma_{zz}}{\partial y^2}\right]_{\substack{non\\local}} = \left(\sigma_{zz}\right)_{local} = \frac{E}{(1-\upsilon^2)} \cdot \left(\varepsilon_{zz} + \upsilon \cdot \varepsilon_{yy}\right) \quad (4.13)$$

$$\left(\sigma_{yy}\right)_{\substack{non\\local}} - \left(e_0 \cdot a\right)^2 \cdot \left[\frac{\partial^2 \sigma_{yy}}{\partial z^2} + \frac{\partial^2 \sigma_{yy}}{\partial y^2}\right]_{\substack{non\\local}} = \left(\sigma_{yy}\right)_{local} = \frac{E}{(1-\upsilon^2)} \cdot \left(\varepsilon_{yy} + \upsilon \cdot \varepsilon_{zz}\right) \quad (4.14)$$

$$\left(\sigma_{zy}\right)_{\substack{non\\local}} - \left(e_0 \cdot a\right)^2 \cdot \left[\frac{\partial^2 \sigma_{zy}}{\partial z^2} + \frac{\partial^2 \sigma_{zy}}{\partial y^2}\right]_{\substack{non\\local}} = \left(\sigma_{zy}\right)_{local} = \frac{E}{(1+\upsilon)} \cdot \varepsilon_{zy} \quad (4.15)$$

4.2 Euler-Bernoulli Beam Theory

Many beam theories are developed based on different approaches and they have different levels of accuracy. One of the simplest and most useful of these is the theory, commonly known as the Euler-Bernoulli beam theory, originally proposed by Euler and Bernoulli.The Euler-Bernoulli beam theory is a simplistic form of the elasticity of a straight isotropic beam. Using this theory, load bearing and collapsing behavior of beams are determined. One of the basic assumptions of this theory is that the cross section of the beam is infinitely rigid in its plane, that is, no deformation occurs in the cross section plane (Bauchau and Craig, 2009).

The Euler-Bernoulli Theory was first mentioned in 1750, but it was not widely accepted in the period until the Eiffel Tower and Ferris Wheel structures in the 19th century.

The first studies on the calculation of the load carrying capacity of materials date back to the 17th century. Galileo Galilei (well known as Galileo) is one of the scientists who have worked in this field. Galileo's work is generally based on the study of the forces of materials under different stress conditions. In this context, the analysis of beams has played an important role in his studies. In the years following Galileo, Robert Hooke's studies on the elasticity of materials was a pioneer in this field. Mariotte is another researcher who worked on the elasticity of materials during Hooke's research (Timoshenko, 1953).

4.2.1 Euler-Bernoulli beam equations

Euler-Bernoulli expressions are the equation expressing the relationship between the deflection of the beam depending on the load applied to the beam.

Assume that *z* indicates the normal direction of the beam axis and *y* is the deflection axis. Vertical displacement *v* at any point d_1 at a distance *z* from the origin expresses the displacement of that point in the *y* direction measured from the *z*-axis to its elastic curve. Therefore, the downward deflection value should be positive and the upward deflection value should be negative. When *v* is stated as a function of *z*, the elastic curve equation is obtained. (Gere and Timoshenko, 1984).

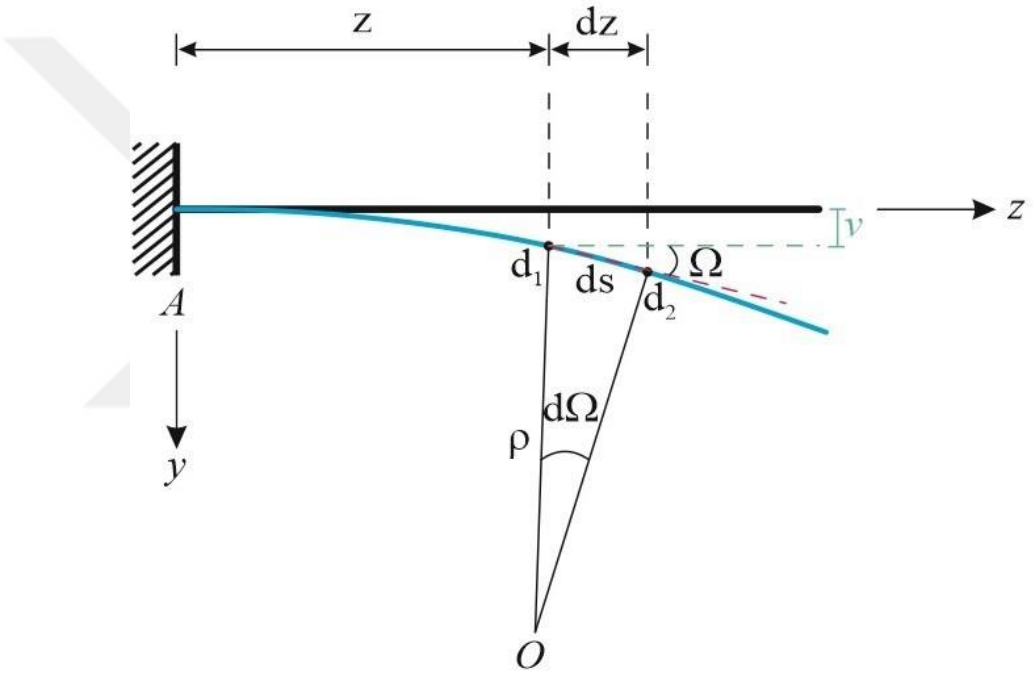

Figure 4.1 : Elastic curve of the beam.

The angle of rotation Ω of the beam axis at point d_1 is the angle between the z-axis and the tangent of the deflection curve. Besides, assume that there is a second point d_2 on the deflection curve along the slope at a distance *ds* and a distance $z + dz$ from the origin. In this case, the deflection value will be $v + dv$. In addition, the rotation angle at the point d_2 will be $\Omega + d\Omega$. If lines perpendicular to the tangent of the elastic curve are formed from d_1 and d_2 points, the intersection point of these lines represent the center of the curvature (*O*). The distance from point *O* to the slope is the radius of curvature (ρ). Thus, the curvature is represented by the following equation (Gere and Timoshenko, 1984).

$$\frac{1}{\rho} = \frac{d\Omega}{ds} \tag{4.16}$$

The first derivative of the deflection (dv/dz) is called slope. Since the slope is extremely small, it is equal to the tangent of Ω. That is,

$$\frac{dv}{dz} = \tan\Omega \tag{4.17}$$

Elastic curves are almost even due to very small rotation values when many beams are loaded. In this case, since Ω has a very small value, simplification operations can be performed as follows.

$$ds = \frac{dz}{\mathrm{Cos}\,\Omega} \tag{4.18}$$

In this case $\mathrm{Cos}\,\Omega \approx 1$, and $ds \approx dz$.

$$\frac{1}{\rho} = \frac{d\Omega}{dz} \tag{4.19}$$

It is also considered as $\tan\Omega \approx \Omega$.

$$\Omega = \tan\Omega = \frac{dv}{dz} \tag{4.20}$$

In this case, the angle of rotation and the slope are equal for the small rotational situations that will occur in the beam. If the Ω derivates with tespect to the *z*, then;

$$\frac{d\Omega}{dz} = \frac{d^2v}{dz^2} \tag{4.21}$$

If equation (4.21) is combined with equation (4.19) the following equation is obtained:

$$\frac{1}{\rho} = \frac{d\Omega}{dz} = \frac{d^2v}{dz^2} \tag{4.22}$$

If the beam material is elastic, the expression of curvature is expressed as follows:

$$\frac{1}{\rho} = -\frac{M}{EI} \tag{4.23}$$

Where M indicates the bending moment and EI is the flexural rigidity of the beam. This equation is valid for both small and large rotations. When this equation is combined with the previous equations, the basic differential equation for the elastic curve of beams emerges.

$$\frac{d\Omega}{dz} = \frac{d^2v}{dz^2} = -\frac{M}{EI} \tag{4.24}$$

If the above equation is differentiated with respect to z then we get,

$$\frac{d^3v}{dz^3} = -\frac{T}{EI} \tag{4.25}$$

$$\frac{d^4v}{dz^4} = \frac{q}{EI} \tag{4.26}$$

Where T is the shear force, q is the uniform load.

4.2.2 Stress-strain relationships in Euler-Bernoulli beams

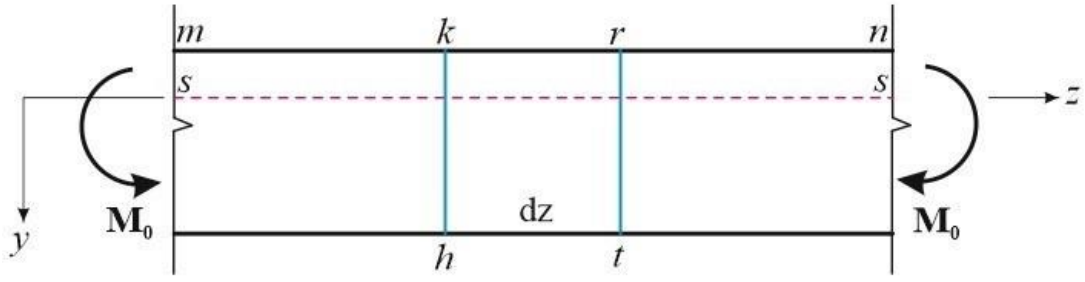

Figure 4.2 : *mn* section of the beam under the bending effect.

To find the internal deformation of the beam, the slope of the beam and final displacement which stem from that behavior must be taken into account (Janečka, Průša, and Rajagopal, 2016). For the section ***ab*** given in the figure, the M_0 moments create a positive curvature. Therefore, negative bending moment develops.

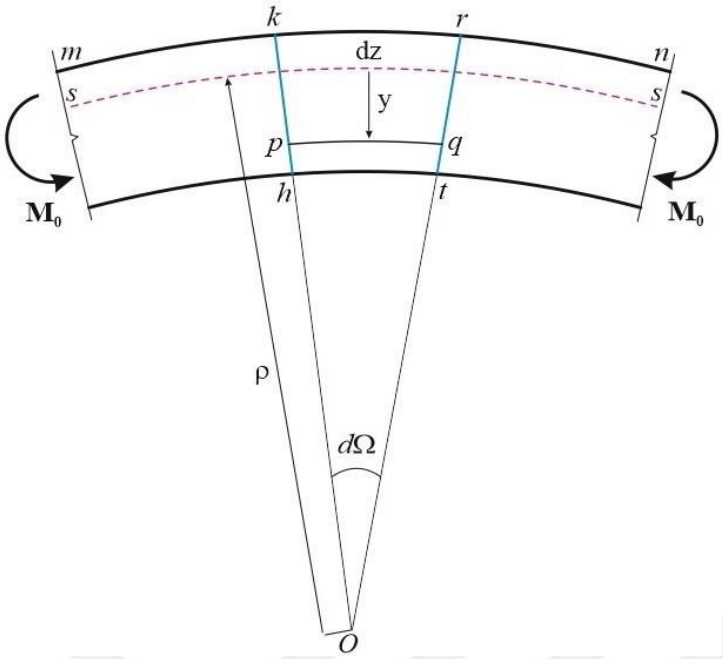

Figure 4.3 : Deformed shape of the *mn* beam section.

The Euler-Bernoulli beam theory is based on the assumption that cross-section of the beam remains plane and it is perpendicular to the deformed axis after deformation.

As all the fibers except the fiber, which is called the neutral axis, will shorten or elongate, the strain (ε_z) occurs along the beam. In order to calculate this deformation, considering a ***pq*** fiber on the beam at a distance *y* from the neutral surface, the length of the fiber *L* is found as:

$$L = (\rho - y)d\Omega = dz - \frac{y}{\rho}dz \tag{4.27}$$

From this equation the strain can be calculated using following expression:

$$\varepsilon_z = -\frac{y}{\rho} \tag{4.28}$$

If we check over the equations dealing with the stress and strain relationship, for a homogeneous, isotropic elastic material, the stress and strain are related by Hook's formula denoted with $\sigma = E\varepsilon$. With the help of the equations (4.24) and (4.28) the stress on the beam is expressed as follows:

$$\sigma_z = -yE\frac{d^2v}{dz^2} \tag{4.29}$$

5. GRADIENT ELASTICITY

The strain energy was first expressed as the deformation (F) and its gradient (∇_x) Afterwards, with the help of some mechanical principles, the strain energy density has become the following form for the given any X reference position (Bertram, 2020).

$$w = \frac{1}{2}\left(E_{IJ} C_{IJKL} E_{KL} + 2E_{IJ,K} H_{IJKLP} E_{LP} + E_{IJ,K} G_{IJKLPQ} E_{LP,Q} \right) \tag{5.1}$$

Where uppercase indices indicate a representation and distinction with respect to Cartesian coordinates (Bertram,2019). The stiffness tensors C, H and G demonstrate fourth, fifth and sixth order tensors, respectively. In this case Green-Lagrange Tensor $\boldsymbol{\varepsilon}$,

$$\boldsymbol{\varepsilon} = \frac{1}{2}\left(F^T \cdot F - I \right) \tag{5.2}$$

If the material is isotropic, then H disappears since the Green-Lagrange tensor is symmetrical. Thus, C and G can be written as follows;

$$C_{IJKL} = \lambda \delta_{IJ} \delta_{KL} + \mu \left(\delta_{IJ} \delta_{KL} + \delta_{IL} \delta_{JK} \right), \qquad H_{IJKLP} = 0 \tag{5.3}$$

$$\begin{aligned} G_{IJKLPQ} &= c_2 \left(\delta_{IJ} \delta_{KL} \delta_{PQ} + \delta_{IJ} \delta_{KP} \delta_{LQ} + \delta_{IK} \delta_{JQ} \delta_{LP} + \delta_{IQ} \delta_{JK} \delta_{LP} \right) + \\ & c_3 \cdot \delta_{IJ} \delta_{KQ} \delta_{LP} + c_5 \left(\delta_{IJ} \delta_{JL} \delta_{PQ} + \delta_{IK} \delta_{JP} \delta_{LQ} + \delta_{IK} \delta_{JQ} \delta_{LP} + \delta_{IL} \delta_{JK} \delta_{LP} + \delta_{IP} \delta_{JK} \delta_{LQ} \right) \\ & + c_{11} \left(\delta_{IL} \delta_{JP} \delta_{KQ} + \delta_{IP} \delta_{JL} \delta_{KQ} \right) + \\ & c_{15} \left(\delta_{IL} \delta_{JQ} \delta_{KP} + \delta_{IP} \delta_{JQ} \delta_{KL} + \delta_{IQ} \delta_{JL} \delta_{KP} + \delta_{IQ} \delta_{JP} \delta_{KL} \right) \end{aligned} \tag{5.4}$$

To analyze and / or model the deformation behavior of solids, the linear strain tensor is calculated for small deformations as follows;

$$\varepsilon = \frac{1}{2}\left(\nabla u + u \nabla \right) \tag{5.5}$$

5.1 Strain Gradient Elasticity

This theory is based on the assumption that the strain gradient tensor can also be included in the calculations to calculate the elastic strain energy. Thus, in addition to the Lame constants, new characteristic length parameters are added to the constitutive equations (Sadeghi et al., 2012).

$$w = \frac{1}{2}\lambda\varepsilon_{ii}\varepsilon_{jj} + \mu\varepsilon_{ij}\varepsilon_{ij} + a_1\varepsilon_{ijj}{}^{(2)}\varepsilon_{ikk}{}^{(2)} + a_2\varepsilon_{iik}{}^{(2)}\varepsilon_{kjj}{}^{(2)} + a_3\varepsilon_{iik}{}^{(2)}\varepsilon_{jjk}{}^{(2)} + a_4\varepsilon_{ijk}{}^{(2)}\varepsilon_{ijk}{}^{(2)} + a_5\varepsilon_{ijk}{}^{(2)}\varepsilon_{kji}{}^{(2)} \tag{5.6}$$

Where λ and μ are Lamê constants, and a_i indicates the second order constant. Herein second-order strain tensor denoted as;

$$\varepsilon^{(2)} = \nabla\nabla u \tag{5.7}$$

With the help of the Castigliano theorem, high-order stresses are calculated as follows:

$$\sigma^{(2)} = \frac{\partial w}{\partial \varepsilon}, \qquad \sigma^{(3)} = \frac{\partial w}{\partial^{(2)}\varepsilon} \tag{5.8}$$

The Green-Lagrange strain tensor (E_{IJ}) can be written as the gradient of displacement (u):

$$\varepsilon_{IJ} = \frac{1}{2}\left(u_{I,J} + u_{J,I} + u_{K,I}\cdot u_{K,J}\right) \tag{5.9}$$

Lam et al. (2003) expressed the strain energy density equation that includes three additional length parameters (l_0, l_1, l_2) required to model a material with almost incompressible structure in the form below;

$$w = \frac{1}{2}\lambda\varepsilon_{ii}\varepsilon_{jj} + \mu\varepsilon_{ij}\varepsilon_{ij} + \mu l_0{}^2\varepsilon_{mm,i}\varepsilon_{nn,i} + \mu l_1{}^2\varepsilon_{ijk}{}^{(2)}\varepsilon_{ijk}{}^{(2)} + \mu l_2{}^2\kappa_{ij}{}^S\kappa_{jjk}{}^S \tag{5.10}$$

Where second-order strain gradient tensor is,

$$\varepsilon'^{(2)}_{ijk} = \varepsilon^{(2)}_{ijk}{}^S - \frac{1}{5}\left(\delta_{ij}\,\varepsilon^{(2)}_{mmk}{}^S + \delta_{jk}\,\varepsilon^{(2)}_{mmi}{}^S + \delta_{ki}\,\varepsilon^{(2)}_{mmj}{}^S\right) \tag{5.11}$$

The second order symmetric strain tensor and the symmetric curvature tensor in the above expression are expressed respectively as follows:

$$\overset{(2)}{\varepsilon^{S}}_{ijk} = \frac{1}{3}\left(\overset{(2)}{\varepsilon}_{ijk} + \overset{(2)}{\varepsilon}_{jki} + \overset{(2)}{\varepsilon}_{kij} \right) \tag{5.12}$$

$$\overset{(2)}{\kappa_{ij}}^{S} = \frac{1}{4}\left(\varepsilon_{ipq} + \overset{(2)}{\varepsilon}_{jpq} + \varepsilon_{jpq}\, \overset{(2)}{\varepsilon}_{ipq} \right) \tag{5.13}$$

Li, Li and Hu (2015) derived a size-dependent Timoshenko model that explains the thickness-strength variation of a two-component functional graded material within the framework of the non-local strain gradient theory. Akgöz and Civalek (2013) investigated the buckling of tapered micro columns using the modified strain gradient elasticity theory. In their studies, Rayleigh-Ritz solution method is used for different taper ratios to determine the critical buckling loads of cantilever tapered micro columns. The strain gradient theory modified by Lam et al. (2003) which includes two high-order stress components in addition to the classical and couple stress. Moreover, this theory is also used to analyze the static and dynamic behavior of linear homogeneous micro beams (Akgöz and Civalek, 2011a, b, 2012,2013b).

5.2 Functionally Graded Materials (FGMs)

Basically, FGMs are composite materials where mechanical properties can change from one surface to another without problems and continuously (Ozturk and Gulgec,2011). FGMs are now frequently used to achieve successful results in many different topics such as alleviation of residual stresses, reducing stresses throughout the life of the structure, preventing fracture and fatigue (Birman, 2014). Along with the technological developments, FGMs are used as thin films in micro and nano structure alloy electromechanical systems (MEMS/NEMS) (Lü et al., 2009b).

Most of the studies on FGMs are related to the fact that the material properties are changing in one direction. However, there may be situations where macroscopic properties are graded in two and /or three directions. According to an information reported by Steinberg (1986), it is observed that an aircraft body used in aviation is exposed to extreme temperature gradient and an extremely high temperature effect during flight, at high speed and at an altitude of about 29km, on the surface and

thickness of the aircraft body. In this context, it is of great importance to developing macroscopic properties of FGMs that change in two or three directions in order for such structures to have a more comprehensive temperature field (Nejad and Hadi, 2016).

There are very few studies in the literature on beams and plates made of bi-directional FGMs. Lü et al.(2009) carried out some studies on thermo-elastic analysis of bi-directional FGM plates. Zhao, Chen and Lü (2012) presented a study on the plane problems of bi-directional FGMs where the modulus of elasticity varies exponentially in both longitudinal and transverse directions. Wang et al. (2016) examined the free vibration behavior of a two-directional functionally graded beam with variable material properties along the length and thickness of the beam. Nejat, Hadi and Rastgoo (2016) analyzed the buckling analysis of arbitrary two-directional functionally graded (FG) Euler-Bernoulli nano beams based on the theory of non-local elasticity. In another study of Nejad and Hadi (2016), they examined the free vibration behavior of the bi-directional functionally graded (BDFG) Euler-Bernoulli nano beams using the non-local theory of elasticity. Using the non-local elasticity theory (Eringen, 1983), Lim and Wang (2017) examined the static bending problem of nano-beams and obtained the governing equation and boundary conditions with the help of a variational principle.

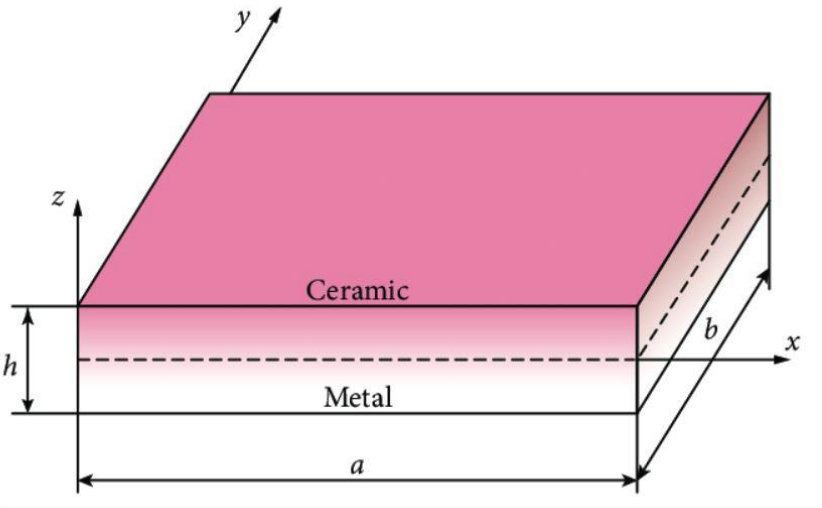

Figure 5.1 : FGM plate (Do et al., 2020).

6. MECHANICAL BEHAVIOR OF THE BI-DIRECTIONAL BEAMS

Determining the mechanical behavior of Euler-Bernoulli nano beams has come into prominence in the last decades. In order for such nano structures to be designed and used in industry, their mechanical behaviors such as bending, buckling and vibration should be well analyzed. The use of FGM nano beams and plates has become widespread in the medical, aviation and electronic device industries with the developing technology.

Kahrobaiyan et al. (2011) developed a size-dependent functionally graded Euler-Bernoulli beam model based on the strain gradient theory that can define the size effect in micro-scale structures. In the study, the governing equation was obtained using a variational approach to both classical and non-classical boundary conditions. In the past years, non-classical continuity theories such as non-local strain gradient and couple stress theories are developed and used to investigate micro-scale structures (Fleck et al., 1994; Ashby and Hutchinson, 1994; Lam et al., 2003). Considering the first and second derivatives of the stress tensor, Mindlin (1965) proposed a higher order gradient theory for the behavior of elastic materials. Fleck and Hutchinson (1993, 2001) used Mindlin's formulations considering only the first derivative of the tensile tensor, and called it the strain gradient theory. Unlike the couple stress theory, the strain gradient theory includes some high-order stress components in addition to the classical and couple stress. In fact, the couple stress theory is in one respect a special case of strain gradient theory. With a similar consideration for the modification of couple stress theory by Yang et al. (2002), Lam et al. (2003) developed a modified strain gradient theory for a particular case. Strain gradient theory is used by researchers such as Kong, Zhou, Nie, Wang (2009) and Wang Zhao, Zhou (2010) to formulate the static and dynamic behavior of linear Euler-Bernoulli and Timoshenko beam models. In their studies, these researchers analyzed the effect of the ratio of beam thickness to the material length scale parameter on the static deflection and natural frequencies of microbeams. Furthermore, the size-dependent non-linear Euler-Bernoulli beam model is developed by Kahrobaiyan et al. (2011) based on the strain gradient theory. In

addition, this non-classical theory is used to investigate the buckling behavior of micro scale beams (Akgoz and Civalek, 2011).

6.1 Static Bending of a Bi-Directional Strain-Gradient Euler-Bernoulli Nano Beams (BDSGEB)

In this section, the bending behavior of the beam whose material properties are vary both axially and thickness directions is investigated. By defining the arbitrary function for the variability of material properties, the effect of size parameters on bending behavior was presented. Kahrobaiyan et al. (2011) have demonstrated that static and dynamic torsional behavior of micro rods is size-dependent. Linear FG Euler-Bernoulli and Timoshenko beam models were formulated in some important studies by Asghari et al. (2010,2011) using the modified couple stress theory. Li and Hu (2015) analytically derived the post-buckling deflection and critical buckling loads of the size-dependent simply supported beams. The results obtained from the study were compared with strain gradient theory, non-local elasticity theory, and classical theory of elasticity. As a result of their study, it is observed that the deflections that occur after buckling can be increased either by increasing the non-local parameter or by decreasing the material characteristic parameter. Reddy (2007) examined the buckling and vibration behavior -which are based on Eringen's non-local model-of different linear beam models.

6.1.1 Basic equations and boundary conditions of bi-directional beam

According to the Euler-Bernoulli beam theory, if the horizontal displacement is expressed as *w* and vertical displacement is *v* at any point on the beam (see Figure 6.1);

$$v(z) = v(z), \qquad w(z) = y\psi(z) \tag{6.1}$$

Where

$$\psi(z) = v'(z) \tag{6.2}$$

The axial strain ε_{zz} ,

$$\varepsilon_{zz} = w'(z) \Rightarrow \varepsilon_{zz} = yv'' \tag{6.3}$$

Considering the modulus of elasticity as an arbitrary function both in the direction of the axis and thickness of the beam as shown in the figure and following term (Nejad and Hadi,2016).

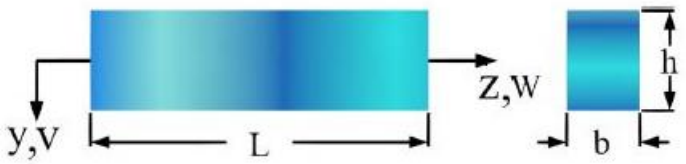

Figure 6.1 : Bi-directional beam.

Elastic modulus *E*,

$$E = f(z)g(y) \tag{6.4}$$

Where $f(z)$ and $g(y)$ are arbitrary functions.

In the frame of gradient elasticity, Cauchy, double stresses and total stress are expressed as follows, respectively (Vardoulakis and Sulem, 1995).

$$\tau_{zz} = E\varepsilon_{zz} \tag{6.5}$$

$$\mu_{zz} = \gamma^2 E\varepsilon'_{zz} \tag{6.6}$$

$$\sigma_{zz} = \tau_{zz} - \mu'_{zz} \tag{6.7}$$

Where γ is the characteristic length of the material.

The governing equation and all boundary conditions are constructed with the help of the Hamilton's principle.

Such that,

$$\delta\Pi = \delta U - \delta W = 0 \tag{6.8}$$

Strain energy (U) for a gradient elastic Euler-Bernoulli beam is expressed as follows:

$$U = \frac{1}{2}\left(\tau_{zz}\varepsilon_{zz} + \mu_{zz}\varepsilon'_{zz}\right) dzdA \tag{6.9}$$

Where A is the cross-sectional area of the given beam. And the work stem from external forces can be calculated following integral:

$$W = \int q(z) v dz \tag{6.10}$$

Where $q(z)$ is the uniform distributed load. Thus, constitutive equations and boundary conditions are obtained as follows:

$$I_2((f(z)v'')'' - \gamma^2(f(z)v''')''') + q(z) = 0 \tag{6.11}$$

$$T\,\delta v\,\Big|_0^L = 0 \tag{6.12}$$

$$M\,\delta v'\,\Big|_0^L = 0 \tag{6.13}$$

$$v'''\,\delta v''\,\Big|_0^L = 0 \tag{6.14}$$

Moment and shear force are expressed as,

$$M = \int \sigma_{zz} y\, dA \Rightarrow M = I_2(f(z)v'' - \gamma^2(f(z)v''')') \tag{6.15}$$

$$T = I_2((f(z)v'')' - \gamma^2(f(z)v''')'') \tag{6.16}$$

Where I_2 is,

$$I_2 = \int y^2 g(y)\, dA \tag{6.17}$$

It is useful to define some dimensionless parameters for convenience in calculations.

$$u = \frac{z}{L},\quad \bar{\gamma} = \frac{\gamma}{L},\quad \bar{v} = \frac{v}{v_0},\quad v_0 = \frac{q_0 L^4}{I_2},\quad \bar{q} = \frac{q}{q_0},\quad \bar{M} = \frac{M}{q_0 L^2},\quad \bar{T} = \frac{T}{qL} \tag{6.18}$$

If we substitute the above parameters into the equations (6.11) and (6.14), the following expressions and boundary conditions are obtained.

$$(f(u)\bar{v}'')'' - \bar{\gamma}^2(f(u)\bar{v}''')''') + \bar{q}(z) = 0 \tag{6.19}$$

$$\bar{M} = f(u)\bar{v}'' - \bar{\gamma}^2(f(u)\bar{v}''')' \tag{6.20}$$

$$\bar{T} = (f(u)\bar{v}'')' - \bar{\gamma}^2(f(u)\bar{v}''')'' \tag{6.21}$$

$$\bar{T}\,\delta\bar{v}\,\Big|_0^L = 0 \tag{6.22}$$

$$\bar{M}\,\delta\bar{v}'\Big|_0^L = 0 \tag{6.23}$$

$$\bar{v}'''\,\delta\bar{v}''\Big|_0^L = 0 \tag{6.24}$$

Let us define new variables for some parameters mentioned in the expressions above.

$$\bar{v}' = \bar{\psi}, \quad \bar{\psi}' = \bar{\alpha}, \quad \bar{\alpha}' = \bar{\mu}, \quad \bar{M}' = T, \quad \bar{T}' = -q(u) \tag{6.25}$$

With the help of the eqn. (6.20), $\bar{\mu}'$ is found as follows.

$$\bar{\mu}' = \frac{1}{\bar{\gamma}^2}\bar{\alpha} - \frac{f'(u)}{f(u)}\bar{\mu} - \frac{1}{\bar{\gamma}^2 f(u)}\bar{M} \tag{6.26}$$

The initial value problem given in equations (6.22) and (6.25) is expressed in matrix form as follows.

$$\frac{d\bar{\mathbf{y}}}{du} = \mathbf{A}\bar{\mathbf{y}} + \mathbf{g}, \qquad \bar{\mathbf{y}}(0) = \bar{\mathbf{y}}_0 \tag{6.27}$$

Where,

$$\mathbf{A} = \begin{bmatrix} 0 & 1 & 0 & 0 & 0 & 0 \\ 0 & 0 & 1 & 0 & 0 & 0 \\ 0 & 0 & 0 & 0 & 0 & 0 \\ 0 & 0 & \frac{1}{\bar{\gamma}^2} & -\frac{f'(u)}{f(u)} & -\frac{1}{\bar{\gamma}^2 f(u)} & 0 \\ 0 & 0 & 0 & 0 & 0 & 1 \\ 0 & 0 & 0 & 0 & 0 & 0 \end{bmatrix} \tag{6.28}$$

$$\bar{\mathbf{y}} = \begin{bmatrix} \bar{v} \\ \bar{\psi} \\ \bar{\alpha} \\ \bar{\mu} \\ \bar{M} \\ \bar{T} \end{bmatrix}, \qquad \bar{\mathbf{y}}_0 = \begin{bmatrix} \bar{v}_0 \\ \bar{\psi}_0 \\ \bar{\alpha}_0 \\ \bar{\mu}_0 \\ \bar{M}_0 \\ \bar{T}_0 \end{bmatrix}, \qquad \bar{\mathbf{g}} = \begin{bmatrix} 0 \\ 0 \\ 0 \\ 0 \\ 0 \\ -\bar{q}(u) \end{bmatrix} \tag{6.29}$$

In this case, the solution of the initial value problem is calculated with the help of the formula below.

$$\bar{\mathbf{y}}(u) = \mathbf{TM}(u) \cdot \bar{\mathbf{y}}_0 + \int_0^u \mathbf{TM}(u - \tau) \cdot \mathbf{g}(\tau) d\tau \tag{6.30}$$

Where **TM(*u*)** is the transfer matrix. If we substitute $f(u) = e^{\beta u}$, the components of the transfer matrix become following form (Nejad and Hadi, 2016).

$$TM_{11} = 1, \quad TM_{12} = u \tag{6.31}$$

$$TM_{13} = \left(\bar{\gamma}^2 \left(-\Gamma e^{\frac{\beta u}{2}} \left(\beta^2 \bar{\gamma}^2 + \beta u + 1 \right) + \beta \bar{\gamma} \left(\beta^2 \bar{\gamma}^2 + 3 \right) \sinh\left(\frac{\Gamma u}{2\bar{\gamma}} \right) + \Gamma \left(\beta^2 \bar{\gamma}^2 + 1 \right) \cosh\left(\frac{\Gamma u}{2\bar{\gamma}} \right) \right) \right) / \left(\Gamma e^{\frac{\beta u}{2}} \right) \tag{6.32}$$

$$TM_{14} = \left(\bar{\gamma}^2 \left(\bar{\gamma} \left(-\beta^2 \bar{\gamma}^2 + \beta \Gamma \bar{\gamma} + \left(\beta \bar{\gamma} (\beta \bar{\gamma} + \Gamma) + 2 \right) e^{\frac{\Gamma u}{\bar{\gamma}}} - 2 \right) - 2\Gamma \left(\beta \bar{\gamma}^2 + u \right) e^{\frac{u(\beta\bar{\gamma} + \Gamma)}{2\bar{\gamma}}} \right) \right) / \left(2\Gamma e^{\frac{u(\beta\bar{\gamma} + \Gamma)}{2\bar{\gamma}}} \right) \tag{6.33}$$

$$TM_{15} = \bar{\gamma}^2 \left(1 - \frac{e^{-\frac{\beta u}{2}} \left(\beta \bar{\gamma} \sinh\left(\frac{\Gamma u}{2\bar{\gamma}} \right) + \Gamma \cosh\left(\frac{\Gamma u}{2\bar{\gamma}} \right) \right)}{\Gamma} \right) + \frac{\beta u + e^{\beta(-u)} - 1}{\beta^2} \tag{6.34}$$

$$TM_{16} = \left(-\beta^2 \bar{\gamma}^2 \left(\frac{2\beta\bar{\gamma} e^{-\frac{\beta u}{2}} \sinh\left(\frac{\Gamma u}{2\bar{\gamma}} \right)}{\Gamma} + e^{\beta(-u)} - 1 \right) + \beta u + e^{\beta(-u)} (\beta u + 2) - 2 \right) / \left(\beta^3 \right) \tag{6.35}$$

$$TM_{21} = 0, \quad TM_{22} = 1 \tag{6.36}$$

$$TM_{23} = \left(\bar{\gamma} \left(\beta \bar{\gamma} \left(-\beta \bar{\gamma} - 2\Gamma e^{\frac{u(\beta\bar{\gamma} + \Gamma)}{2\bar{\gamma}}} + \left(\beta \bar{\gamma} + \Gamma \right) e^{\frac{\Gamma u}{\bar{\gamma}}} + \Gamma \right) + 2 \left(e^{\frac{\Gamma u}{\bar{\gamma}}} - 1 \right) \right) \right) / \left(2\Gamma e^{\frac{u(\beta\bar{\gamma} + \Gamma)}{2\bar{\gamma}}} \right) \tag{6.37}$$

$$TM_{24} = \bar{\gamma}^2 \left(\frac{e^{-\frac{u(\beta\bar{\gamma}+\Gamma)}{2\bar{\gamma}}} \left(-\beta\bar{\gamma} + \left(\beta\bar{\gamma}+\Gamma\right) e^{\frac{\Gamma u}{\bar{\gamma}}} + \Gamma \right)}{\Gamma} - 2 \right) / 2 \tag{6.38}$$

$$TM_{25} = \left(\frac{2\sinh\left(\frac{\beta u}{2}\right)}{\beta} - \frac{2\bar{\gamma}\sinh\left(\frac{\Gamma u}{2\bar{\gamma}}\right)}{\Gamma} \right) / \left(e^{\frac{\beta u}{2}} \right) \tag{6.39}$$

$$\begin{aligned} TM_{26} = \Bigg(& \beta^2\bar{\gamma}^2 \left(e^{\frac{\beta u}{2}} \left(\beta\bar{\gamma}\sinh\left(\frac{\Gamma u}{2\bar{\gamma}}\right) - \Gamma\cosh\left(\frac{\Gamma u}{2\bar{\gamma}}\right) \right) + \Gamma \right) \\ & + \Gamma\left(\beta(-u) + e^{\beta u} - 1\right) \Bigg) / \left(\beta^2 \Gamma e^{\beta u} \right) \end{aligned} \tag{6.40}$$

$$TM_{31} = 0, \quad TM_{32} = 0 \tag{6.41}$$

$$TM_{33} = e^{-\frac{\beta u}{2}} \left(\frac{\beta\bar{\gamma}\sinh\left(\frac{\Gamma u}{2\bar{\gamma}}\right)}{\Gamma} + \cosh\left(\frac{\Gamma u}{2\bar{\gamma}}\right) \right) \tag{6.42}$$

$$TM_{34} = \frac{2\bar{\gamma} e^{-\frac{\beta u}{2}} \sinh\left(\frac{\Gamma u}{2\bar{\gamma}}\right)}{\Gamma} \tag{6.43}$$

$$TM_{35} = \frac{e^{\beta(-u)} \left(e^{\frac{\beta u}{2}} \left(\beta\bar{\gamma}\sinh\left(\frac{\Gamma u}{2\bar{\gamma}}\right) - \Gamma\cosh\left(\frac{\Gamma u}{2\bar{\gamma}}\right) \right) + \Gamma \right)}{\Gamma} \tag{6.44}$$

$$\begin{aligned} TM_{36} = \Bigg(& \bar{\gamma} \Bigg(-\beta\Gamma\bar{\gamma} - e^{\frac{\beta u}{2}} \left(\beta^2\bar{\gamma}^2 + 2\right) \sinh\left(\frac{\Gamma u}{2\bar{\gamma}}\right) \\ & + \beta\Gamma\bar{\gamma} e^{\frac{\beta u}{2}} \cosh\left(\frac{\Gamma u}{2\bar{\gamma}}\right) \Bigg) + \Gamma u \Bigg) / \left(\Gamma e^{\beta u} \right) \end{aligned} \tag{6.45}$$

$$TM_{41} = 0, \quad TM_{42} = 0 \tag{6.46}$$

$$TM_{43} = \frac{2e^{-\frac{\beta u}{2}} \sinh\left(\frac{\Gamma u}{2\bar{\gamma}}\right)}{\Gamma\bar{\gamma}} \tag{6.47}$$

$$TM_{44} = e^{-\frac{\beta u}{2}}\left(\cosh\left(\frac{\Gamma u}{2\bar{\gamma}}\right) - \frac{\beta\bar{\gamma}\sinh\left(\frac{\Gamma u}{2\bar{\gamma}}\right)}{\Gamma}\right) \tag{6.48}$$

$$TM_{45} = \left(-2\beta\Gamma\bar{\gamma}e^{\frac{\Gamma u}{2\bar{\gamma}}} + \left(\beta\bar{\gamma}\left(\Gamma - \beta\bar{\gamma}\right) - 2\right)e^{\frac{\Gamma u}{\bar{\gamma}} + \frac{\beta u}{2}} + e^{\frac{\beta u}{2}}\left(\beta\bar{\gamma}\left(\beta\bar{\gamma} + \Gamma\right) + 2\right)\right) / \left(2\Gamma\bar{\gamma}e^{\frac{\Gamma u}{2\bar{\gamma}} + \beta u}\right) \tag{6.49}$$

$$TM_{46} = \left(\beta^2\Gamma\bar{\gamma}^2 + \beta\bar{\gamma}e^{\frac{\beta u}{2}}\left(\beta^2\bar{\gamma}^2 + 3\right)\sinh\left(\frac{\Gamma u}{2\bar{\gamma}}\right) - \Gamma e^{\frac{\beta u}{2}}\left(\beta^2\bar{\gamma}^2 + 1\right)\cosh\left(\frac{\Gamma u}{2\bar{\gamma}}\right) + \Gamma - \beta\Gamma u\right) / \left(\Gamma e^{\beta u}\right) \tag{6.50}$$

$$TM_{51} = 0, \quad TM_{52} = 0, \quad TM_{53} = 0 \tag{6.51}$$

$$TM_{54} = 0, \quad TM_{55} = 1, \quad TM_{56} = u \tag{6.52}$$

$$TM_{61} = 0, \quad TM_{62} = 0, \quad TM_{63} = 0 \tag{6.53}$$

$$TM_{64} = 0, \quad TM_{65} = 0, \quad TM_{66} = 1 \tag{6.54}$$

Where Γ is,

$$\Gamma = \sqrt{4 + \beta^2\gamma^2} \tag{6.55}$$

6.1.2 Examples

6.1.2.1 A simply supported beam subjected to distributed load

In this section we will discuss two types of boundary conditions in order to obtain initial values.

First type of boundary conditions

In this section, three of initial values are known as can be seen from the equations (6.22,6.23 and 6.24).

$$\bar{v}_0 = 0, \quad \bar{\alpha}_0 = 0, \quad \bar{M}_0 = 0 \tag{6.56}$$

And the end conditions are,

$$\bar{v}(1)=0, \quad \bar{\alpha}(1)=0, \quad \bar{M}(1)=0 \tag{6.57}$$

By means of the eqn. (6.30) other initial values are obtained as an analytical functions as seen in the figures (6.2-6.3, and 6.4).

Second type of boundary conditions

In this section, three of initial values are known as can be seen from the equations (6.22,6.23 and 6.24).

$$\bar{v}_0=0, \quad \bar{\mu}_0=0, \quad \bar{M}_0=0 \tag{6.58}$$

And the end conditions are,

$$\bar{v}(1)=0, \quad \bar{\mu}(1)=0, \quad \bar{M}(1)=0 \tag{6.59}$$

By means of the eqn. (6.30) other initial values are obtained as an analytical functions as seen in the figures (6.5 and 6.6). The situations described in the first and second cases are compared in terms of given notations as also seen in Figures (6.10 and 11).

$\bar{v}(u,\bar{\gamma},\beta)$: Deflections in the bi-directional beams

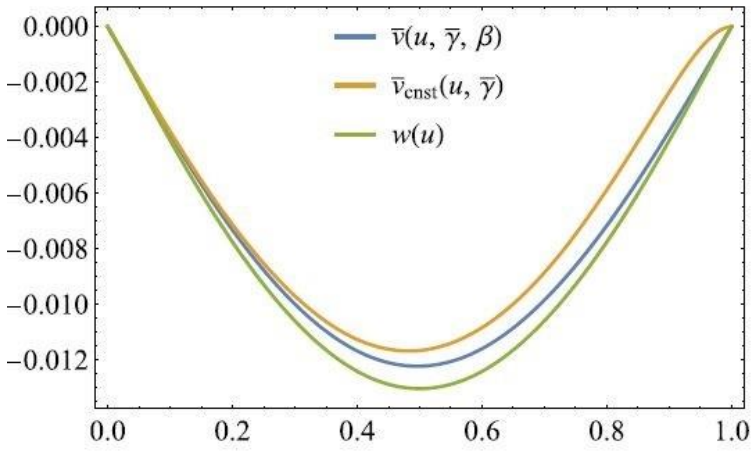

Figure 6.2 : Deflections of the bi-directional gradient elastic beam. For the simply supported beam $\gamma=0,05$ and $\beta=0,05$ and E is constant (Initial conditions are $\bar{v}_0=0, \ \bar{\alpha}_0=0, \ \bar{M}_0=0$, and end conditions are $\bar{v}(1)=0, \ \bar{\alpha}(1)=0, \ \bar{M}(1)=0$).

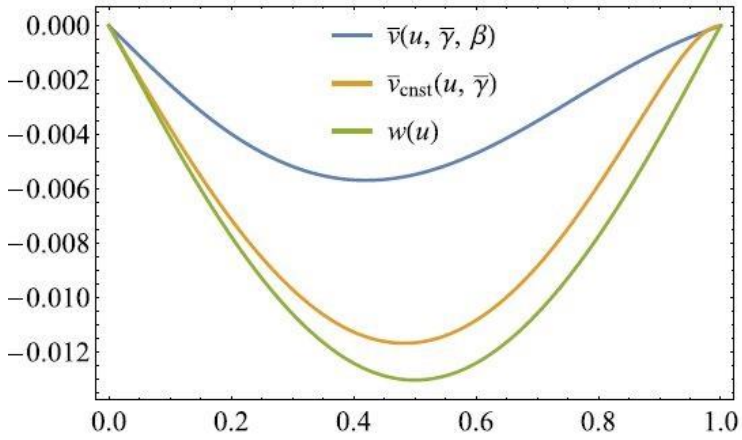

Figure 6.3 : Deflections of the bi-directional gradient elastic beam. For simply supported beam $\gamma = 0.05$ and $\beta = 1$ and E is constant (Initial conditions are $\bar{v}_0 = 0,\ \ \bar{\alpha}_0 = 0,\ \ \bar{M}_0 = 0$, and end conditions are $\bar{v}(1) = 0,\ \ \bar{\alpha}(1) = 0,\ \ \bar{M}(1) = 0$).

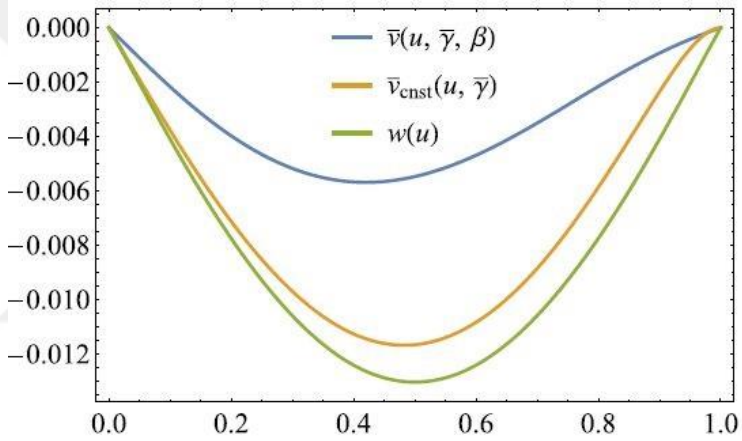

Figure 6.4 : Deflections of the bi-directional gradient elastic beam. For simply supported beam $\gamma = 0.1$ and $\beta = 1$ and E is constant (Initial conditions are $\bar{v}_0 = 0,\ \ \bar{\alpha}_0 = 0,\ \ \bar{M}_0 = 0$, and end conditions are $\bar{v}(1) = 0,\ \ \bar{\alpha}(1) = 0,\ \ \bar{M}(1) = 0$).

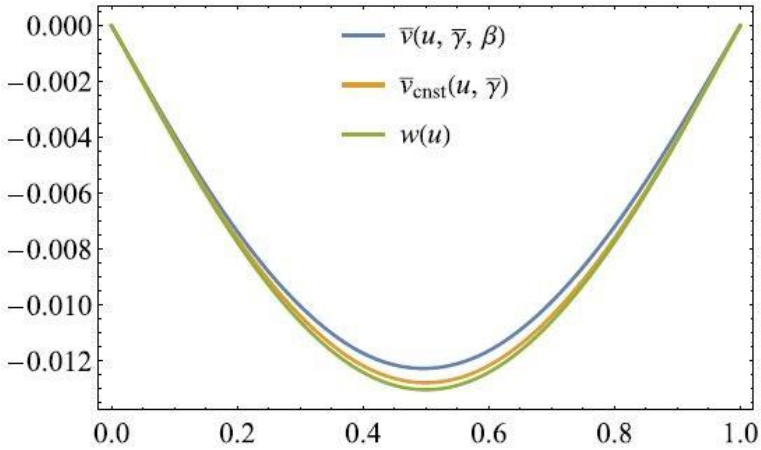

Figure 6.5 : Deflections of the bi-directional gradient elastic beam. For simply supported beam $\gamma = 0.05$ and $\beta = 0.05$ and E is constant (Initial conditions are $\bar{v}_0 = 0, \quad \bar{\mu}_0 = 0, \quad \bar{M}_0 = 0$, and end conditions are $\bar{v}(1) = 0, \quad \bar{\mu}(1) = 0, \quad \bar{M}(1) = 0$).

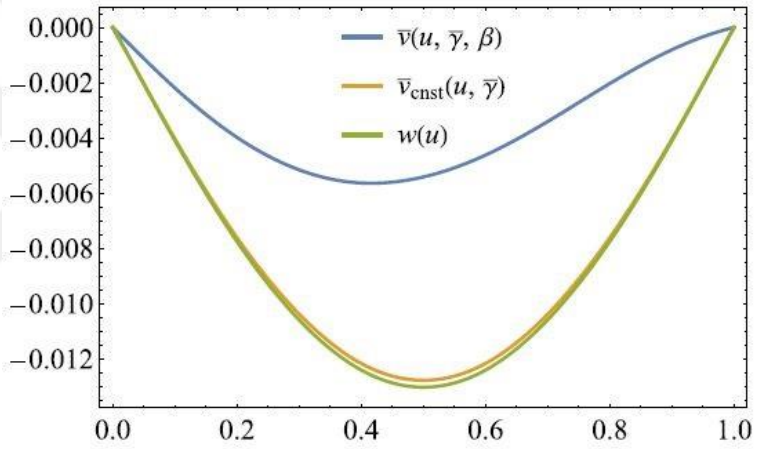

Figure 6.6 : Deflections of the bi-directional gradient elastic beam. For simply supported beam $\gamma = 0.05$ and $\beta = 1$ and E is constant (Initial conditions are $\bar{v}_0 = 0, \quad \bar{\mu}_0 = 0, \quad \bar{M}_0 = 0$, and end conditions are $\bar{v}(1) = 0, \quad \bar{\mu}(1) = 0, \quad \bar{M}(1) = 0$).

6.1.2.2 The beam fixed at both ends subjected to distributed load

First type of boundary conditions

In this section, three of initial values are known as can be seen from the equations (6.22,6.23 and 6.24).

$$\bar{v}_0 = 0, \quad \bar{\psi}_0 = 0, \quad \bar{\alpha}_0 = 0 \tag{6.60}$$

And, the end conditions are;

$$\bar{v}(1) = 0, \quad \bar{\psi}(1) = 0, \quad \bar{\alpha}(1) = 0 \tag{6.61}$$

By using the eqn. (6.30) other initial values are obtained as an analytical functions as seen in the figures (6.7 and 6.8).

Second type of boundary conditions

In this section, three of initial values are known as can be seen from the equations (6.22,6.23 and 6.24).

$$\bar{v}_0 = 0, \quad \bar{\psi}_0 = 0, \quad \bar{\mu}_0 = 0 \tag{6.62}$$

And, the end conditions are;

$$\bar{v}(1) = 0, \quad \bar{\psi}(1) = 0, \quad \bar{\mu}(1) = 0 \tag{6.63}$$

By using the eqn. (6.30) other initial values are obtained as an analytical functions as seen in the figures (6.9 and 6.10). The situations described in the first and second cases are compared in terms of given notations as also seen in Figures (6.11).

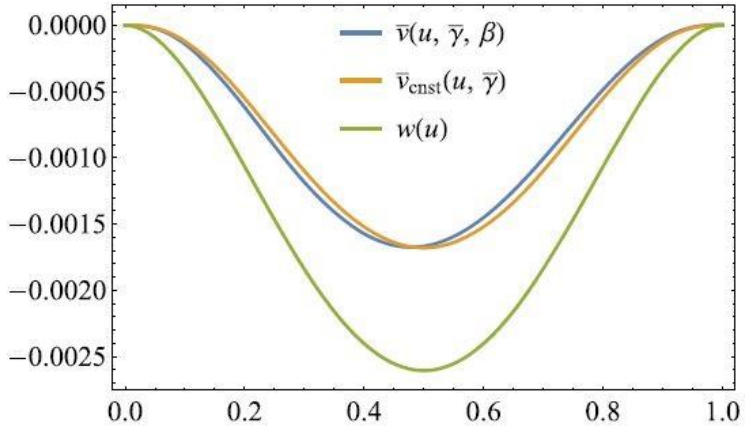

Figure 6.7 : Deflections of the bi-directional gradient elastic beam. For the beam fixed at both ends $\gamma = 0,05$ and $\beta = 1$ and E is constant (Initial conditions are $\bar{v}_0 = 0,\ \bar{\psi}_0 = 0,\ \bar{\alpha}_0 = 0$, and end conditions are $\bar{v}(1) = 0,\ \bar{\psi}(1) = 0,\ \bar{\alpha}(1) = 0$).

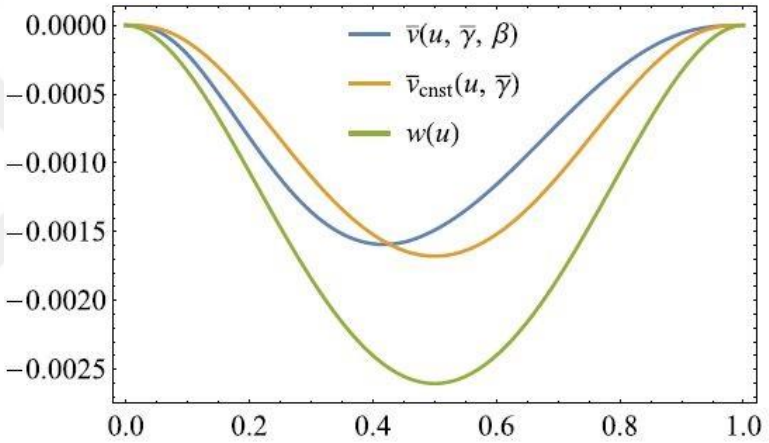

Figure 6.8 : Deflections of the bi-directional gradient elastic beam. For the beam fixed at both ends $\gamma = 0,05$ and $\beta = 4$ and E is constant (Initial conditions are $\bar{v}_0 = 0,\ \bar{\psi}_0 = 0,\ \bar{\alpha}_0 = 0$, and end conditions are $\bar{v}(1) = 0,\ \bar{\psi}(1) = 0,\ \bar{\alpha}(1) = 0$).

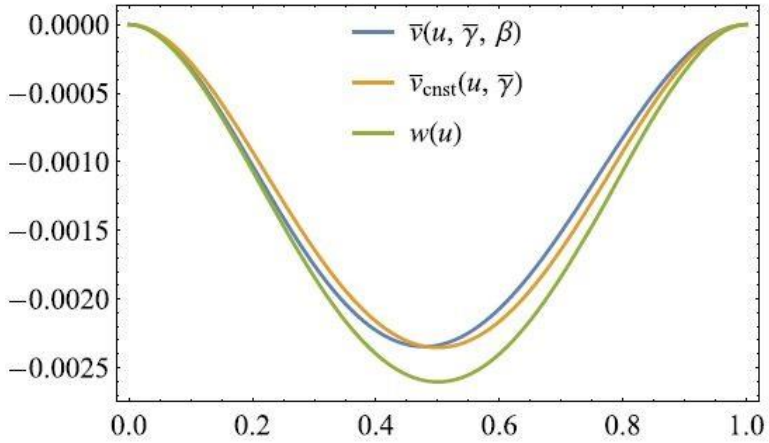

Figure 6.9 : Deflections of the bi-directional gradient elastic beam. For the beam fixed at both ends $\gamma = 0,05$ and $\beta = 1$ and E is constant (Initial conditions are $\bar{v}_0 = 0,\ \bar{\psi}_0 = 0,\ \bar{\mu}_0 = 0$, and end conditions are $\bar{v}(1) = 0,\ \bar{\psi}(1) = 0,\ \bar{\mu}(1) = 0$).

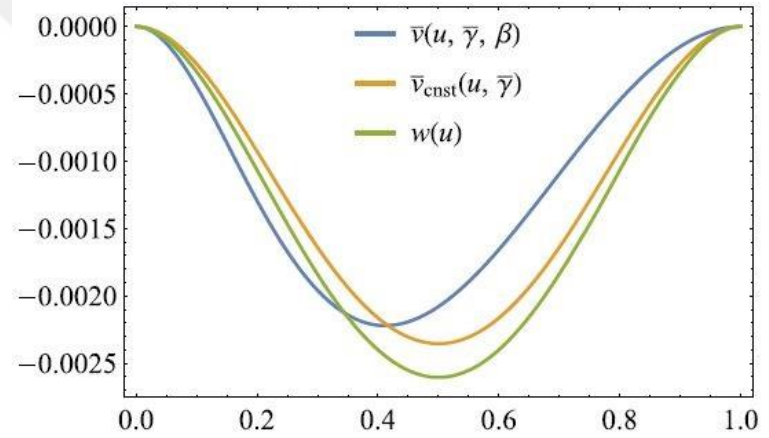

Figure 6.10 : Deflections of the bi-directional gradient elastic beam. For the beam fixed at both ends $\gamma = 0,05$ and $\beta = 4$ and E is constant (Initial conditions are $\bar{v}_0 = 0,\ \bar{\psi}_0 = 0,\ \bar{\mu}_0 = 0$, and end conditions are $\bar{v}(1) = 0,\ \bar{\psi}(1) = 0,\ \bar{\mu}(1) = 0$).

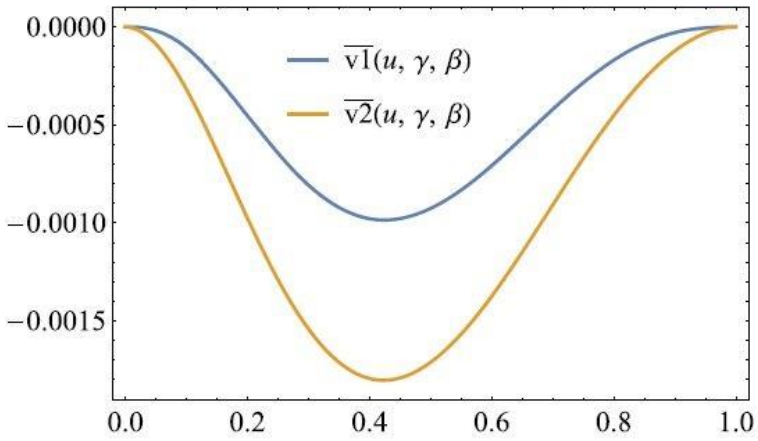

Figure 6.11 : Deflections of the bi-directional gradient elastic beam. For the fixed-fixed beam with the first and second types of boundary conditions for $\gamma = 0{,}1$ and $\beta = 4$.

6.2 Buckling Analysis of a Bi-Directional Strain-Gradient Euler-Bernoulli Nano Beams

In this section, the buckling behavior of an Euler-Bernoulli nano beam whose material properties change in two directions is investigated. Since the transport matrix cannot be calculated analytically, the approximate transport matrix (matricant) method was used in the solution of the problem. Equations and boundary conditions are derived with the help of Hamilton's principle. (Celik and Artan, 2020).

Nejat et al. (2016) examined the buckling behavior of a bi-directional FGM beam within the framework of the non-local elasticity theory. Deng and Cheng (2016) studied the buckling and vibration behavior of a bi-directional nano-beam.

The novelty that this study brings to the literature is that both the size effect and the effect of the non-local parameter on the buckling load were presented for the first time with the method of initial values.

6.2.1 A brief introduction to the Initial Values Method

The solution of the initial values problem is,

$$\frac{dy}{dz} = \mathbf{A}\mathbf{y}, \qquad \mathbf{y}(0) = \mathrm{y}_0 \tag{6.64}$$

is,

$$\mathbf{y}(z) = \mathbf{Y}(z,0) \tag{6.65}$$

Where $\mathbf{Y}(z,0)$ is the transfer matrix, $\mathbf{y}$ is the column matrix containing unknowns, $\mathbf{y}(0)$ is the column matrix whose elements are initial values, and $\mathbf{A}$ is the coefficient matrix. The Matricant can be calculated with the help of the consecutive approximations.

$$\begin{aligned}\mathbf{TM}(z,z_1) = \mathbf{I} + \int_{z_1}^{z} \mathbf{A}(\tau)d\tau + \int_{z_1}^{z} \mathbf{A}(\tau)\int_{z_1}^{\tau} \mathbf{A}(\sigma)d\sigma d\tau + \int_{z_1}^{z} \mathbf{A}(\tau)\int_{z_1}^{\tau} \mathbf{A}(\sigma) \\ + \int_{z_1}^{\sigma} \mathbf{A}(\beta)d\beta d\sigma d\tau + \ldots\end{aligned} \tag{6.66}$$

Where $\mathbf{I}$ is the identity matrix, and $\mathbf{TM}$ satisfied following expressions:

$$\mathbf{TM}(z,z) = \mathbf{I} \tag{6.67}$$

$$\mathbf{TM}(z,z_n) = \mathbf{TM}(z,z_1)\cdot\mathbf{TM}(z_1,z_2)\cdots\mathbf{TM}(z_{n-1},z_n) \tag{6.68}$$

If we known the value $\mathbf{TM}$ $(z,0)$ at the point z, then the solution of the initial value problem can be calculated.

6.2.2 Classical beam

For the convenience of calculations, some dimensionless parameters are defined as follows:

$$\bar{M} = \frac{M}{PL}, \quad \bar{v} = \frac{v}{L}, \quad u = \frac{z}{L}, \quad \bar{T} = \frac{T}{P}, \quad \bar{P} = \frac{PL^2}{EI} \tag{6.69}$$

Where $\bar{v}$ is the vertical deflection, $\bar{M}$ is the bending moment, $\bar{T}$ is the shear force, u is axis of the bar and L is the length of the beam. P indicates the axial compression force. Then, the basic equations can be esppressed in the following form:

$$\frac{d\bar{v}}{du} = \varphi, \quad \frac{d\varphi}{du} = -\bar{P}\bar{M}, \quad \frac{d\bar{M}}{du} = \bar{T} + \varphi, \quad \frac{d\bar{T}}{du} = 0 \tag{6.70}$$

Here, φ shows the rotation. Then, $\mathbf{y}$ and $\mathbf{A}$ can be written as:

$$\mathbf{y} = \begin{bmatrix} \bar{v} \\ \varphi \\ \bar{M} \\ \bar{T} \end{bmatrix}, \qquad \mathbf{A} = \begin{bmatrix} 0 & 1 & 0 & 0 \\ 0 & 0 & -\bar{P} & 0 \\ 0 & 1 & 0 & 1 \\ 0 & 0 & 0 & 0 \end{bmatrix} \tag{6.71}$$

6.2.2.1 Simply-supported beam

The initial conditions are,

$$v(0) = v_0 = 0, \qquad M(0) = M_0 = 0 \tag{6.72}$$

And, the end conditions are,

$$v(1) = 0, \qquad M(1) = 0 \tag{6.73}$$

The transport matrix can be written by using the equation (6.68). The end conditions also can be espressed as follows:

$$\begin{bmatrix} \bar{v}(1) \\ \bar{M}(1) \end{bmatrix} = \begin{bmatrix} TM_{12}(1) & TM_{14}(1) \\ TM_{32}(1) & TM_{34}(1) \end{bmatrix} \begin{bmatrix} \bar{\varphi}_0 \\ \bar{T}_0 \end{bmatrix} = \begin{bmatrix} 0 \\ 0 \end{bmatrix} \tag{6.74}$$

The solution of the above differential equation is possible if and only if determinant of the coefficient matrix is zero. Hence, the buckling loads calculated for different term numbers (n_t) and interval numbers (n_i) by using that condtions (see, Table 6.1). All calculated values for the given conditions were demonstrated as follows. In this problem the exact solution is $\bar{P} = 9.8696$.

6.2.2.2 Beam fixed from the both ends

The initial conditions are,

$$v(0) = v_0 = 0, \qquad \varphi(0) = \varphi_0 = 0 \tag{6.75}$$

And, the end conditions are,

$$v(1) = 0, \qquad \varphi(1) = 0 \tag{6.76}$$

Table 6.1 : Critical loads calculated for simply- supported beam with the help of the classical elasticity theory.

n_i/ n_t	2	3	4
12	9.6570	9.8665	9.8704
16	9.7470	9.8686	9.8698
20	9.7902	9.8692	9.8697

Table 6.2 : Critical loads calculated for the fixed ends beam with the help of the classical elasticity theory.

n_i/ n_t	2	3	4
12	36.5975	39.2912	39.5233
16	37.6970	39.4176	39.4932
20	38.2851	39.4532	39.4846

The transformation matrix can be obtained by using the eqn. (6.66), and the end conditions are expressed as follows:

$$\begin{bmatrix} \bar{v}(1) \\ \bar{\varphi}(1) \end{bmatrix} = \begin{bmatrix} TM_{13}(1) & TM_{14}(1) \\ TM_{23}(1) & TM_{24}(1) \end{bmatrix} \begin{bmatrix} \bar{M}_0 \\ \bar{T}_0 \end{bmatrix} = \begin{bmatrix} 0 \\ 0 \end{bmatrix} \tag{6.77}$$

The solution of the above differential equation is possible if and only if determinant of the coefficient matrix is zero. Hence, the buckling loads calculated for different term numbers (n_t) and interval numbers (n_i) by using that condtions (see, Table 6.2). All calculated values for the given conditions were demonstrated as follows. In this problem the exact solution is $P = 39.4784$.

6.2.3 Basic equations and boundary conditions of bi-directional Euler-Bernoulli beam

According to Euler-Bernoulli beam theory, the axial displacement (w) and the vertical displacement (v) of the beam at any point can be expressed with the following equations:

$$v(z) = v(z), \qquad w(z) = y\psi(z) \tag{6.78}$$

Where,

$$\psi(z) = v'(z) \tag{6.79}$$

The axial strain ε_{zz} is,

$$\varepsilon_{zz} = w'(z) \Rightarrow \varepsilon_{zz} = yv'' \tag{6.80}$$

Considering the modulus of elasticity (E) as an arbitrary function both in the direction of the axis and thickness of the beam as shown in the figure and following term.

$$E = f(z)g(y) \tag{6.81}$$

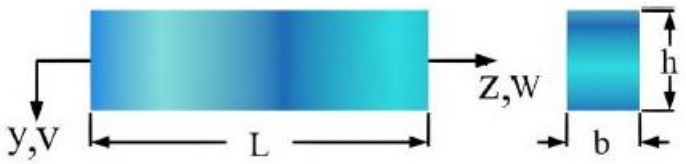

Figure 6.12 : Bi-directional beam.

Where f(z) and g(y) are the arbitrary functions. In the frame of gradient elasticity, Cauchy, double stresses and total stress are expressed as follows, respectively (Vardoulakis and Sulem, 1995; Papargyri-Beskou, Tsepoura et al., 2003).

$$\tau_{zz} = E\varepsilon_{zz} \tag{6.82}$$

$$\mu_{zz} = \gamma^2 E\varepsilon'_{zz} \tag{6.83}$$

$$\sigma_{zz} = \tau_{zz} - \mu'_{zz} \tag{6.84}$$

Where γ indicates the characteristic length of the material. The governing equation and boundary conditions are obtained with the help of the Hamilton's principle. As it known the first derivation of the total potential energy must be zero.

Such that,

$$\delta\Pi = \delta U - \delta W = 0 \tag{6.85}$$

The strain energy (U) can be written for a gradient elastic Euler-Bernoulli beam in terms of W which shows the work done by external load.

$$U = \frac{1}{2}\left(\tau_{zz}\varepsilon_{zz} + \mu_{zz}\varepsilon'_{zz}\right)dzdA \tag{6.86}$$

A is the cross-sectional area of the beam, and W can be calculated with the aim of the following integral:

$$W = \frac{1}{2}\int P v'^{2} dz \tag{6.87}$$

Where P is the axial force. With the help of the minimum potential energy, the equilibrium equation and boundary conditions are obtained as:

$$I_2(f(z)v'')'' - \gamma^2(f(z)v''')''') + Pv'' = 0 \tag{6.88}$$

$$\left\{I_2\left[-\left(f(z)v''\right)' + \gamma^2(f(z)v''')''\right] - Pv'\right\}\delta\Big|_0^L = 0 \tag{6.89}$$

$$I_2\left[f(z)v'' - \gamma^2(f(z)v''')'\right]\delta v'\Big|_0^L = 0 \tag{6.90}$$

$$\gamma^2 I_2 f(z)v'''\,\delta v''\Big|_0^L = 0 \tag{6.91}$$

Where

$$I_2 = \int y^2 g(y)\, dA \tag{6.92}$$

Let us write some dimensionless parameters for convenience in calculations:

$$u = \frac{z}{L},\quad \bar{\gamma} = \frac{\gamma}{L},\quad \bar{v} = \frac{v}{v_0},\quad \bar{P} = \frac{PL^2}{I_2},\quad \bar{M} = \frac{M}{PL},\quad \bar{T} = \frac{T}{P},\quad v_0 = \frac{PL^3}{I_2} \tag{6.93}$$

Equilibrium equations and the boundary conditions are can be expressed in terms of dimensionless parameters with the help of the equations (6.88-6.91).

$$\bar{T}' + \bar{P}\bar{v}'' = 0 \tag{6.94}$$

$$\left(-\bar{T} - \bar{P}\bar{v}'\right)\delta\bar{v}\Big|_0^L = 0 \tag{6.95}$$

$$\bar{M}\,\delta\bar{v}'\Big|_0^L = 0 \tag{6.96}$$

$$\bar{v}'''\,\delta\bar{v}''\Big|_0^L = 0 \tag{6.97}$$

Where,

$$\bar{M} = f(u)\bar{v}'' - \bar{\gamma}^2(f(u)\bar{v}''')' \tag{6.98}$$

$$\bar{T} = (f(u)\bar{v}'')' - \bar{\gamma}^2 (f(u)\bar{v}''')'' \tag{6.99}$$

And new variables are defined as:

$$\begin{aligned}
&\bar{v}' = \bar{\psi}, \\
&\bar{v}'' = \bar{\alpha}, \\
&\bar{v}''' = \bar{\mu}, \\
&\bar{v}^{IV} = \frac{1}{\gamma^2}\bar{\alpha} - \frac{f'(u)}{f(u)}\bar{\mu} - \frac{1}{\gamma^2 f(u)}\bar{M}, \\
&\bar{M}' = \bar{T} \\
&\bar{T}' = -\bar{P}\bar{\alpha}
\end{aligned} \tag{6.100}$$

If we write the above equation in a matrix form:

$$\frac{d}{dz}\begin{bmatrix} \bar{v} \\ \bar{\psi} \\ \bar{\alpha} \\ \bar{\mu} \\ \bar{M} \\ \bar{T} \end{bmatrix} = \begin{bmatrix} 0 & 1 & 0 & 0 & 0 & 0 \\ 0 & 0 & 1 & 0 & 0 & 0 \\ 0 & 0 & 0 & 1 & 0 & 0 \\ 0 & 0 & \frac{1}{\bar{\gamma}^2} & -\frac{f'(u)}{f(u)} & -\frac{1}{\bar{\gamma}^2 f(u)} & 0 \\ 0 & 0 & 0 & 0 & 0 & 1 \\ 0 & 0 & -\bar{P} & 0 & 0 & 0 \end{bmatrix} \begin{bmatrix} \bar{v} \\ \bar{\psi} \\ \bar{\alpha} \\ \bar{\mu} \\ \bar{M} \\ \bar{T} \end{bmatrix} \tag{6.101}$$

6.2.4 Bi-directional strain-gradient beam and Matricant

With the help of the eq. (6.66) and $f(u) = e^{\beta u}$ the components of the matricant can be obtained by using its first three terms.

$$TM_{11} = 1, \qquad TM_{12} = z - z_1, \qquad TM_{13} = \frac{1}{2}(z - z_1)^2 \tag{6.102}$$

$$TM_{14} = \frac{1}{6}(z - z_1)^3, \qquad TM_{15} = 0, \qquad TM_{16} = 0, \qquad TM_{21} = 0 \tag{6.103}$$

$$TM_{22} = 1, \qquad TM_{23} = \frac{(z - z_1)\left(6\bar{\gamma}^2 + (z - z_1)^2\right)}{6\bar{\gamma}^2} \tag{6.104}$$

$$TM_{24} = -\frac{1}{6}(z - z_1)^2 (\beta z - \beta z_1 - 3) \tag{6.105}$$

$$TM_{25} = \frac{e^{-\beta(z+z_1)}\left(2e^{\beta z_1} - e^{\beta z}\left(\beta(z - z_1)(\beta z - \beta z_1 - 2) + 2\right)\right)}{2\beta^3\bar{\gamma}^2} \tag{6.106}$$

$$TM_{26}=0,\qquad TM_{31}=0,\qquad TM_{32}=0 \tag{6.107}$$

$$TM_{33}=\frac{6\bar{\gamma}^2-\left(z-z_1\right)^2\left(\beta z-\beta z_1-3\right)}{6\bar{\gamma}^2} \tag{6.108}$$

$$\begin{aligned}TM_{34}=&\left(z-z_1\right)\left(\bar{\gamma}^2\left(\beta z\left(\beta z-3\right)+\beta z_1\left(-2\beta z+\beta z_1+3\right)+6\right)\right.\\&\left.+\left(z-z_1\right)^2\right)/6\bar{\gamma}^2\end{aligned} \tag{6.109}$$

$$TM_{35}=\frac{e^{-\beta\left(z+z_1\right)}\left(e^{\beta z}\left(\beta\left(-z\right)\beta z_1+2\right)^2-4e^{\beta z_1}\right)}{2\beta^2\bar{\gamma}^2} \tag{6.110}$$

$$TM_{36}=\frac{e^{-\beta\left(z+z_1\right)}\left(e^{\beta z}\left(\beta\left(-z\right)\beta z_1-2\right)+e^{\beta z}\left(\beta\left(-z\right)+\beta z_1+2\right)\right)}{\beta^3\bar{\gamma}^2} \tag{6.111}$$

$$TM_{41}=0,\qquad TM_{42}=0,\qquad TM_{43}=0 \tag{6.112}$$

$$\begin{aligned}TM_{44}=&\left(\bar{\gamma}^2\left(\beta\left(-z\right)\beta z\left(\beta z-3\right)+6\right)\beta z_1\left(3\beta z\left(\beta z-2\right)\right.\right.\\&\left.+\beta z_1\left(-3\beta z+\beta z_1+3\right)+6\right)+6\Big)\\&-\left(z-z_1\right)^2\left(2\beta z-2\beta z_1-3\right)/6\bar{\gamma}^2\Big)/6\bar{\gamma}^2\end{aligned} \tag{6.113}$$

$$\begin{aligned}TM_{45}=&2e^{\beta z_1}\left(3\beta^2\bar{\gamma}^2+1\right)\\&-e^{\beta z}\left(\beta^2\bar{\gamma}^2\left(\beta\left(z-z_1\right)\left(\beta z-\beta z_1-4\right)+6\right)\right.\\&\left.+\beta\left(z-z_1\right)\left(\beta z-\beta z_1-2\right)+2\right)\\&\times\left(2\beta^3\bar{\gamma}^4e^{\beta\left(z+z_1\right)}\right)\end{aligned} \tag{6.114}$$

$$TM_{46}=\frac{e^{-\beta\left(z+z_1\right)}\left(e^{\beta z_1}\left(2\beta z-2\beta z_1+3\right)+e^{\beta z}\left(\beta z-\beta z_1-3\right)\right)}{\beta^2\bar{\gamma}^2} \tag{6.115}$$

$$TM_{51}=0,\qquad TM_{52}=0,\qquad TM_{53}=-\frac{1}{2}\left(z-z_1\right)^2\bar{P} \tag{6.116}$$

$$TM_{54}=-\frac{1}{6}\left(z-z_1\right)^3\bar{P},\qquad TM_{55}=1,\qquad TM_{56}=z-z_1 \tag{6.117}$$

$$TM_{61}=0,\qquad TM_{62}=0,\qquad TM_{63}=-\frac{\left(z-z_1\right)\bar{P}\left(6\bar{\gamma}^2+\left(z-z_1\right)^2\right)}{6\bar{\gamma}^2} \tag{6.118}$$

$$TM_{64} = \frac{1}{6}\left(z - z_1\right)^2 \bar{P}\left(\beta z - \beta z_1 - 3\right) \tag{6.119}$$

$$TM_{65} = \frac{\bar{P}e^{-\beta(z+z_1)}\left(e^{\beta z}\left(\beta\left(z - z_1\right)\left(\beta z - \beta z_1 - 2\right) + 2\right) - 2e^{\beta z_1}\right)}{2\beta^3\bar{\gamma}^2} \tag{6.120}$$

$$TM_{66} = 1 \tag{6.121}$$

6.2.4.1 Simply-supported beam

Calculation of critical loads for the first type of boundary conditions

The initial values for the first case are:

$$\bar{v}(0) = \bar{v}_0 = 0, \quad \bar{M}(0) = \bar{M}_0 = 0, \quad \bar{\alpha}(0) = \bar{\alpha}_0 = 0 \tag{6.122}$$

The end conditions are,

$$\bar{v}(1) = 0, \quad \bar{M}(1) = 0, \quad \bar{\alpha}(1) = 0 \tag{6.123}$$

The transport matrix is obtained with the help of the eqn. (6.66), then, the end conditions can be written as follows:

$$\begin{bmatrix} \bar{v}(1) \\ \bar{\alpha}(1) \\ \bar{M}(1) \end{bmatrix} = \begin{bmatrix} TM_{12}(1) & TM_{14}(1) & TM_{16}(1) \\ TM_{32}(1) & TM_{34}(1) & TM_{36}(1) \\ TM_{52}(1) & TM_{54}(1) & TM_{56}(1) \end{bmatrix} \begin{bmatrix} \bar{\varphi}_0 \\ \bar{\mu}_0 \\ \bar{T}_0 \end{bmatrix} = \begin{bmatrix} 0 \\ 0 \\ 0 \end{bmatrix} \tag{6.124}$$

The solution of the above differential equation is possible if and only if determinant of the coefficient matrix is zero. Hence, the buckling loads calculated for different term numbers (n_t) and interval numbers (n_i) by using this conditions (see, Table 6.3-6.6). All calculated values for the given conditions were demonstrated as follows.

Table 6.3 : Critical loads calculated for simply- supported beam for the first type of conditions for $\bar{\gamma} = \frac{1}{20}, \quad \beta = \frac{1}{10}$.

n_i/ n_t	2	3	4
12	10.3944	10.5256	10.6298
16	10.4936	10.6279	10.6292
20	10.5413	10.6285	10.6291

Table 6.4 : Critical loads calculated for simply- supported beam for the first type of conditions for $\bar{\gamma}=\frac{1}{10},\ \ \beta=\frac{1}{10}$.

$n_i/\ n_t$	2	3	4
12	11.1299	11.3936	11.3983
16	11.2429	11.3962	11.3976
20	11.2973	11.3969	11.3975

Table 6.5 : Critical loads calculated for simply- supported beam for the first type of conditions for $\bar{\gamma}=\frac{1}{20},\ \ \beta=1$.

$n_i/\ n_t$	2	3	4
12	15.8817	16.2575	16.2647
16	16.0424	16.2614	16.2637
20	16.1201	16.2625	16.2634

Table 6.6 : Critical loads calculated for simply- supported beam for the first type of conditions for $\bar{\gamma}=\frac{1}{10},\ \ \beta=1.$

$n_i/\ n_t$	2	3	4
12	17.0815	17.5136	17.5208
16	17.2665	17.5175	17.5196
20	17.3555	17.5184	17.5192

Bi-directional-buckled shapes- gradient elastic beam

i) $\bar{\gamma}=\frac{1}{20},\ \beta=\frac{1}{10}$ and $\bar{P}=10.6291.$

For this case, $\bar{\psi}_0$ and $\bar{\mu}_0$ are calculated in terms of $\bar{T}_0$ with the aid of eqn. (6.124) as,

$$\bar{\psi}_0=-0.0940824\bar{T}_0,\qquad \bar{\mu}_0=0.970296\bar{T}_0 \tag{6.125}$$

Deformed (buckled) shapes of this beam can be plotted with the help of the eqn. (6.124), as shown in the figure (6.13).

ii) $\bar{\gamma}=\frac{1}{10},\ \beta=\frac{1}{10}$ and $\bar{P}=11.3975.$

For this case, $\bar{\psi}_0$ and $\bar{\mu}_0$ are calculated in terms of $\bar{T}_0$ with the aid of eqn. (6.124) as;

$$\bar{\psi}_0=-0.0877398\bar{T}_0,\qquad \bar{\mu}_0=0.89982\bar{T}_0 \tag{6.126}$$

Deformed (buckled) shapes of this beam can be plotted as shown in the figure (6.14).

iii) $\bar{\gamma} = \dfrac{1}{20}$, $\beta = 1$ and $\bar{P} = 16.2634$. For this case, $\bar{\psi}_0$ and $\bar{\mu}_0$ are calculated in terms of $\bar{T}_0$ with the aid of eqn. (6.124) as,

$$\bar{\psi}_0 = -0.0614885\bar{T}_0, \qquad \bar{\mu}_0 = 0.920583\bar{T}_0 \tag{6.127}$$

Deformed (buckled) shapes of this beam can be plotted as shown in the figure (6.15).

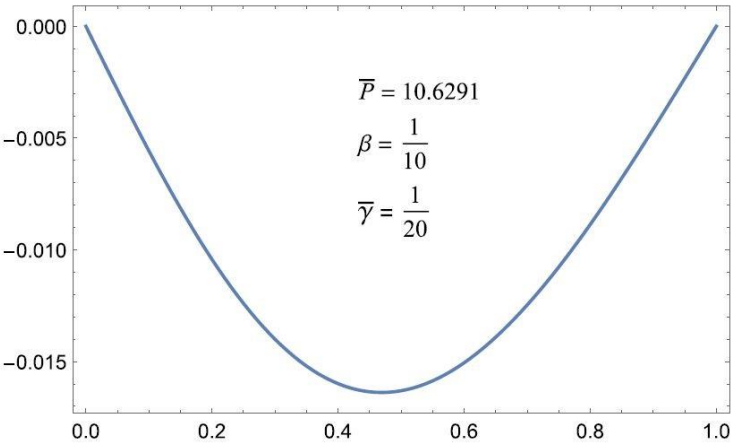

Figure 6.13 : For the first type of boundary conditions buckled shapes of the beam.

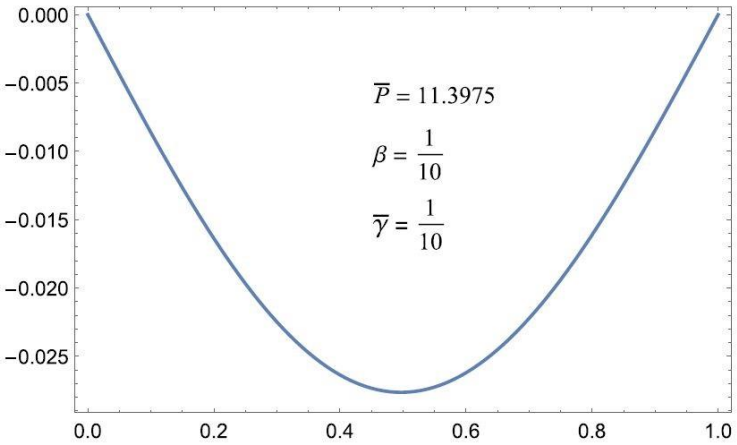

Figure 6.14 : For the first type of boundary conditions buckled shapes of the beam.

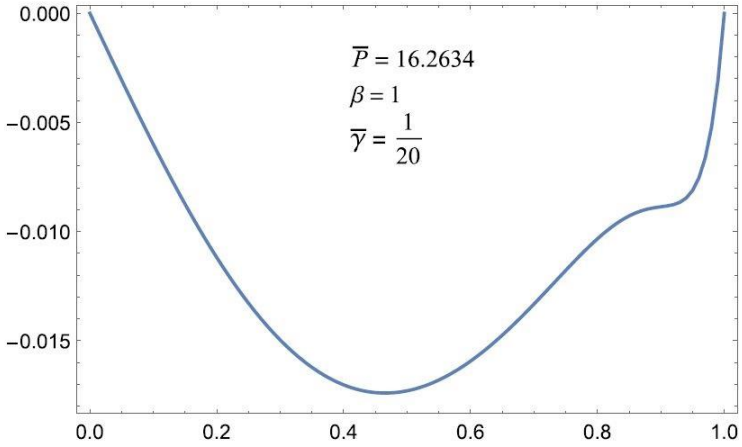

Figure 6.15 : For the first type of boundary conditions buckled shapes of the beam.

iv) $\bar{\gamma} = \frac{1}{10}$, $\beta = 1$ and $\bar{P} = 17.5192$. For this case, $\bar{\psi}_0$ and $\bar{\mu}_0$ are calculated in terms of $\bar{T}_0$ with the aid of eqn. (6.124) as,

$$\bar{\psi}_0 = -0.0614885\bar{T}_0, \qquad \bar{\mu}_0 = 0.920583\bar{T}_0 \tag{6.128}$$

Buckled shapes of the beam can be plotted as shown in the figure (6.16).

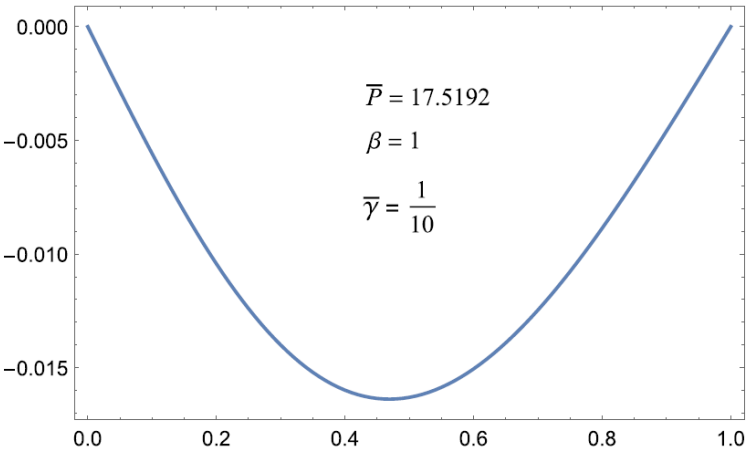

Figure 6.16 : For the first type of boundary conditions buckled shapes of the beam.

Calculation of critical loads for the second type of boundary conditions

The initial values for the second case,

$$\bar{v}(0) = \bar{v}_0 = 0, \qquad \bar{\mu}(0) = \bar{\mu}_0, \qquad \bar{M}(0) = \bar{M}_0 = 0 \tag{6.129}$$

And, the end conditions are:

$$\bar{v}(1)=0, \qquad \bar{\mu}(1)=0, \qquad \bar{M}(1)=0 \tag{6.130}$$

The transport matrix can be obtained with the aim of the eqn. (6.66). And, the end contions are expressed as follows:

$$\begin{bmatrix} \bar{v}(1) \\ \bar{\mu}(1) \\ \bar{M}(1) \end{bmatrix} = \begin{bmatrix} TM_{12}(1) & TM_{13}(1) & TM_{16}(1) \\ TM_{42}(1) & TM_{43}(1) & TM_{46}(1) \\ TM_{52}(1) & TM_{53}(1) & TM_{56}(1) \end{bmatrix} \begin{bmatrix} \bar{\varphi}_0 \\ \bar{\alpha}_0 \\ \bar{T}_0 \end{bmatrix} = \begin{bmatrix} 0 \\ 0 \\ 0 \end{bmatrix} \tag{6.131}$$

The solution of the above differential equation is possible if and only if determinant of the coefficient matrix is zero. Hence, the buckling loads calculated for different term numbers (n_t) and interval numbers (n_i) by using this conditions (see, Table 6.7-6.10). All calculated values for the given conditions were demonstrated as follows:

Table 6.7 : Critical loads calculated for simply- supported beam for the second type of conditions $\bar{\gamma}=\frac{1}{20}, \ \beta=\frac{1}{10}$.

n_i/ n_t	2	3	4
12	10.3439	10.5744	10.5783
16	10.4441	10.5766	10.5778
20	10.4912	10.5771	10.5776

Table 6.8 : Critical loads calculated for simply- supported beam for the second type of conditions $\bar{\gamma}=\frac{1}{10}, \ \beta=\frac{1}{10}$.

n_i/ n_t	2	3	4
12	10.7547	10.9916	10.9953
16	10.8565	10.9936	10.9948
20	10.9052	10.9942	10.9947

Table 6.9 : Critical loads calculated for simply- supported beam for the second type of conditions $\bar{\gamma}=\frac{1}{20}, \ \beta=1$.

n_i/ n_t	2	3	4
12	15.7738	16.1693	16.1739
16	15.9537	16.1721	16.1734
20	16.0319	16.1728	16.1732

Table 6.10 : Critical loads calculated for simply- supported beam for the second type of conditions $\bar{\gamma} = \frac{1}{10}, \quad \beta = 1.$

n_i / n_t	2	3	4
12	16.4622	16.8579	16.8599
16	16.6323	16.8589	16.8591
20	16.7128	16.8590	16.8589

6.2.4.2 Beam fixed from the both ends

Calculation of the critical loads for the first type of boundary conditions

The initial values:

$$\bar{v}(0) = \bar{v}_0 = 0, \quad \bar{\psi}(0) = \bar{\psi}_0 = 0, \quad \bar{\alpha}(0) = \bar{\alpha}_0 = 0 \tag{6.132}$$

And, the end conditions:

$$\bar{v}(1) = 0, \quad \bar{\psi}(1) = 0, \quad \bar{\alpha}(1) = 0 \tag{6.133}$$

The transport matrix is obtained with the help of the eqn. (6.66), then, the end conditions can be written as follows:

$$\begin{bmatrix} \bar{v}(1) \\ \bar{\psi}(1) \\ \bar{\alpha}(1) \end{bmatrix} = \begin{bmatrix} TM_{14}(1) & TM_{15}(1) & TM_{16}(1) \\ TM_{24}(1) & TM_{25}(1) & TM_{26}(1) \\ TM_{34}(1) & TM_{35}(1) & TM_{36}(1) \end{bmatrix} \begin{bmatrix} \bar{\mu}_0 \\ \bar{M}_0 \\ \bar{T}_0 \end{bmatrix} = \begin{bmatrix} 0 \\ 0 \\ 0 \end{bmatrix} \tag{6.134}$$

The critical loads for the buckling calculated for different calues of the parameters as seen in the tables (6.11-6.14).

Table 6.11 : Critical loads calculated for fixed-fixed beam for the first type of conditions $\bar{\gamma} = \frac{1}{16}, \quad \beta = \frac{1}{10}.$

n_i / n_t	2	3	4
12	55.6275	61.7977	62.5201
16	58.0959	62.1906	62.4285
20	59.4659	62.3036	62.4020

Table 6.12 : Critical loads calculated for fixed-fixed beam for the first type of conditions $\bar{\gamma} = \frac{1}{10}, \quad \beta = \frac{1}{10}$.

n_i / n_t	2	3	4
12	76.0658	86.4590	87.8191
16	80.1378	87.1941	87.6427
20	82.4734	87.4045	87.5912

Table 6.13 : Critical loads calculated for fixed-fixed beam for the first type of conditions $\bar{\gamma} = \frac{1}{16}, \quad \beta = 1.$

n_i / n_t	2	3	4
12	85.7056	95.6253	96.9654
16	89.7676	96.3425	96.7862
20	91.9765	96.5483	96.7338

Table 6.14 : Critical loads calculated for fixed-fixed beam for the first type of conditions $\bar{\gamma} = \frac{1}{10}, \quad \beta = 1.$

n_i / n_t	2	3	4
12	117.2770	134.3020	136.4950
16	123.9660	135.4770	136.1780
20	127.7810	135.8030	136.0850

Calculation of the critical loads for the second type of boundary conditions

The initial values are:

$$\bar{v}(0) = \bar{v}_0 = 0, \qquad \bar{\psi}(0) = \bar{\psi}_0 = 0, \qquad \bar{\mu}(0) = \bar{\mu}_0 = 0 \tag{6.135}$$

And, the end conditions:

$$\bar{v}(1) = 0, \qquad \bar{\psi}(1) = 0, \qquad \bar{\mu}(1) = 0 \tag{6.136}$$

The transport matrix is obtained with the help of the eqn. (6.66), then, the end conditions can be written as follows:

$$\begin{bmatrix} \bar{v}(1) \\ \bar{\psi}(1) \\ \bar{\mu}(1) \end{bmatrix} = \begin{bmatrix} TM_{13}(1) & TM_{15}(1) & TM_{16}(1) \\ TM_{23}(1) & TM_{25}(1) & TM_{26}(1) \\ TM_{43}(1) & TM_{45}(1) & TM_{46}(1) \end{bmatrix} \begin{bmatrix} \bar{\mu}_0 \\ \bar{M}_0 \\ \bar{T}_0 \end{bmatrix} = \begin{bmatrix} 0 \\ 0 \\ 0 \end{bmatrix} \tag{6.137}$$

The critical loads for the buckling calculated for different calues of the parameters as seen in the tables (6.15-6.18).

Table 6.15 : Critical loads calculated for fixed-fixed beam for the second type of conditions $\bar{\gamma} = \frac{1}{16}, \ \beta = \frac{1}{10}$.

n_i / n_t	2	3	4
12	43.9598	47.6409	47.9587
16	45.4560	47.8145	47.9180
20	46.2594	47.8631	47.9053

Table 6.16 : Critical loads calculated for fixed-fixed beam for the second type of conditions $\bar{\gamma} = \frac{1}{10}, \ \beta = \frac{1}{10}$.

n_i / n_t	2	3	4
12	52.5294	57.5346	57.9673
16	54.5559	57.7702	57.9104
20	55.6478	57.8362	57.8941

Table 6.17 : Critical loads calculated for fixed-fixed beam for the second type of conditions $\bar{\gamma} = \frac{1}{16}, \ \beta = 1.$

n_i / n_t	2	3	4
12	67.8507	73.8222	73.3621
16	70.2647	74.1151	74.2880
20	71.5724	74.1978	74.2659

Table 6.18 : Critical loads calculated for fixed-fixed beam for the second type of conditions $\bar{\gamma} = \frac{1}{10}, \ \beta = 1.$

n_i / n_t	2	3	4
12	81.3164	89.5266	90.2095
16	84.6253	89.8953	90.1063
20	86.4112	89.9940	90.0769

Bi-directional-buckled shapes-gradient elastic fixed beam

i) $\bar{\gamma} = \frac{1}{16}, \ \beta = \frac{1}{10}$ and $\bar{P} = 62.4020$.

For this case, $\bar{\mu}_0$ and $\bar{M}_0$ are calculated in terms of $\bar{T}_0$ with the aid of eqn. (6.134) as,

$$\bar{\mu}_0 = 661.0945\bar{T}_0, \qquad \bar{M}_0 = 45.3428\bar{T}_0 \tag{6.138}$$

ii) $\bar{\gamma} = \frac{1}{10}$, $\beta = \frac{1}{10}$ and $\bar{P} = 87.5912$.

For this case, $\bar{\mu}_0$ and $\bar{M}_0$ are calculated in terms of $\bar{T}_0$ with the aid of eqn. (6.134) as;

$$\bar{\mu}_0 = 414.9989\bar{T}_0, \qquad \bar{M}_0 = 51.8689\bar{T}_0 \tag{6.139}$$

iii) $\bar{\gamma} = \frac{1}{16}$, $\beta = 1$ and $\bar{P} = 96.7338$.

For this case, $\bar{\mu}_0$ and $\bar{T}_0$ are calculated in terms of $\bar{M}_0$ with the aid of eqn. (6.134) as;

$$\bar{\mu}_0 = 14.0180\bar{T}_0, \qquad \bar{T}_0 = 0.2436\bar{M}_0 \tag{6.140}$$

iv) $\bar{\gamma} = \frac{1}{10}$, $\beta = 1$ and $\bar{P} = 136.0850$.

For this case, $\bar{\mu}_0$ and $\bar{T}_0$ are calculated in terms of $\bar{M}_0$ with the aid of eqn. (6.134) as;

$$\bar{\mu}_0 = 35.6888\bar{T}_0, \qquad \bar{T}_0 = 0.2104\bar{M}_0 \tag{6.141}$$

Deformed (buckled) shapes of this beam can be plotted with the help of the eqn. (6.134), as shown in the figures (6.17-6.20).

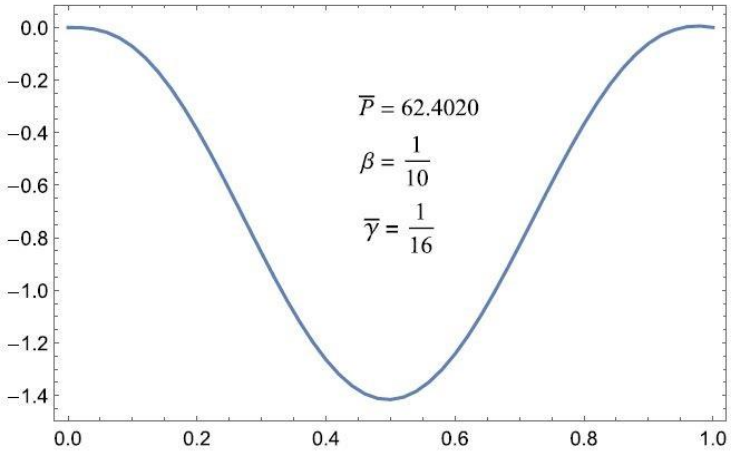

Figure 6.17 : For the second type of boundary conditions buckled shapes of the beam (fixed at both ends).

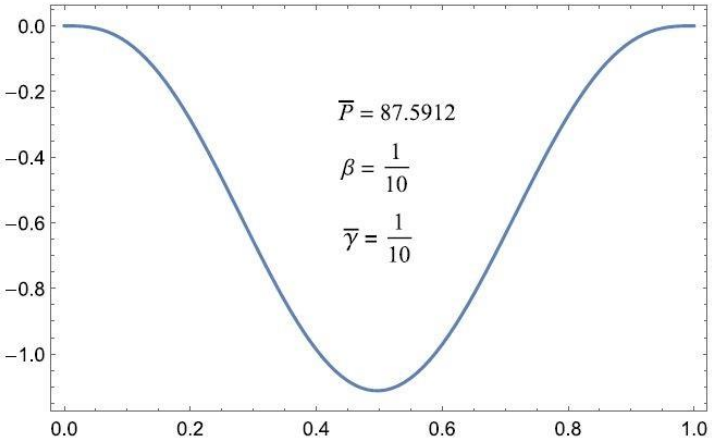

Figure 6.18 : For the second type of boundary conditions buckled shapes of the beam (fixed at both ends).

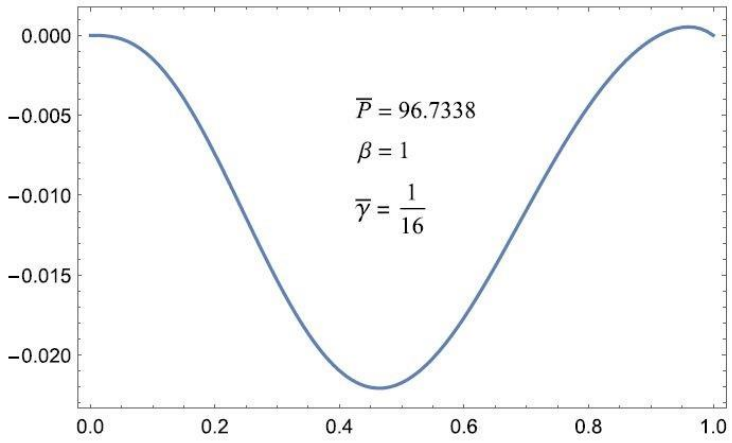

Figure 6.19 : For the second type of boundary conditions buckled shapes of the beam (fixed at both ends).

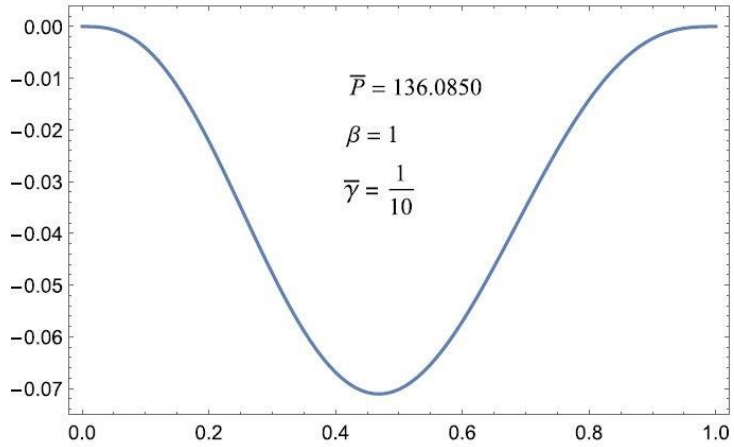

Figure 6.20 : For the second type of boundary conditions buckled shapes of the beam (fixed at both ends).

7. CONCLUSIONS AND RECOMMENDATIONS

In recent years, important breakthroughs have been made in areas such as nanotechnology with the advances in technology. The design and analysis of nanoscale structures is important for the integration of such structures into today's engineering. From this point of view, the topology and mechanical analysis of micro or nano-sized structures draw attention as a very important issue. With the introduction of classical elasticity theory almost a century ago, analysis of many mechanical problems has become very easy. Although the local theory, which is widely used today, is an important approach for the solution of the aforementioned problems, it has shown that the classical eleasticity theory is insufficient in the analysis of such structures if the dimensions of the analyzed structural element are at the level that can be compared with the distance between the atoms of the relevant structure. Therefore, the idea of developing a new enriched continuum model in which the size effect is also taken into account was put forward by published scientific studies. In the analysis of nanoscale structures, the importance of the size effect was emphasized with the non-local elasticity theory and the strain gradient theory developed by scientists such as Eringen and Mindlin (These methods are explained in more detail in Chapters 4 and 5).

In this thesis, static bending and buckling analyzes of bi-directional Euler-Bernoulli nanobeams are investigated within the scope of strain gradient theory.

In the first part of the study, the bending behavior of the Euler-Bernoulli beam, whose material properties vary along the beam axis and thickness, is investigated. The problem solved with the help of Initial Values Method and Transport matrix approach. As it is known, in the Initial Values Method, the transport matrix is unique for the problem. The transport matrix of the problem is created to analyze the bending behavior of the bi-directional strain gradient Euler-Bernoulli (BDSGEB) beam. The modulus of elasticity of beam is defined in terms of arbitrary functions. In the strain gradient theory, in addition to the total stress, Cauchy and double stresses are also expressed. Accordingly, the governing equations and boundary conditions are obtained with the help of the minimum potential energy principle. The bending of the

Euler-Bernoulli beam under uniformly distributed load for two different boundary conditions is investigated. In fact, 4 end conditions can be written in the classical elasticity theory, while 6 end conditions can be written in the gradient elasticity theory. The displacements obtained for two different boundary conditions are presented in the figures (see 6.2-6.11).

As a result of the study, the following informations are presented:

i) It is observed that the size effect decreases depending on the length of the nano beam. That is, in other words, the difference between local and non-local theory becomes important in small-scale structures.

ii) It is observed that the inhomogeneous material constant causes lower displacement in the nanobeams.

iii) The contribution of material characteristic length and inhomogeneous material constant to displacement depending on different boundary conditions are demonstrated with the help of graphs.

In the second part of the study, the buckling behavior of the bi-directional Euler-Bernoulli beam is analyzed within the framework of the gradient elasticity theory. The modulus of elasticity is expressed in terms of arbitrary functions to represent the thickness and beam axis. In the calculation of the critical buckling load-within the scope of the Initial Values Method-since the transport matrix cannot be obtained analytically, the approximate transport matrix (Matricant) approach is used. The governing equations and boundary conditions obtained with the help of Hamilton's principle.

As a result of the study, the following informations are presented:

i) It is shown that if the convergence interval number is large enough, the value of the transport matrix calculated for the first two terms converges significantly to the exact value.

ii) It is shown that the critical buckling load values obtained for the second type boundary condition were always smaller than the values found for the first type boundary condition.

iii) It is observed that the buckled shape of the beam shows a symmetry as the material characteristic length increases.

iv) It is observed that the buckling resistance of the beam increased with the increase of the material characteristic length.

In the calculation of the critical buckling load; It is considered that both types of boundary conditions may be suitable for different types of materials. That is, the type of material to be used may depend on boundary conditions. The accuracy of such a proposition can only be demonstrated by experimental studies. The information provided as a result of both studies is expected to be an important guide in the design and analysis of functionally graded nanostructures.

REFERENCES

Adalı, S. (2008). Variational principles formulti-walled carbon nanotubes undergoing buckling based on nonlocal elasticity theory. *Physics Letters Section A: General, Atomicand Solid State Physics*, (*vol.372*, no.35, pp.5701-5705). doi:10.1016/j.physleta.2008.07.003.

Aksencer, T. and Aydoğdu, M. (2011). Levy type solution method for vibration and buckling of nanoplates using nonlocal elasticity theory. *Phys. E, 43*:954-959.

Akgöz, B. and Civalek, Ö. (2013). A size-dependent shear deformation beam model based on the strain gradient elasticity theory. *International Journal of Engineering Science, 70*:1-14.

Aksoy, Y. and Özkan, M., (2017). *Diferansiyel Denklemler*, Yıldız Teknik Üniversitesi.

Allarakhia, M., & Walsh, S. (2011). Managing knowledge assets under conditions of radical change: The case of the pharmaceutical industry. *Technovation, 31*(2–3): 105–117.

Allhoff, F. (2007). What Is Nanotechnology and Why Does It Matter? From Scienceto Ethics, John Wiley & Sons, Incorporated.

Alotta, G., Failla, G. & Zingales, M. (2014). Finite element method for a nonlocal Timoshenko beam model. *Finite Elements in Analysis and Design, 89*:77-92.

Al Rjoub, Y. ve Hamad A., G. (2017). Free vibration of functionally Euler-Bernoulli and Timoshenko graded porous beams using the transfer matrix method. *KSCE Journal of Civil Engineering, 21*(3):792-806.

Altan, B. (1982). *Yerel olmayan elastisitede bazı konular.* (Doktora tezi). İstanbul Teknik Üniversitesi, Fen Bilimleri Enstitüsü, İstanbul.

Ansari, R., & Sahmani, S. (2011). Bending behavior and buckling of nanobeams including surface stress effects corresponding to different beam theories. *International Journal of Engineering Science, 49*(11):1244–1255.

Ansari, R., Arash, B. ve Rouhi, H. (2011). Vibration characteristics of embedded multi-layered graphene sheets with different boundary conditions via nonlocal elasticity. *Composite* Structures, *93*:2419-2429.

Ansari, R. ve Gholami, R. (2017). Size-dependent buckling and postbuckling analyses of first-order shear deformable magneto-electro-thermo elastic nanoplates based on the nonlocal elasticity theory. *International Journal of Structural Stability and Dynamics, 17*(01):1750014.

Aqel, A., Abou El-Nour, K. M. M., Ammar, R. A. A., & Al-Warthan, A. (2012). Carbon nanotubes, science and technology part (I) structure, synthesis and characterisation. *Arabian Journal of Chemistry*, *5*(1), 1–23.

Arash, B. ve Wang Q., (2014). *A Review on the Application of Nonlocal Elastic Models in Modelling of Carbon Nanotubes and Graphenes,* pages 57-82. Springer International Publishing, Cham.

Arda, M. (2016). *Nano ölçekli yapılarda burulma davranışının yerel olmayan elastisite teorisi kullanılarak statik ve dinamik analizi.* (Yüksek lisans tezi). Trakya Üniversitesi, Fen Bilimleri Enstitüsü, Edirne.

Arslan, A. (2004). *Varyasyonel türev yöntemi ile Euler-Bernoulli kirişlerinin çözümü.* (Yüksek lisans tezi). Selçuk Üniversitesi, Fen Bilimleri Enstitüsü, Konya.

Artan, R. (1992). *Yerel olmayan plastisitede varlık ve teklik problemleri.* (Doktora tezi). İstanbul Teknik Üniversitesi, Fen Bilimleri Enstitüsü, İstanbul.

Artan, R. (1997). The analytical calculation of circular rods of variable cross-section by the initial values method. *Computers of Strucutres, 62*(3):445-461.

Artan, R. ve Batra, R., C. (2012). Free vibrations of a strain gradient beam by the method of initial values. *Acta Mechanica, 223*:2393-2409.

Artan, R. ve Tepe, A. (2008). The initial values method for buckling of nonlocal bars with application in nanotechnology. *European Journal of Mechanics-A/Solids, 27*(3):469-447.

Artan, R. ve Toksöz, A. (2013). Stability analysis of gradient elastic beams by method of initial value. *Archive of Applied Mechanics, 83*(8):1129-1144.

Avcar, M. (2014). Free vibration analysis of beams considering different geometric characteristics and boundary conditions. *Journal of Mechanics and Applications, 4*(3):94-100.

Aykanat, B., A. (2007). *Düzgün yayılı yükle yüklenmiş ankastre mesnetli çubuğun yerel olmayan elastisite yöntemiyle incelenmesi.* (Yüksek lisans tezi). İstanbul Teknik Üniversitesi, Fen Bilimleri Enstitüsü, İstanbul.

Bağdatlı, S., M. ve Toğun, N. (2017). Yerel olmayan elastisite teorisine göre akışkan taşıyan nanokirişin serbest titreşimlerinin analizi. Nanoteknoloji ve antic çağlara uzanan killi nanoyapılar. *Pamukkale Üniversitesi Mühendislik Bilim Dergisi, 23*(1):6-11. doi:10.5505/pajes.2016.85579.

Baretta, R., Feo, L., Luciano, R. ve Marotti de Sciarra, F. (2015). Variational formulations for functionally graded nonlocal Euler-Bernoulli nanobeams. *Composite Structures, 129*:80-89.

Bazant, Z., P. ve Jirasek, M. (2002). Nonlocal integral formulations of plasticity and damage: survey and progress. *J. Eng. Mech., 128*(11):1119-1149.

Benli, B. (2009). Nanoteknoloji ve antic çağlara uzanan killi nanoyapılar. *Kil Bilimi ve Teknoloji Dergisi*, 143-162.

Berger, M. (2016). *Nanotechnology: the future is Tiny*. Cambridge, England: The Royal Society of Chemistry.

Bertram, A. (2020). *Mechanics of Strain Gradient Materials.* Springer.

Bertram, A. (2019). *Compendium on gradient materials including solids and fluids.* Magdeburg, Berlin.

Besseghier, A., Tounsi, A., Houari, M., S., A., Benzair, A., Boumia, L. ve Heireche, H. (2011). Thermal effect on wave propagation in double-walled carbon nanotubes embedded in a polymermatrix using nonlocal elasticity. *Physica E: Low Dimensional Systems and Nanostructures,* (*vol.43,* no.7, pp.1379-1386). doi:10.1016/j.physe.2011.03.008.

Bhagyaraj, S. M., & Oluwafemi, O. S. (2018). *Nanotechnology: The Science of the Invisible. Synthesis of Inorganic Nanomaterials:* Advances and Key Technologies (ss. 1–18). Cambridge, MA: Woodhead Publishing.

Brodie, B.C. (1859). On the Atomic Weight of Graphite. *Philosophical Transactions of the Royal Society of London, 149*:249-259.

Celik, M., Artan, R. (2020). An investigation of static bending of a bi-directional strain-gradient Euler–Bernoulli nano-beams with the method of initial values. *Microsystem Technologies, 26*:2921–2929.

Celik, M., Artan, R. (2020). Buckling Analysis of a Bi-Directional Strain-Gradient Euler–Bernoulli Nano-Beams. *International Journal of Structural Stability and Dynamics, 20* (11): 2050114.

Challamel, N. ve Wan, G., C., M. (2008). The small length scale effect for a nonlocal cantilever beam a paradox solved. Erişim: 21 Ekim, 2019, https://iopscience.iop.org/article/10.1088/0957-4484/19/34/345703/meta.

Chakraverty, S., & Behera, L. (2016). *Static and dynamic problems of nanobeams and nanoplates*. 5 Toh Tuck Link, Singapur: World Scientific Publishing Co. Pte. Ltd.

Chopra, N., G. ve Zetl, A. (1998). Measurement of the elastic modulus of a multiwalled boron nitride nanotube. *Solid State Communications, 105*(5):297-300.

Cıracı, S. (2005). Nanoteknolojide yeni ufuklar. *Bilim ve Teknik Dergisi*.

Clayton, G. (2018). Nanoscience and Nanotechnology. Essex, England: *Ed-Tech Press.*

Cosserat, E., Cosserat, F. (1909). *Théorie des corps déformables*, Herman et fils, Paris.

Coşkun, Y., E. ve Özdemir, Ö. (2016). Kompozit bir helicopter palinin katman dizilimlerinin pal titreşim özellikleri üzerindeki etkisinin incelenmesi. *VI. Ulusal Havacılık ve Uzay Konferansı.* Kocaeli, Türkiye: Kocaeli Üniversitesi.

Da Silva, J., F., do Nascimento, L., A., D. ve dos Santos Hoefel, S. (2016). Free vibration analysis of Euler-Bernoulli beams under non-classical boundary conditions. *IX Congresso Nacional de Engenharia Mecanica.* Fortaleza, Brasil. doi: 10.20906/CPS/CON-2016-1053.

Daneshfaraz, R. (2008). *Bir boyutlu akım problemlerinin çözümünde taşıma matrisi yöntemi.* (Doktora tezi). Ege Üniversitesi, Fen Bilimleri Enstitüsü, İzmir.

de Oliveira, O., Ferreira, M., Da Róz, A. L., & de Lima Leite, F. (2017). *Nanostructures*. Oxford, England: William Andrew Publishing.

De Rosa, M., A. ve Lippiello, M. (2017). Nonlocal Timoshenko frequency analysis of single-walled carbon nanotube with attached mass: An alternative hamiltonian approach. *Composites Part B: Engineering, 111*:409-418.

Demir, C. (2010). *Production of boron nitride nanotubes and their uses in polymer composites.* (Master's thesis). Middle East Technical University, Chemical Engineering, Ankara.

Demiray, H. (1972). On the nonlocal theory of quasi-static elastic dielectrics. *International Journal of Engineering Science, 10*(3):285-292.

Demirkan, E., & Artan, R. (2019). Buckling Analysis of Nanobeams Based on Nonlocal Timoshenko Beam Model by the Method of Initial Values. *International Journal of Structural Stability and Dynamics*, *19*(4), 1–17.

Demirkan, E. (2020). *Yerel olmayan Tımoshenko çubuklarında burkulma probleminin başlangıç değerleri yöntemiyle incelenmesi.* (Doktora Tezi). İstanbul Teknik Üniversitesi, Fen Bilimleri Enstitüsü, İstanbul.

Diaz de Anda, A., Flores, J., Gutierrez, L., Mendez Sanchez, R., A., Monsivais, G. ve Morales, A. (2012). Experimental study of the Timoshenko beam theory predictions. *Journal of Sound and Vibration, 331*(26):5732-5744.

Do, V. T. et al. (2020). On the Development of Refined Plate Theory for Static Bending Behavior of Functionally Graded Plates. *Mathematical Problems in Engineering*, *2020*:2836763.

Duan, W., H., Wang, C., M. ve Zhang, Y., Y. (2007). Calibration of nonlocal scaling effect parameter for free vibration of carbon nanotubes by molecular dynamics. *Journal of Applied Physics,101*(2):024305.

Ebrahimi, F., Dehghan, M. ve Seyfi, A. (2019). Eringen's nonlocal elasticity theory for wave propagation analysis of magneto-electro-elastic nanotubes. *Advances in Nano Research,* (*vol.7*, no.1, pp.1-11).

Edelen, D., G., B. (1969). On nonlocal variational mechanics I. *International Journal of Engineering Science, 7*(3):269-285.

Ekinci, K., L. ve Roukes, M., L. (2005). Nanoelectromechanical systems. *Review of Scientific Instruments, 76*(6):061101.

Elmas, M. (1988). *Elastik zemine outran sonlu kirişlerin deneysel incelenmesi..* (Doktora tezi). İstanbul Teknik Üniversitesi, Fen Bilimleri Enstitüsü, İstanbul.

Eltaher, M., A., Khater, M., E. ve Emam, S., A. (2016). A review on nonlocal elastic models for bending, buckling, vibrations and wave propagation of nanoscale beams. *Applied Mathematical Modelling, 40*(5-6):4109-4128.

Eringen, A., C. (1972). Nonlocal polar elastic continua. *International Journal of Engineering Science, 10*(1):1-6.

Eringen, A., C. ve Edelen, D., G., B. (1972). On nonlocal elasticity. *International Journal of Engineering Science, 10*(3):233-248.

Eringen, A., C. (1973). On nonlocal microfluid mechanics. *International Journal of Engineering Science, 11*(2):291-306.

Eringen, A., C. ve Kim, B., S. (1974). On the problem of crack tip in nonlocal elasticity. *Continuum Mechanics Aspect of Geodynamics and Rock Fracture,* 81-105.

Eringen, A., C. (1983). On differantial equations of nonlocal elasticity and solutions of screw dislocation and surface waves. *Journal Applied Physics, 54*(9):4703-4710.

Eringen, A., C. (2002). *Nonlocal continuum field theories.* Springer-Verlag, New York, USA. ISBN:978-0-387-22643-9.

Erkoç, Ş. 2001. *Karbon nano yapılar,* Bilim ve Teknik Dergisi.

Erkut, Ş. (2007). *Nanobilim ve nanoteknoloji.* ODTÜ Geliştirme Vakfı Yayıncılık, 2. Baskı, ISBN:9944344289.

Ersöz, M., Işıtan, A. Ve Balaban, M. (2018). Nanoteknoloji 1: nanoteknolojinin temelleri. Denizli: Pamukkale Üniversitesi Yayınları. Erişim adresi http://acikerisim.pau.edu.tr:8080/xmlui/handle/11499/3117.

Faghidian, S., A. (2018). On non-linear flexure of beams based on non-local elasticity theory. *International Journal of Engineering Science, 124*:49-63.

Fleck, N. A., Muller, G. M., Ashby, M. F., & Hutchinson, J. W. (1994). Strain gradient plasticity: Theory and experiment. *Acta Metallurgica Et Materialia*, *42*(2):475–487.

Fleck, N. A., & Hutchinson, J. W. (1997). Strain gradient plasticity. *Advances in Applied Mechanics*, *33*:296–358.

Gere, J., M. ve Timoshenko, S., P. (1984). *Mechanics of Materials.* (2nd edition) PWS Engineering.

Gholami, R., Ansari, R., Darvizeh, A. ve Sahmani, S. (2015). Axial buckling and dynamic stability of functionally graded microshells based on the modified couple stress theory. *International of Strutural Stability and Dynamics, 15*(04):1450070.

GR, C. (1966). The shear coefficient in Timoshenko's beam theory. *J. ASME Appl. Mech., 33*(2):335-340.

Grubu, N., S. (2004). Nanobilim ve nanoteknoloji stratejileri. *Nano Teknoloji Strateji Grubu,* TÜBİTAK, Ankara.

Gurtin, M., E. (1965). Thermodynamics and possibility of spatial interactions in elastic materials. *Archive for Rational Mechanics and Analysis, 19*:339-352.

Güçlü, G. (2020). *Nanoçubuklarda büyük yer değiştirme ve yerel olmayan elastisite teorilerine göre deplasman hesabı.* (Doktora Tezi) İstanbul Teknik Üniversitesi, Fen Bilimleri Enstitüsü, İstanbul.

Gül, U. (2015). *Kirişlerin dinamik davranışlarının kayma deformasyonlu kiriş teorileri ile analizi.* (Yüksek lisans tezi). Trakya Üniversitesi, Fen Bilimleri Enstitüsü, Edirne.

Gül, U., E. ve Aydoğdu, M. (2015). Elastik zemin üzerinde outran Timoshenko kirişlerinde dalga yayınımı. *Uluslararası Katılımlı 17. Makina Teorisi Sempozyumu.* İzmir.

Han, S., M., Benaroya, H. ve Wei, T. (1999). Dynamics of transversely vibrating beams using four engineering theories. *Journal of Sound and Vibration, 225*(5):935-988.

Hasan, A., G. (2012). *Hareketli yüke maruz Euler-Bernoulli tipi kirişlerin dinamik davranışlarının incelenmesi.* (Yüksek lisans tezi). İstanbul Teknik Üniversitesi, Fen Bilimleri Enstitüsü, İstanbul.

Hosseini, S., A., H. ve Rahmani, O. (2016). Surface effects on buckling of double nanobeam system based on nonlocal Timoshenko model. *International of Strutural Stability and Dynamics, 16*(10):1550077.

Ishigami, M., Aloni, S. ve Zettl, A. (2003). Properties of boron nitridenanotubes. *InAIP Conference Proceedings,* (*vol.696,* no.1, pp.94-99). AIP.

Işık, Ç. (2011). *Nano ve mikro yapıların yerel olmayan elastisite teorisi ile eğilme ve titreşim hesabı.* (Yüksek lisans tezi). Akdeniz Üniversitesi, Fen Bilimleri Enstitüsü, Antalya.

İlhan, E. (2011). *Diferansiyel denklemlerin varyasyonel iterasyon metodu ile yaklaşık analitik çözümleri.* (Yüksek lisans tezi). Ahi Evran Üniversitesi, Fen Bilimleri Enstitüsü, Kırşehir.

İnan, M. (1964). *Başlangıç değerleri metodu ve taşıma matrisi.* İTÜ İnşaat Fakültesi Matbaası.

İnan, M. (1966). *Elastik çubukların genel teorisi.* İTÜ Yayınları, İstanbul.

İnan, M. (1981). *Cisimlerin Mukavemeti.* İTÜ İnşaat Fakültesi Matbaası.

Janecka, A., Prusa, V. ve Rajagopal, K., R. (2016). Euler-Bernoulli type beam theory for elastic bodies with nonlinear reponse in the small strain range. *Arch. Mech., 68*(1):3-25.

Kahrobaiyan, M. H. et al. (2011). A strain gradient functionally graded Euler–Bernoulli beam formulation. *International Journal of Engineering Science, 52*:65-76.

Karataş, F., Ö. ve Ülker, N. (2014). Kimya öğrencilerinin nanobilim ve nanoteknoloji konularındaki bilgi düzeyleri. *Journal of Turkish Science Education, 11*(3):103-118.

Kaneko, T. (1975). On Timoshenko's correction for shear in vibration beams. *Journal of Physics D: Applied Physics, 8*(16):1927-1936.

Kelly, P. (2012). *Solid mechanics lecture notes.* University of Auckland, Department of Engineering Science, New Zeland.

Khademolhosseini, F., Phani, A., S., Nojeh, A. ve Rajapakse, N. (2012). Nonlocal continuum modeling and molecular dynamics simulation of torsional

vibration of carbon nanotubes. *IEEE Transactions on Nanotechnology, 11*(1):34-43.

Kızılkaya, D. (2016). *Diferansiyel denklemler ve başlangıç değer problemleri.* https://slideplayer.biz.tr/slide/3092541/

Kong, S., Zhou, S., Nie, Z., & Wang, K. (2009). Static and dynamic analysis of micro beams based on strain gradient elasticity theory. *International Journal of Engineering Science, 47*:487–498.

Kösegil, Toksöz, A. (2010). *Yerel olmayan elastisite teorisinde açı ve ritz yöntemlerinin nanoteknolojiye uygulanması.* (Doktora tezi). İstanbul Teknik Üniversitesi, Fen Bilimleri Enstitüsü, İstanbul.

Krishnan, A. et al. (1997). Graphitic cones and the nucleation of curved carbon surfaces. *Nature 388*, 451–454 (1997).

Kunin, I., A. (1982). *Elastic media with microstructure: One-dimensional models.* Elastic Media with Microstructure. Springer.

Lam, D. C. C., Yang, F., Chong, A. C. M., Wang, J., & Tong, P. (2003). Experiments and theory in strain gradient elasticity. *Journal of the Mechanics and Physics of Solids*, *51*(8), 1477–1508.

Lavrik, N., V., Sepaniak, M., J. ve Datskos, P., G. (2004). Cantilever transducers as a platform for chemical and biological sensors. *Review of Scientific Instruments*, *75*(7):2229-2253.

Lee, Y.-G., & Song, Y. I. (2007). Selecting the key research areas in nano-technology field using technology cluster analysis: A case study based on National R&D Programs in South Korea. *Technovation*, *27*(1–2), 57–64.

Lee, J., Mahendra, S., & Alvarez, P. J. J. (2010). Nanomaterials in the construction industry: a review of their applications and environmental health and safety considerations. *ACS Nano*, *4*(7), 3580–3590.

Li, C. ve Chou, T., W. (2004). Modeling of elastic buckling of carbon nanotubes by molecular structural mechanics approach. *Mechanics of Materials, 36*(11):1047-1055.

Li, C. (2014). Torsional vibration of carbon nanotubes: Comparison of two nonlocal models and a semi-continuum model. *International Journal of Mechanical Sciences, 82*(4):25-31.

Liang, Y., J. ve Han, Q. (2012). Prediction of nonlocal scale parameter for carbon nanotubes. *Science China Physics, Mechanics and Astronomy, 55*(9):1670-1678.

Li Li & Hu, Y. (2015). Buckling analysis of size-dependent nonlinear beams based on a nonlocal strain gradient theory. *International Journal of Engineering Science*, *97*, 84–94.

Lim, C., W. ve Xu, R. (2012). Analytical solutions for coupled tension-bending of nanobeam-columns considering nonlocal size effects. *Acta Mechanica, 223*(4):789-809.

Lin, H., P. (2004). Direct and inverse methods on free vibration analysis of simply supported beams with crack. *Engineering Structures, 26*(4):427-436.

Liu, C., Ke, L., L., Wang, Y., S., Yang, J. ve Kitipornchai, S. (2014). Buckling and post-buckling of size-dependent piezoelectric Timoshenko nanobeams subject to thermo-electro-mechanical loadings. *International Journal of Structural Stability and Dynamics, 14*(03):1350067.

Loveridge, D., Dewick, P., & Randles, S. (2008). Converging technologies at the nanoscale: The making of a new world? *Technology Analysis & Strategic Management, 20*(1), 29–43.

Maclurcan, D. (2005). Nanotechnology and developing countries-part 2: What realities?.*Online Journal of Nanotechnology*, 1. Available at SSRN: https://ssrn.com/abstract=1697859.

Mattevi, C. et al. (2012). Solution-processable organic dielectrics for graphene electronics. *Nanotechnology, 23*(34):344017.

Mercan, K., Civalek, Ö. (2017). Buckling analysis of Silicon carbide nanotubes (SiCNTs) with surface effect and nonlocal elasticity using the method of HDQ. *Composites Part B: Engineering*, *114*:34-45, 2017.

Mindlin, R., D. ve Deresiewicz, H. (1953). *Timoshenko's shear coefficient for flexural vibrations of beams* (Technical Report No-10) Columbia University, New York.

Mindlin, R. ve Tiersten, H.F. (1962). Effects of couple-stresses in linear elasticity. *Archive for Rational Mechanics and Analysis*, *11*(1), 415–448.

Murmu, T. ve Pradhan, S., C. (2009). Buckling analysis of a single-walled carbon nantube embedded in an elastic medium based on nonlocal elasticity and Timoshenko beam theory and using dqm. *Physica E: Low-dimensional Systems and Nanostrutures, 41*(7):1232-1239.

Murmu, T. ve Pradhan, S., C. (2009). Buckling of biaxially compressed orthotropic plates at small scales. *Mechanics Research Communications*, *36*(8):933-938.

Murmu, T. ve Pradhan, S., C. (2009). Thermo-mechanical vibration of a single-walled carbon nanotube embedded in an elastic medium based on nonlocal elasticity theory. *Computational Materials Science*, *46*(4):854-859.

Murmu, T. ve Pradhan, S., C. (2010). Small scale effect on the buckling analysis of single-layered graphene sheet embedded in an elastic medium based on nonlocal plate theory. *Physica E: Low-dimensional Systems and Nanostrutures, 42*(5):1293-1301.

Mutluay, İ., Soysal, F., ve Çiçek, B. (2008). Düşük maliyetli bir raman spektrometresinin karbon nanotüp analizi için modifikasyonu. *Eskişehir Osmangazi Üniversitesi Mühendislik ve Mimarlık Fakültesi Dergisi, 21*(2):27-38.

Nam, M., H. ve Lee, K., H. (2000). Unsymetrically loaded cylindrical tank on elastic foundation. *ASCE Journal of Engineering Mechanics, 126*(12):1257-1261.

Nejad, M. Z. Hadi, A. (2016). Eringen's non-local elasticity theory for bending analysis of bi-directional functionally graded Euler–Bernoulli nano-beams. *International Journal of Engineering Science*, *106*:1-9.

Nejad, M. Z. Hadi, A., Rastgoo, A. (2016). Buckling analysis of arbitrary two-directional functionally graded Euler–Bernoulli nano-beams based on nonlocal elasticity theory**.** *International Journal of Engineering Science, 103*:1-10.

Novoselov, K. S. et al. (2005). Two-dimensional atomic crystals. *Proc. Natl Acad. Sci. USA 102,* 10451–10453.

Numanoğlu, H., M. (2017). *Nanoyapıların kiriş ve çubuk modelinin yerel olmayan elastisite teorisi kullanılarak titreşim analizi.* (Lisans tezi) Akdeniz Üniversitesi, Antalya.

Oğulbulan, T. (2007). *Yerel kesite sahip gergi çubuğun yerel olmayan elastisite yöntemiyle incelenmesi.* (Yüksek lisans tezi) İstanbul Teknik Üniversitesi, Fen Bilimleri Enstitüsü, İstanbul.

Orhon, A., V. (2014). Kendini temizleyen cephe sistemleri. *7. Ulusal Çatı ve Cephe Sempozyumu*, İstanbul.

Oruçoğlu, K. (1991). *Yerel olmayan elastisitede çatlak problemi.* (Doktora tezi) İstanbul Teknik Üniversitesi, Fen Bilimleri Enstitüsü, İstanbul.

Ovid'ko, I. A. (2013). Mechanical properties of graphene. *Rev. Adv. Mater. Sci*, *34* (1), 1–11.

Özbay, E. (2006). Günümüzde nanoteknoloji ve uygulamaları. *Dergi Bilkent, 5*:12-15.

Özbora, A., A., Tarhan, M. ve Engin, Y. (2013). Nanoteknolojinin betonun geleceğindeki rolü. *Hazır Beton Kongresi*, İstanbul.

Paola, M., D., Failla, G., Sofi, A. ve Zingales, M. (2011). A mechanically based approach to non-local beam theories. *International Journal of Mechanical Sciences, 53*(9):676-687.

Peddieson, J. (1972). An application of the micropolar fluid model to the calculation of a turbulent shear flow. *International Journal of Engineering Science, 10*(1):23-32.

Pestel, E., C. ve Leckie, F., A. (1963). *Matrix methods in elastomechanics.* Mc-Graw Hill.

Polizotto, C. (2001). Nonlocal elasticity and related variational principles. *International Journal of Solids and Structures, 38*(42-43):7359-7380.

Pradhan, S., C. (2012). Nonlocal finite element analysis and small scale effects of CNTs with Timoshenko beam theory. *Finite Elements in Analysis and Design, 50*:8-20.

Pradhan, S., C. ve Mandal, U. (2013). Finite element analysis of CNTs based on nonlocal elasticity and Timoshenko beam theory including thermal effect. *Physica E: Low-dimensional Systems and Nanostructures, 53*:223-232.

Rao, C. N. R., & Cheetham, A. K. (2001). Science and technology of nanomaterials: Current status and future prospects. *Journal of Materials Chemistry, 11* (12), 2887–2894.

Reddy, J. N. (2007). Nonlocal theories for bending, buckling and vibration of beams. *International Journal of Engineering Science, 45*(2–8), 288–307.

Roco, M. C. (2011). The Long View of Nanotechnology Development: The National Nanotechnology Initiative at 10 Years. *Nanotechnology Research Directions for Societal Needs in 2020 (ss. 1–28)*. Haarlem, Nerherlands: Springer Netherlands.

Rosinger, H., E. ve Ritchie, I., G. (1977). On Timoshenko's correction for shear in vibrating isotropic beams. *Journal of Physics D: Applied Physics, 10*(11):1461-1466.

Ru, C., Q. (2004). Elastic models for carbon nanotubes. *In: Encycl. Nanosci. Nanotechnology, American Scientific Publishers,* (pp. 731-744).

Rui, X., Wang, G. ve Zhang, J. (2018). *Transfer matrix method for multibody systems: Theory and applications*. Wiley.

Ruoff, R., S. ve Yu, M., F. (2005). Nanoscale mechanical characterization of carbon nanotubes. *Microscale Diagnostic Techniques, Springer Berlin Heidelberg,* (pp. 197-226).

Ruotolo, R. ve Surace, C.(2004). Natural frequencies of a bar with multiple cracks. *Journal of Sound and Vibration, 272*(1-2):301-316.

Sağlam, N. ve Emül, E. (2016). Bilimlerin buluşma noktası: Nanoteknolojiye kısa bir bakış. *Yeni Türkiye Dergisi,* 88.

Sari, M., S. ve Al Kouz, W., G. (2016). Vibration analysis of non-uniform orthotropic Kirchhoff plates resting on elastic foundation based on nonlocal elasticity theory. *International Journal of Mechanical Sciences, 114*:1-14.

Sevinç, E. (2017). Nanoteknoloji inovasyon sistemi: Türkiye tekstil sektörü örneği. *Anadolu Üniversitesi Sosyal Bilimler Dergisi, 19*(2):23-48.

Solmaz, S. (2017). *Nano ölçekli kirişlerin static yükler altında yerel olmayan elastisite ile optimum tasarımı.* (Yüksek lisans tezi) Akdeniz Üniversitesi, Antalya.

Staudenmaier, L. (1898). Verfahren zur Darstellung der Graphitsäure. *Berichte der deutschen chemischen Gesellschaft, 31*, 1481-1499.

Stephen, N., G. (1980). Timoshenko's shear coefficient from a beam subjected to gravity loading. *Journal of Applied Mechanics, 47*(1):121-127.

Sun, Y., Z. ve Liew, K., M. (2008). The buckling of single-walled carbon nanotubes upon bending: The higher order gradient continuum and mesh-free method. *Computer Methods in Applied Mechanics and Engineering, 197*(33-40):3001-3013.

Taourirte, M., Eladlani, N., Rhazi, M. et al. (2016). Preparation and characterization of α-chitin whiskers, chitosan nanoparticles and chitosan nanoscaffold from Parapenaeus longirostris. *Materials Today: Proceedings*, *3*(8), 2590–2598.

Tepe, A. (2007). *Nanoteknolojide nano ölçekteki yapıların yerel olmayan elastisite çerçevesinde incelenmesi.* (Doktora tezi) İstanbul Teknik Üniversitesi, Fen Bilimleri Enstitüsü, İstanbul.

Timoshenko, S., P. (1921). On the correction factor for shear of the differential equation for transverse vibrations of bars of uniform cross-section. *Philosophical Magazine, 6*:742-746.

Timoshenko, S., P. (1922). On the transverse vibrations of bars of uniform cross-section. *Philosophical Magazine and Journal of Science, 43*(253):125-131.

Timoshenko, S., P. (1953). *History of Strength of Materials*. McGraw-Hill Book Company, New York.

Thomson, W., T. (1981). *Theory of Vibration with Applications*. Prentice-Hall, New Jersey.

Togun, N. ve Bagdatli, S., M. (2016). Nonlinear vibration of a nano bema on a pasternak elastic foundation based on nonlocal Euler-Bernoulli beam theory. *Mathematical and Computational Appliations, 21*(3):1-19.

Toksöz, A.K. (2010). *Yerel olmayan elastisite teorisinde Açı ve Ritz yöntemlerinin nanoteknolojiye uygulanması*. Doktora tezi, İstanbul Teknik Üniversitesi, İstanbul, 134s.

Tserpes, K. ve Silvestre, N. (2014). *Modeling of carbon nanotubes, graphene and their composites*. Springer Series in Materials Science. Springer, Cham.

URL-1 <*https://en.wikipedia.org/wiki/File:Types_of_Carbon_Nanotubes.png*>, date retrieved 05.06.2021.

Uyan, U. (2018). *Yerel olmayan elastisite teorisi ile bor nitrür nano çubukların eksenel titreşimi.* (Yüksek lisans tezi) Akdeniz Üniversitesi, Fen Bilimleri Enstitüsü, Antalya.

Uysal, S. (2010). *Yüksek teknolojik ürünlerin pazara sunulmasında yenilikçi yaklaşımlar: Boya sanayi uygulaması.* (Doktora tezi) Dokuz Eylül Üniversitesi, Sosyal Bilimler Enstitüsü, İzmir.

Wallace, P. R. (1947). The band theory of graphite. *Phys. Rev. 71*, 622–634.

Wang, C., M., Zhang, Y., Y., Ramesh, S., S. ve Kitipornchai, S. (2006). Buckling analysis of micro and nano-rods/tubes based on nonlocal Timoshenko beam theory. *Journal of Physics D: Applied Physics, 39*(17):3904.

Wang, K., F. ve Wang, B., L. (2011). Vibration of nanoscale plates with surface energy via nonlocal elasticity. *Physica E: Low Dimensional Systems and Nanostrutures, 44*(2):448-453.

Wang, L. ve Hu, H. (2005). Flexural wave propagation in single-walled carbon nanotubes. *Physical Review B, 71*(19):195412.

Wang, L. (2011). A modified nonlocal beam model for vibration and stability of nanotubes conveying fluid. *Physica E: Low Dimensional Systems and Nanostrutures, 44*(1):25-28.

Wang, Q. (2005). Wave propagation in carbon nanotubes via nonlocal continuum mechanics. *Journal of Applied Physics, 98*(12):124301.

Wang, Q. ve Shindo, Y. (2006). Nonlocal continuum models for carbon nanotubes subjected to static loading. *Journal of Mechanics of Materials and Structures, 1*(4):663-680.

Wang, Q. ve Varadan, V., K. (2006). Vibration of carbon nanotubes studied using nonlocal continuum mechanics. *Smart Materials and Structures, 15*(2):659.

Wang, Q., Varadan, V., K. ve Quek, S., T. (2006). Small scale effect on elastic buckling of carbon nanotubes with nonlocal continuum models. *Physics Letters A, 357*(2):130-135.

Wang, Q., Zhou, G., Y. ve Lin, K., C. (2006). Scale effect on wave propagation of double-walled carbon nanotubes. *International Journal of Solids and Structures, 43*(20):6701-6804.

Wang, Q., Han, Q., K. ve Wen, B., C. (2008). Estimate of material property of carbon nanotubes via nonlocal elasticity. *ADV. Theor. Appl. Mech., 1*(1):1-10.

Wang, Q. ve Arash, B. (2012). A review on the application of nonlocal elastic models in modeling of carbon nanotubes and graphenes. *Elsevier Computational Materials Science, 51*(1):303-313.

Weckner, O., Brunk, G., Epton, M., A., Silling, S., A. ve Askari, E. (2009). *Comparison between local elasticity and non-local peridynamics.* Erişim: 21 Ekim 2019, http://citeseerx.ist.psu.edu/viewdoc/download?doi=10.1.1.504.3855&rep=rep1&type=pdf.

Wei, G., W., Zhao, Y., B. ve Xiang, Y. (2002). Discrete singular convolution and its application to the analysis of plates with internal supports part 1: theory and algorithm. *International Journal for Numerical Methods in Engineering, 55*(8):913-946.

Witmer, E., A. (1992). *Elementary Euler-Bernoulli beam theory.* Erişim: 08 Şubat 2020, http://web.mit.edu/16.20/homepage/7_SimpleBeamTheory_files/module_7_with_solutions.pdf

Wu, H., Kitipornchai, S. ve Yang, J. (2015). Free vibration and buckling analysis of sandwich beams with functionally graded carbon nanotube-reinforced composite face sheets. *International Journal of Structural Stability and Dynamics, 15*(07):1540011.

Yang, J., Ke, L., L. ve Kitipornchai, S. (2010). Nonlinear free vibration of single-walled carbon nanotubes using nonlocal Timoshenko beam theory. *Physica E, 42*(5):1727-1735.

Yang, Y., Q., Xiong, G., Ding, K., Nie, S., Zhang, W., Hu, Y. ve Dai, G. (2016). Experimental and numerical studies on lateral-torsional buckling of gj structural steel beams under a concentrated loading condition. *International Journal of Structural Stability and Dynamics, 16*(01):1640004.

Yaylı, M., Ö. (2010). *Yerel olmayan elastisite teorisine göre nano ölçekteki kirişlerin doğrusal olmayan teoriye göre incelenmesi.* (Yüksek lisans tezi) İstanbul Teknik Üniversitesi, Fen Bilimleri Enstitüsü, İstanbul.

Yürüm, Y., Saner Okan, B., Kocabaş, Ö., Z., Okyay, F., Nalbant Ergün, A., Dumanlı, A., G. ve Yürüm, A. (2011). Bor ve karbon nano malzemelerin üretimi ve karakterizasyonu. *Kocaeli Nanoteknoloji Günleri,* Sabancı Üniversitesi, Mühendislik ve Doğa Bilimleri Fakültesi.

Zhang, Y., Q., Liu, G., R. ve Wang, J., S. (2004). Small scale effects on buckling of multi walled carbon nanotubes under axial compression. *Phys. Rev. B, 70*(20):205430.

Zhang, Y., Q., Liu, G., R. ve Xie, X., Y. (2005). Free transverse vibration of double walled carbon nanotubes using a theory of nonlocal elasticity. *Phys. Rev. B, 71*(19):195404.

Zhang, Y., Y., Wang, C. ve Tan, V., B, C. (2009). Assessment of Timoshenko beam models for vibrational behavior of single-walled carbon nanotubes using molecular dynamics. *In advances in Applied Mathematics and Mechanics, 1*(1):89-106.

Zhang, Y., Y., Wang, C., M., Duan, W., H., Xiang, Y. ve Zong, Z. (2009). Assessment of continuum mechanics models in predicting buckling strains of single-walled carbon nanotubes. *Nanotechnology, 20*(39):395707.

Zhang, Y., Zhang, L., W., Liwe, K., M. ve Yu, J., L. (2016). Buckling analysis of graphene sheets embedded in a elastic medium based on the kp-Ritz method and non-local elasticity theory. *Engineering Analysis with Boundary Elements, 70*:31-39.

Zhu, R., Pan, E. ve Roy, A., K. (2007). Molecular dynamics study of the stress-strain behavior of carbon nanotube reinforced Epon *Composites Materials Science and Engineering: A, 447*(1-2):51-57.

Ziegler, H. (1982). Arguments for and against engesser's buckling formulas.*Ingenieur-Archiv, 52*(1):105-113.

APPENDICES

APPENDIX A: Bending Figures

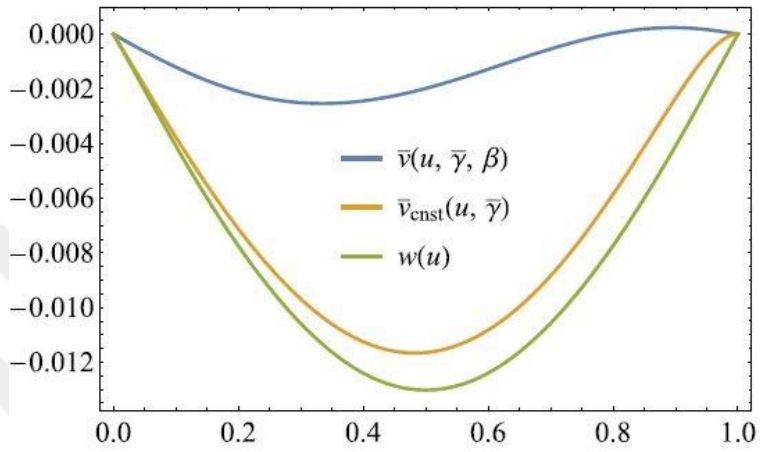

Figure A.1 : Deflections of the bi-directional gradient elastic beam. For the simply supported beam $\gamma = 0.1$ and $\beta = 2$ and E is constant (Initial conditions are $\bar{v}_0 = 0,\ \bar{\alpha}_0 = 0,\ \bar{M}_0 = 0$, and end conditions are $\bar{v}(1) = 0,\ \bar{\alpha}(1) = 0,\ \bar{M}(1) = 0$).

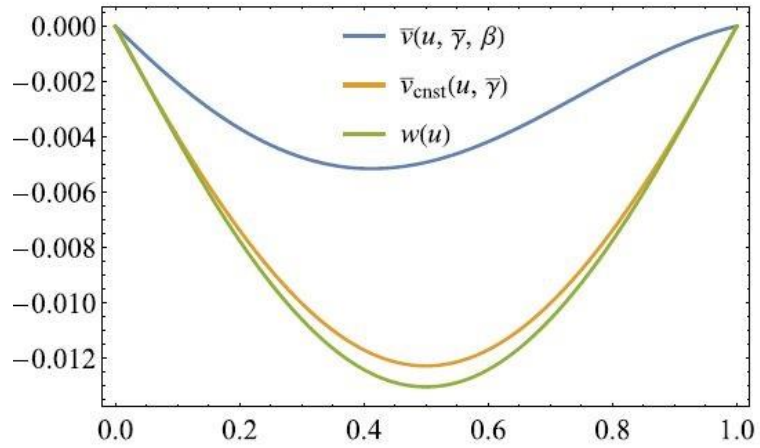

Figure A.2 : Deflections of the bi-directional gradient elastic beam. For the simply supported beam $\gamma = 0.1$ and $\beta = 1$ and E is constant (Initial conditions are $\bar{v}_0 = 0,\ \bar{\mu}_0 = 0,\ \bar{M}_0 = 0$, and end conditions are $\bar{v}(1) = 0,\ \bar{\mu}(1) = 0,\ \bar{M}(1) = 0$).

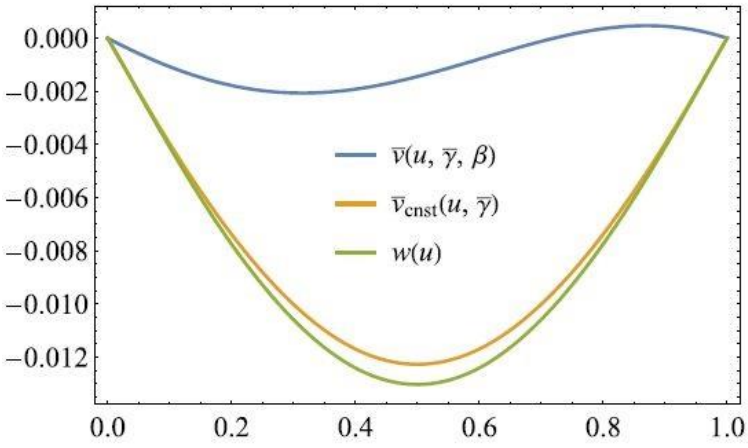

Figure A.3 : Deflections of the bi-directional gradient elastic beam. For the simply supported beam $\gamma = 0.1$ and $\beta = 2$ and E is constant (Initial conditions are $\bar{v}_0 = 0, \quad \bar{\mu}_0 = 0, \quad \bar{M}_0 = 0$, and end conditions are $\bar{v}(1) = 0, \quad \bar{\mu}(1) = 0, \quad \bar{M}(1) = 0$).

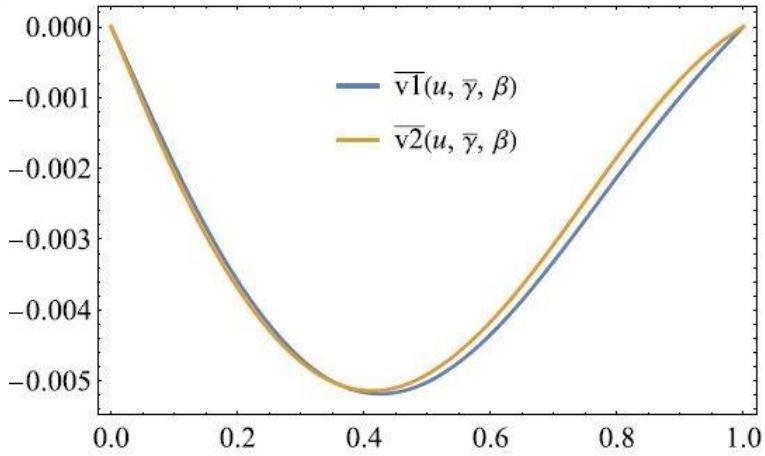

Figure A.4 : Deflections of the bi-directional gradient elastic beam. Simply supported beam with the first and second type of boundary conditions $\gamma = 0.1$ and $\beta = 2$.

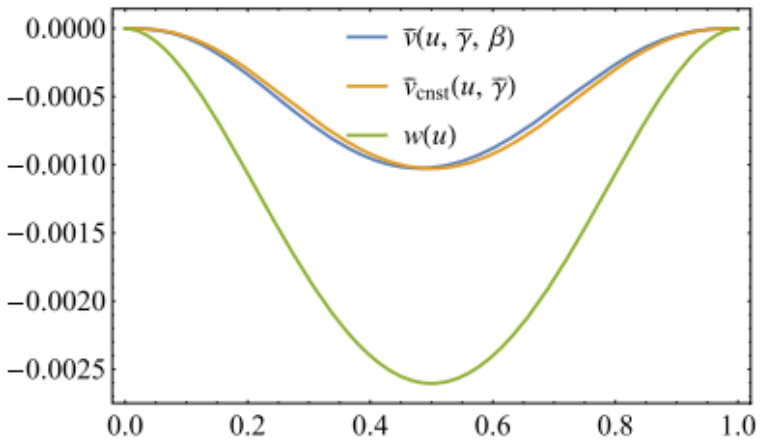

Figure A.5 : Deflections of the bi-directional gradient elastic beam. For beam fixed at both ends $\gamma = 0.1$ and $\beta = 1$ and E is constant (Initial conditions are $\bar{v}_0 = 0,\ \bar{\psi}_0 = 0,\ \bar{\alpha}_0 = 0$, and end conditions are $\bar{v}(1) = 0,\ \bar{\psi}(1),\ \bar{\alpha}(1) = 0$).

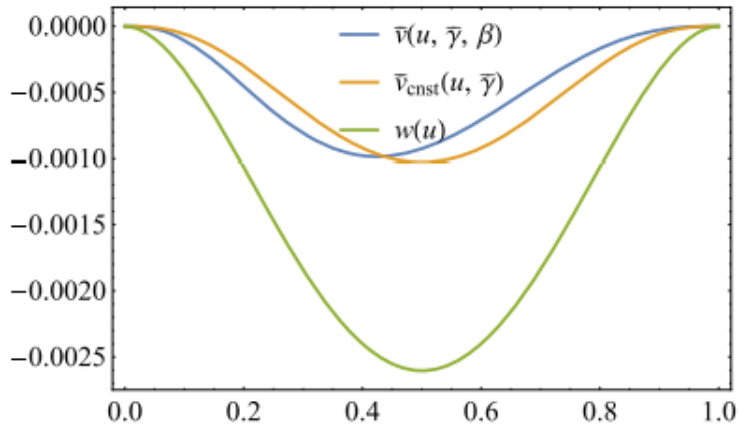

Figure A.6 : Deflections of the bi-directional gradient elastic beam. For beam fixed at both ends $\gamma = 0.1$ and $\beta = 4$ and E is constant (Initial conditions are $\bar{v}_0 = 0,\ \bar{\psi}_0 = 0,\ \bar{\alpha}_0 = 0$, and end conditions are $\bar{v}(1) = 0,\ \bar{\psi}(1),\ \bar{\alpha}(1) = 0$).

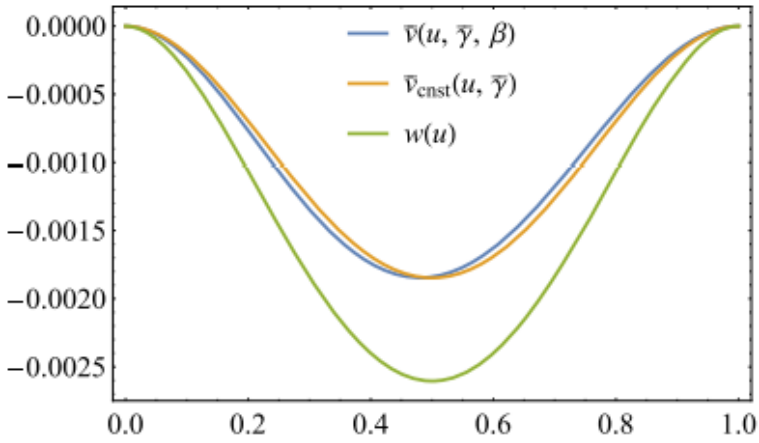

Figure A.7 : Deflections of the bi-directional gradient elastic beam. For beam fixed at both ends $\gamma = 0.1$ and $\beta = 1$ and E is constant (Initial conditions are $\bar{v}_0 = 0,\ \bar{\psi}_0 = 0,\ \bar{\mu}_0 = 0$, and end conditions are $\bar{v}(1) = 0,\ \bar{\psi}(1),\ \bar{\mu}(1) = 0$).

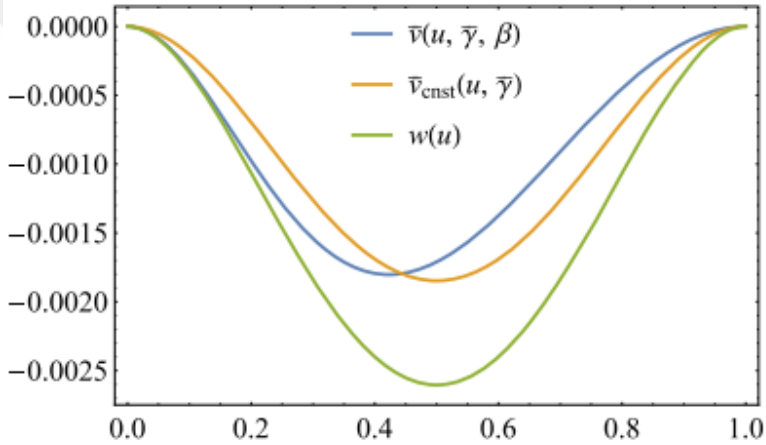

Figure A.8 : Deflections of the bi-directional gradient elastic beam. For beam fixed at both ends $\gamma = 0.1$ and $\beta = 4$ and E is constant (Initial conditions are $\bar{v}_0 = 0,\ \bar{\psi}_0 = 0,\ \bar{\mu}_0 = 0$, and end conditions are $\bar{v}(1) = 0,\ \bar{\psi}(1),\ \bar{\mu}(1) = 0$).

CURRICULUM VITAE

Name Surname **:** Murat ÇELİK

EDUCATION **:**

- **B.Sc.** **:** 2010, Ataturk University, Department of Civil Engineering